Impact of Global Warming on Production Change of Paddy Rice and Its Economic Assessment

January 2007

Toshichika IIZUMI

Impact of Global Warming on Production Change of Paddy Rice and Its Economic Assessment

A Dissertation Submitted to
the Graduate School of Life and Environmental Sciences,
University of Tsukuba
in Partial Fulfillment of the Requirements
for the Degree of Doctor of Philosophy in Science
(Doctoral Program in Geoenvironmental Sciences)

Toshichika IIZUMI

Abstract

Rice is a staple crop in eastern and southeastern Asia, the most populous area in the world. Rice production may change as a result of global warming through the CO_2 increase, temperature rise, and change in precipitation. Thus, policymakers require reliable projections of the regional impacts on the production in order to consider mitigation and adaptation techniques. In particular, paddy rice in Japan is one of the suitable objectives to establish the projection framework because of accumulation of the reliable data regarding phenology, production infrastructures, and weather. The established framework is expected to be applied to other Asian countries as well to Japan.

Most of impact projections use a combination of climate model products and crop models. However, the reliabilities of the projections are often very low due to the accuracy limitation of climate model products. The products generated by climate models e.g., General Circulation Models (GCMs) and Regional Climate Models (RCMs), include a climate-model bias, which is defined as the difference between simulated and observed climates. Especially, the dynamically downscaled products include another RCM biases in addition to GCM biases, although it is highly improved in the temporal and spatial resolutions. Since crop models have been tuned to simulate crop phenology development and yield based on observed climate datasets, the climate-model bias could reduce the accuracy of crop model simulations. Thus, this study demonstrates the effect of climate-model bias on rice model simulation and suggests the adjusted climate scenario for reliable impact projections, which assumes in 2070s under the Special Report on Emission Scenarios (SRES)-A2 scenario.

Adjusted climate scenario is applied to develop the impact projections in extreme events e.g., cool and hot summers after global warming. A cool summer seriously hurts rice production in northern Japan in current climate. Besides, an extremely hot summer after global warming may reduce production by the heat stress during the flowering period. Thus, the assessment is required regard to the hazards of production variability. The results of rice model simulations

show that climate changes will reduce the damage by a cool summer. On the other hand, the climate changes will enhance the damage by heat stress in central and southwestern Japan, but the heat stress will be disappeared in northern Japan even in the hot summer. As a result of the global warming, the damage to yield by a cool summer is mitigated; however, the damage by heat stress is enlarged after global warming.

The crop insurance for rice contributes to stabilize rice farmer's income. However, the global warming may affect the rice insurance payouts because of changes in production variability. Farmers expect the insurance works as an economic mitigation technique against the global warming, while policymakers require projecting the changes in the insurance payouts to examine the balance of income and payouts. Thus, changes in the insurance payouts in the 2070s are projected using a regime of simple rice insurance. The analysis framework is built by combining the climate model, crop model, yield damage assessment model, and insurance payout model. The simulation shows that the mean insurance payout during ten years in the 2070s significantly decreases accompanying an increase in the interannual variability, while the future yield decreases both in the mean and the interannual variability. In addition, regional differences are found in the future changes regarding the yield and the insurance payouts in nine agricultural areas of Japan. The change in the insurance payouts is proportion to that in the stability of rice production. The regional differences in the stability could cause the shift of main source area for rice. Such changes will potentially affect to the agricultural economics.

Key words: crop insurance, dynamic downscaling, economic assessment, global warming, impact assessment, Japan, paddy rice, regional climate model, rice model

Contents

List of Figures

List of Tables

1. Introduction

1.1. Global warming impact on paddy rice production

Agricultural production including paddy rice will be strongly affected by climate change as a result of increasing levels of greenhouse gases. To assess the impact on agricultural production, many studies have projected the impact of global warming on the production of major crops in some countries by combining climate model products and crop models. They have tried to project the future production of, for example, maize, winter wheat, rice (Tsvetsinskaya et al., 2003), cotton (Ruth et al., 2003), and grain crops (Thomson et al., 2005) in the U.S.A., as well as paddy rice in Japan (Toritani et al., 1999; Yokozawa et al., 2003; Nakagawa et al., 2003) and other major crops in China (Tao et al., 2003).

Paddy rice is a staple crop in eastern and southeastern Asia, the most populous areas in the world. Projections of regional climate change and impact on rice production are important in relation to food security for these areas, as stated by the Intergovernmental Panel on Climate Change (IPCC) in its Third Assessment Report (AR3; IPCC, 2001). Reliable projections work as an early warning and contribute to the investigation of mitigation and adaptation techniques. In particular, Japan is one of the suitable countries for which to establish impact projection methods for paddy rice because of the reliable accumulation of data, i.e., phenological data, socio-economic data related to production infrastructure and dense observational weather data. The established projection methods may be applied to other Asian countries as well to Japan.

1.2. Previous studies regarding impact on paddy rice production in Japan

Most impact projections on paddy rice growth and production in Japan are based on the IS92A scenario. The scenario is presented in the IPCC Second Assessment Report (AR2; IPCC,

1996). Several early studies use other simple climate projections instead of the IS92A scenario, such as Seino (1993) and Yonemura et al. (1998).

Projections relating to paddy rice production in Japan are updated accompanying with the improvements in climate models, climate downscaling methods, and crop models. Some projections are shown according to the climate projections under the IS92A scenario presented in the IPCC AR2 (IPCC, 1995). One of them bases on a coupled atmosphere-ocean GCM product and shows that the rice growth period is shortened in current major source areas and cultivatable area shifts northwards (Toritani et al., 1999). The other shows that the rice yield decreases in southwestern Japan whereas it increases in northern Japan by using four GCM products (Horie et al., 1995; Nakagawa et al., 2003), and the projection also demonstrates that the interannual variability becomes larger in entire Japan in 2090s. Such projected changes are partially supported by the projection based on the improved crop model and five current climate projections submitted in the upcoming IPCC Fourth Assessment Report: AR4 (Iizumi et al., 2006).

GCMs seem to be the only tools that allow the projection of global warming by greenhouse gas emissions. Although the spatial resolution of GCMs has been rapidly improving, it is still insufficient to project regional climate changes. Thus, downscaling of climate projection is often used to obtain high-resolution regional climate scenario. The four GCM products are downscaled by the interpolation technique in Yokozawa et al. (2003). Simply, these downscaled climate projections express climate changes by the addition or multiplication of climatological mean differences between the CO_2 increase run and the control run of the GCMs to the observational climate datasets. Thus, the climate projections are limited in analyzing extreme years and inter-annual variability. Therefore, impact projections are still under development when subject to inter-annual variability and extreme years after global warming; e.g., the hot summer year and the cool summer year.

On the other hand, the dynamic downscaling technique is often used to further increase the resolution of GCM products by using regional climate models (RCMs) as well as statistical downscaling and interpolation. The dynamic downscaling technique is one of the key tools for

projecting regional climate change, although it has some limitations regarding the physical parameterization of RCMs. A current study that includes the achievement of dynamic downscaling extends impact assessment to extreme years and displays the impacts on paddy rice production in cool and hot summers after global warming (Iizumi et al., 2007).

1.3. Purpose of the study

As mentioned above, it is under development to provide a reliable assessment of global warming impact on agricultural production, although a reliable impact assessment is strongly required by policymakers to examine countermeasures. No investigation has achieved to clarify the disturbance of climate-model bias on impact assessment. Additionally, less cross-disciplinary studies have conducted in wide-ranging sectors from the projection of regional climate change, estimation of crop production change, and assessment of change in agricultural economy. Thus, this study aims to build a reliable framework for projection to assess the impact of global warming on crop production and agricultural economic system taking paddy rice in Japan as an example.

2. Data and Methods

2.1. Projection framework

The analysis framework in this study is designed to project future rice insurance payouts after global warming in Japan (Figure 2.1). The framework was composed of the following four modules: (1) a climate-projection downscaling module that dynamically downscales global reanalysis datasets and GCM products to obtain regional high-resolution climate projections; (2) a yield estimation module that estimates the typical potential yield of paddy rice in a unit area by using daily weather datasets; (3) a yield damage-assessment module that estimates the yield damage caused by natural hazards; (4) a rice insurance payout projection module that simulates the insurance payout based on the estimated production and a long-term average production. The module details are described in Chapters 2.2, 2.3, and 5.3.

The unit of calculation in this framework is the legal unit, i.e., the prefecture. Forty six out of the forty seven prefectures in Japan are chosen; a prefecture in the southwestern islands is excluded. Simulation results in respective prefectures are aggregated into the nine agricultural areas for display (Figure 2.2). The agricultural areas are defined by the Ministry of Agriculture, Forestry and Fisheries of Japan (MAFF).

2.2. Regional climate model

2.2.1. Dynamically downscaled climate scenario

The role of Regional Climate Model (RCM) is to reproduce the present climate and to project the regional climate in 2070s based on the GCM products under the SRES (IPCC, 2000) - A2 scenario. The Meteorological Research Institute - Coupled GCM ver.2 (MRI-CGCM2; Yukimoto et al., 2001) products are adapted in this study. The GCM products are referred as the

one of climate projections in the IPCC AR3 (IPCC, 2001).

We used a RCM (TERC-RAMS) as the module relating to climate projection downscaling; the TERC-RAMS is a version of the Regional Atmospheric Modeling System (RAMS) modified by the Terrestrial Environmental Research Center (TERC), University of Tsukuba (Yoshikane and Kimura, 2003; Sato and Kimura, 2005, Sato et al., 2006). The original version of the RAMS is developed at the Colorado State University (Pielke et al., 1992). The RCM includes the physical schemes and parameterizations summarized in Table 2.1 and has a two-way nested grid system shown in Figure 2.3. The coarse grid system covers entirety eastern Asia with 120 km grid interval, while the fine one covers entirety Japan with 30 km grid interval with the exception in southeastern islands. Both grid systems include 30 vertical layers in the terrain following coordinate system. The lowest layer locates 110 m up from the screen height.

We conform to a dynamic downscaling method, namely “pseudo warming method” suggested by Kimura (2005). The method is developed to estimate the regional climate change with reducing a GCM bias, the most serious issue for projection (Sato et al., 2006; Misra and Kanematsu 2004). The downscaling method has limitations in the assumption of same interannual variability with current climate, but the method is valid to generate a climate scenario for impact projection. The method is applied in Mongolia (Sato et al. 2006), Japan (Iizumi et al., 2007) and Turkey (Tanaka et al., 2006).

When the RCM projects a climate condition in 2070s, the boundary condition of RCM was assumed to be a linear composite of reanalysis data at 6-hour intervals and the warming component between the 1990s and 2070s in the GCM products. The warming component was given by the following process that firstly, the monthly mean climate data was calculated from the GCM products at 6-hour intervals. Secondly, the 10-year mean data was obtained by averaging the monthly mean data for 1990s and 2070s, respectively. The warming components are the difference in the monthly 10-year mean data between above two periods. The warming components of the GCM include wind speed and temperature, geopotential height, specific humidity, sea surface temperature (SST). The warming components of GCM are loaded on the time series of a reanalysis and SST data, time-independently. The reanalysis data is produced by

the National Center for Environmental Prediction / National Center for Atmospheric Research (NCEP/NCAR). By using the composite including reanalysis data, the synoptic condition of simulated future year is very similar to that of specific present year. Thus the simulated future year is called “pseudo year”, and it means a year after global warming which has very similar synoptic condition to a present year.

On the other hand, the RCM uses the reanalysis data and monthly mean SST (Reynolds et al., 2002) as the boundary condition when the RCM reproduces the present climate. The reanalysis data fed to the RCM is six-hourly NCEP/NCAR reanalysis. The numerical experiment corresponds to the “hindcast”. The hindcast and the projection are carried out for 10 years in 1990s and 2070s (from current and pseudo year 1991 to 2000).

2.2.2. Use of regional climate change scenario

RCMs have the climate-model bias as well as GCMs. The RCM bias is also serious issue when the global warming impact is projected by use of the RCM products. We prepared the warming component of RCM as the differences between projection and hindcast. The warming component of RCM includes temperature, downward shortwave radiation, and precipitation. The warming components of RCM are added to the grid point value of observational datasets, given by the Automated Meteorological Data Acquisition System (AMeDAS) provided by the Japan Meteorological Agency. The value of AMeDAS is interpolated to the grid points of the second coordinate of the Digital Numerical Land Information (DNLI) with temperature adjustment reflecting to the altitude. The DNLI is provided by the Ministry of Land, Infrastructure and Transportation of Japan. The grid interval of the DNLI is 5.0 minutes in latitude and 7.5 minutes in longitude (approximately 10 km $\times$10 km). We call the processed datasets “adjusted climate projection” and assumed as the future regional climate projection.

2.3. Rice model

2.3.1. Yield formation of the SIMRIW

A crop model for rice (SIMRIW) is adapted. The SIMRIW (SImulation Model for RIce and Weather-relationship; Horie et al., 1995a, Nakagawa et al., 2003) estimates potential rice growth and yield under the idealized condition of an irrigated paddy field and good managements of nutrients, pests and diseases. The SIMRIW has adequate capability to reproduce the inter-annual variability and the spatial distribution of rice yield in Japan (Horie 1995a, Nakagawa et al., 2003). The model simulates potential rice growth using data of daily minimum and maximum temperatures and daily total solar radiation. Precipitation is eliminated from the input data in this study for the following two reasons. First, since most of rice is produced in irrigated paddy fields, precipitation is not a critical factor of rice yield in Japan. Second, since precipitation is predicted to increase in the summertime in eastern Asia (IPCC, 2001), water resources are expected to be available under the future climate condition in Japan.

The SIMRIW detail is described by Horie et al. (1995b). Here, we overview the parameterization regarding yield formation suggested by above mentioned work of Horie et al. The constituent elements of parameterization will be shown as a result of the rice model simulations in Chapter 4 for diagnosing the rice response to climate change.

The potential yield (PY) means the potential dry weight of brown rice in this study. The potential dry weight of brown rice is a function of the total dry weight including roots at maturity day (W_t) and the harvest index (h), as follows:

$$PY = hW_t . \tag{2.3.1.1}$$

The harvest index takes account of two types of spikelet sterility; i.e., that due to a cool temperature (h_c) and that due to a high temperature (h_h) during the flowering period. The more influential value is adapted as the h in the model.

The harvest index (h_c) is given as the following function when the harvest index corresponds to stress from cool temperatures:

$$h_c = h_m(1-\gamma_c)\{1-\exp[-K_h(DVI-1.22)]\}, \tag{2.3.1.2}$$

where h_m is the maximum harvest index of the given cultivar and K_h is an empirical constant.

The maximum harvest index of the given cultivar is obtained under optimum conditions for air temperature, solar radiation, nutrients, pests and diseases. The Development Index (DVI) represents the alternation of the crop stage in the range of 0 to 2. The DVI means the heading day, approximately same as the flowering day, when its value reaches 1. The DVI means the maturity day when its value reaches 2. The ratio of sterile spikelets as a result of the damage by a cool summer (γ_c) is approximated as follows:

$$\gamma_c = \gamma_0 - K_q Q_t{}^a , \tag{2.3.1.3}$$

where γ_0, K_q and a are empirical constants. The cooling degree-days Q_t is given as a function of daily mean temperature (T_i) during the period when rice panicles are most sensitive to cool stress. The time period is defined by the DVI and ranges from 0.75 to 1.20. Thus Q_t is given as follows:

$$Q_t = \sum (22 - T_i). \qquad (0.75 \le DVI \le 1.20) \tag{2.3.1.4}$$

Rice yield is also damaged by high temperature during the flowering period. The harvest index (h_h) is given by the following function when the harvest index corresponds to heat stress. The parameterization is suggested by Nakagawa et al. (2003).

$$h_h = h_m (1.00 - 0.95\gamma_h), \tag{2.3.1.5}$$

$$\begin{cases} \gamma_h = \left[\left(\dfrac{\overline{T_{\max}} - T_b}{T_o - T_b} \right) \left(\dfrac{T_c - \overline{T_{\max}}}{T_c - T_o} \right)^{\frac{T_c - T_o}{T_o - T_b}} \right]^{\alpha} & \text{for } T_{\max} > T_o , \\ \gamma_h = 0 & \text{for } T_{\max} \le T_o . \end{cases} \tag{2.3.1.6}$$

where γ_h is the ratio of sterile spikelets as a result of heat damage to unity. $\overline{T_{\max}}$ is the daily maximum temperature averaged over the flowering period. T_b is the lower critical temperature for rice growth. T_o is the optimum daily maximum temperature during the flowering period. T_c is the upper critical temperature. α is the curvature factor. We conform to Nakagawa et al. (2003), and we adapted the same values for the above parameters; i.e., 10 and 43 ^{o}C for T_b and T_c. α is also fixed at 4.77 and 12.78 for CO_2 concentrations below and above 550 ppm, respectively.

We also conformed to Nakagawa et al. (2003) with respect to the cultivars setting in each

prefecture. Additionally, the initial values of leaf area index, DVI, initial dry weight and technical coefficient were regulated to fit the actual yield record, provided by the MAFF. The rice model simulates at each grid point of DNLI, respectively, based on the given climate datasets. The climate datasets include the daily maximum/minimum temperatures and the daily total solar radiation. Precipitation is eliminated from the input elements because the accuracy of precipitation in the RCM products is quite low. However, a slight change in precipitation is not the critical factor in the irrigated paddy rice. Thus, not using precipitation does not spoil the reliability of our simulation results.

The rice model hindcasts the present yield when the model is based on a 330 ppm CO_2 concentration and observational climate datasets. The numerical experiment is named the "Yield-present-run". The rice model projects the future yield when the model is based on a 550 ppm CO_2 concentration and the adjusted climate projection and this experiment is named the "Yield-warming-run".

Despite its good capability, the SIMRIW has limited capability in climate acclimatization. The partial effect of acclimatization is included in the parameters regarding the phenology sub-model of the current model through the parameter optimization process. The current model implicitly considers the effect of climate acclimatization rather than explicitly. Thus, our simulation results have an uncertainty regarding the effect of climate acclimatization.

2.3.2. Modification of the SIMRIW to Regional-Scale Rice Model

A modified version of SIMRIW (SImulation Model for RIce-Weather relationships) was developed as a Regional-scale Rice Model (RRM) and included into the analysis framework as the rice yield estimation module. The RRM is used in Chapter 5. The original version of SIMRIW is a simplified process model to simulate the relation between rice growth in irrigated paddy and surrounding weather condition i.e. daily maximum/minimum temperatures and daily total solar radiation (Horie et al., 1995; Nakagawa et al., 2003). The SIMRIW is validated that it has enough capability to reproduce yield and heading day in their interannual variability and

spatial distribution. Heading day is quite important as well as yield. The time period which at and before heading day is most sensitive to heat and cooling stresses respectively, a correct estimation of heading day is strongly responsible to the accuracy of yield estimation.

The RRM detail will be addressed by Yokozawa et al. (submitting), we briefly note the resultant improvement by modifications. The RRM was improved in its subjective scale with taking over basic parameterizations regarding phenology and yield formation. Crop models used in previous studies have a large disagreement in spatial scale with climate model products. Most crop models assume a field scale, whereas climate models used for climate projection cover the global to regional scale. A regional-scale crop model is required to couple with downscaled climate products. Reduction of disagreement in spatial scale contributes to decrease errors in yield estimation.

The RRM was improved not only in the scale-up but also in the response of spikelet sterility. The model includes the spikelet sterility response to the combination of high temperature and high CO_2 concentration during flowering period (roughly corresponds to heading day) suggested by the work of Nakagawa et al. (2003).

The modification regarding scale-up was carried out through the new parameter setting. The parameters regarding phenology and yield formation are optimized to describe the typical growth and yield in each prefecture for the past 25 years based on the daily time series of area mean weather data on paddy fields. Observed heading day and yield are obtained from “Crop statistics” provided by the MAFF. The gridded AMeDAS provided by the National Institute for Agro-Environmental Sciences (NIAES) is adapted as the observed weather dataset. The parameters were estimated based on the dataset in the odd years, and the estimated heading day and yield were cross-validated with the actual records in the even years.

As the result of cross-validation, the RRM simulates very well the interannual variability and mean of yield and heading day under the present climate condition. The correlation coefficient in yield averaged over 46 prefectures is 0.576 with Root Mean Square Error (RMSE) of 0.609 t/ha, while the heading day is also well simulated with mean correlation coefficient of 0.731 with RMSE of 6.907 days. In spite of such good capability, the model has some limitations

such as a larger RMSE in yield over northern area, and the lack of damage assessments from irregular events (i.e. typhoon and heavy rain). The partial improvement can be seen regarding assessment of irregular events by coupling with the yield damage assessment model. The detail of damage assessment model is described in Chapter 5.

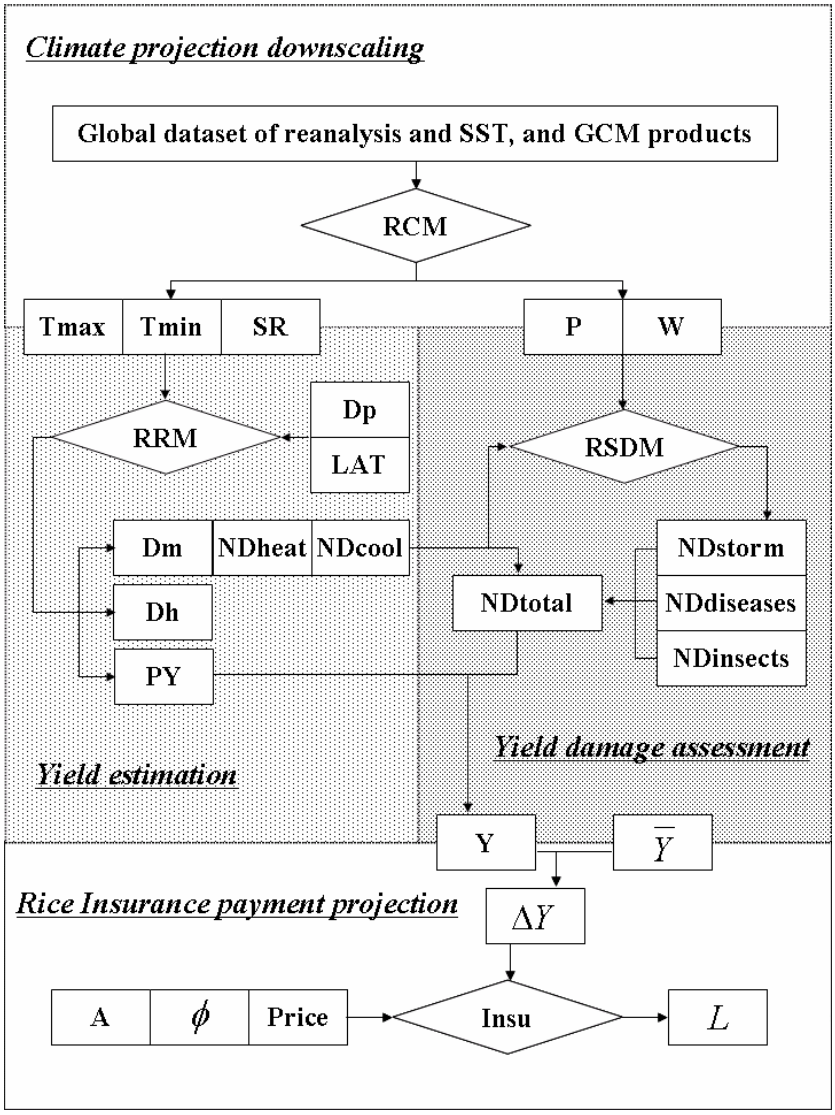

Figure 2.1: Schematic diagram of the analysis framework. The rhombic boxes show the models. RCM: regional climate model, RRM: regional-scale rice model, RSDM: regional stochastic damage model, Insu: insurance payout model. Tmax, Tmin, SR, P, and W are daily values of maximum and minimum air surface temperatures, daily total solar radiation, hourly maximum precipitation, and hourly maximum wind speed, respectively. LAT: latitude, Dp, Dh, and Dm: planting day, heading day, and maturity day, PY: potential yield, NDheat and NDcool: net yield damages caused by heat stress and cool summers, NDstorm, NDdiseases, and NDpests: net yield damage caused by storms, disease, and pests, NDtotal: total yield damage, Y: yield, $\overline{Y}$: long-term mean yield, ΔY: insurance-covered yield damage, A: planted acreage, ϕ: insurance coverage, Price: mean price of rice in the 1990s, and L: rice insurance payment.

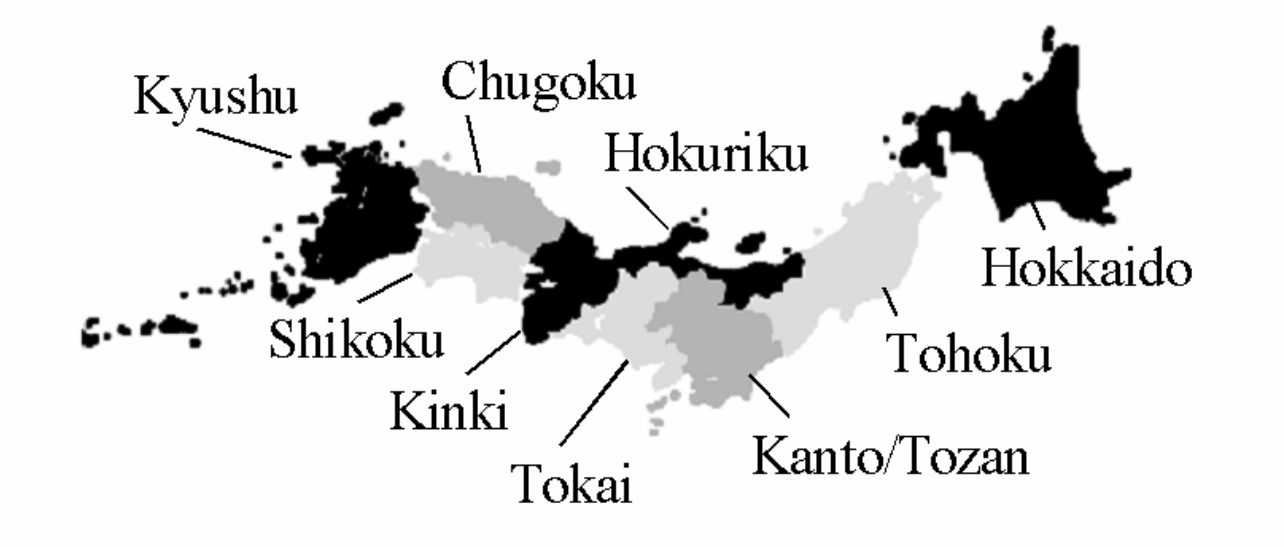

Figure 2.2: Names of agricultural areas in Japan

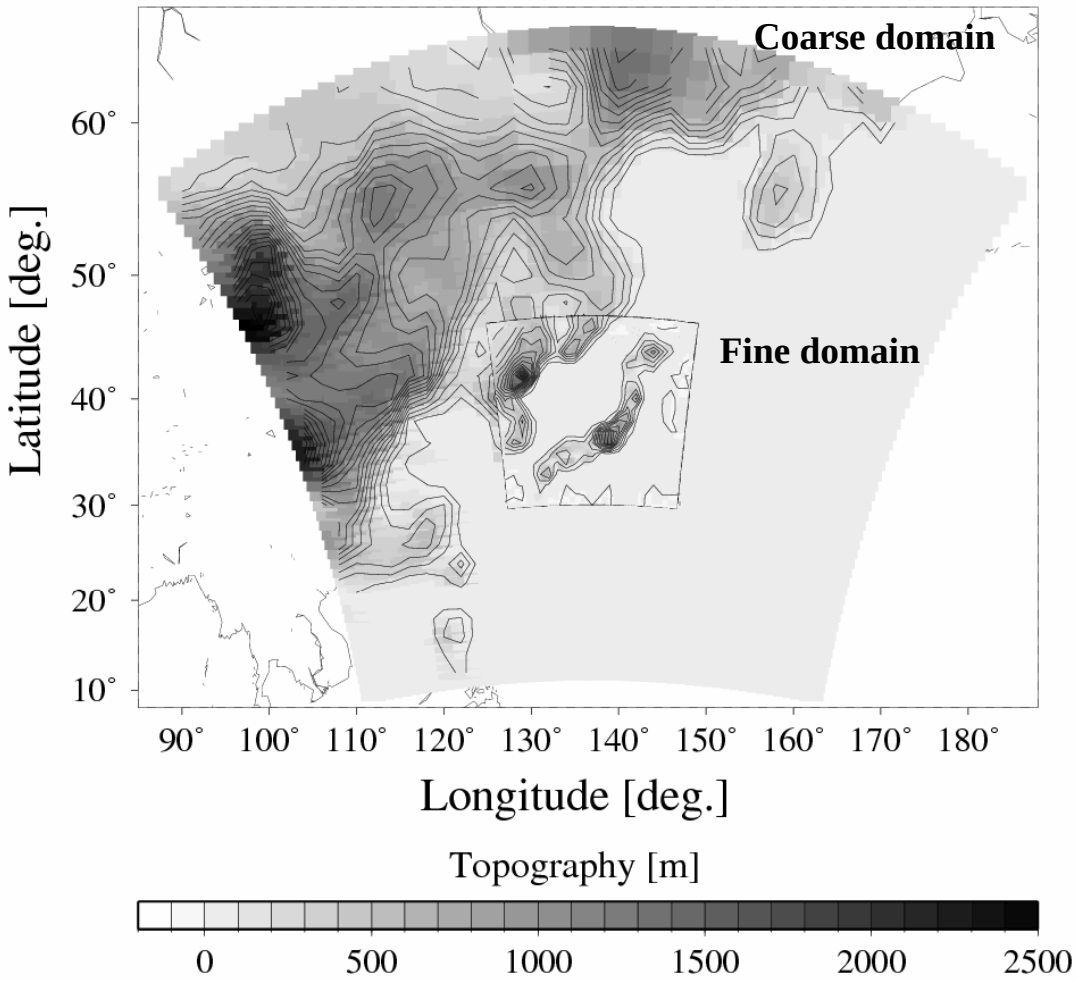

Figure 2.3: Domains of the regional climate model (TERC-RAMS); the shading shows the topography of the RCM, and the contour interval is 100 meters.

Table 2.1: The calculation condition of the RCM

Horizontal grid system:
Coarse grid system: 50 x 50, 120 km grid interval, centered on 137.0^{o}E, 38.5^{o}N
Fine grid system: 62 x 62, 30 km grid interval, centered on same with above
Vertical layer: 30 layers, 110 m thickness in lowest layer
Soil layer: 11 layers
Vegetation type: Short grass
Sea surface temperature: Monthly mean SST (Reynolds et al., 2002)
Start time: 24 hour before the 1st day each month for every integrations
Dynamical process:
Nonhydrostatic equations
Terrian following coordinate system
Physical process:
Radiation: (Nakajima et al., 2000)
Cumulus convection: (Arakawa and Schubert, 1974)
Cloud microphysics: (Walko et al., 1995)
Surface process: (Louis, 1979)
Soil model: (Tremback and Kessler, 1985)

3. Disturbance of climate-model bias

3.1. Climate-model bias

Climate-model bias, the difference between the simulated climate and the actual observation, reduces the accuracy of climate-model products. Each GCM and RCM has its own model bias, so downscaled climate data include both RCM bias and GCM bias. Mearns et al. (2003) stated that the reproduction of the present climate by climate models remains a challenging issue.

Crop models are designed to simulate crop growth and yield based on an observed climate dataset, and the model parameters have been tuned using observed data. Climate-model bias sometimes seriously reduces the accuracy of crop model simulations. Careless application of climate-model products to crop simulation often destroys the reliability of the impact projection. The conventional projection method for the impact of global warming, a simple combination of climate models and crop models, is not sufficient to obtain the accurate simulation results. The reliability of the impact projection must be considered in order to obtain an accurate projection of crop production.

This chapter focuses on the effects of model bias in climate data on yield estimation by a crop model. Three sensitivity tests of rice yields were used. The first test is the sensitivity of the present rice yields to errors in climate data, which can be estimated as the difference between the rice yield based on observed climate data and that based on the present climate data reproduced by RCMs. This difference is the estimation error of the current yield in the impact projection. The second test is the sensitivity of the yield to climate change, which can be estimated by calculating the difference between the estimated yield based on the reproduced present climate data and that based on future climate data projections by RCMs. We propose new, corrected future climate data, a composite of observed climate data and the difference between future and present climates estimated by RCMs. The third type of sensitivity can be estimated by finding the difference between the projected yield based on future climate data directly estimated by

RCMs and the yield based on the future OCD.

3.2. Data and Methods

3.2.1. Use of climate data

Two climate datasets are provided: Model output Climate Datasets (MCDs) and Observed Climate Datasets (OCDs). Each dataset includes present and future climate data. The MCDs were obtained by the downscaling technique based on reanalysis data and GCM products using RCMs (see in Chapter 2.2.1 and 2.2.2).

The RCM estimates the present MCDs in 1991 and 1994 as Run-1, as shown in Figure 1. This run is almost the same as a hindcast, the prediction of past weather through the use of the RCM, and it indicates the reproductive capability of the RCM by a comparison with the present OCD. The RCM also estimates future MCD, Run 2 in Figure 3.1.

Observational climate data are employed as the present OCD, most of which were given by the AMeDAS (the distance to each station is approximately 25 km) and provided by the Japan Meteorological Agency. The solar radiation of the present OCD is estimated from the sunshine duration of AMeDAS. The climate data are also interpolated to the second grid coordinate of DNLI. The future OCD is assumed to be a composition of observational and differential components. The differential component is defined as the difference between the future MCD and the present MCD estimated by the RCM in a fine grid system, which indicates a regional climate change as the result of global warming. The differential components are common to the future MCD and OCD, so these two are only different in the basic climate data hindcast by the RCM and observed data, respectively. The difference between the present MCD and OCD is expected to be the RCM bias.

3.2.2. Rice model simulations

Four rice yield estimations are carried out using a crop model for rice. The crop model calculates the rice yield using MCDs and OCDs. Since each includes the present and future climate datasets, the crop model runs four times in Run-A to Run-D, as shown in Figure 3.1. The crop model adopted here is SIMRIW (Horie, 1990; Toritani et al., 1999; Nakagawa et al., 2003).

The CO_2 concentration is fixed at 330 ppm in both the present and future climates since the simulation focuses on the effects of climate-model bias on yield estimations in this chapter. The outline of the crop-model setting is given in Table 3.1. These setting parameters are common in the four runs.

The crop model hindcasts the present rice yield based on the present MCD in Run-A. The present MCD is obtained by Run-1. This run corresponds to the estimation of the baseline yield in the conventional method of impact projection. Then the crop model projects the yield as Run-B, assuming the climate condition in the 2070s based on the future MCD. The future MCD is projected by Run-2, which corresponds to the future yield estimation by the conventional method. Next, the crop model again hindcasts the present yield, but it is based on the present OCD as Run-C, where the present OCD is obtained from the grid interpolation of observational climate data. The phenological parameters and initial conditions of the crop model have been adjusted using the present OCD and actual yield, so this run demonstrates the reproductive capability of the crop model. Finally, the crop model again projects the future yield, but it is based on the future OCD as Run-D. The future OCD is obtained by the process mentioned above using the present OCD and the results of Run-1 and Run-2.

The difference in estimated yield between Run-A and Run-C is caused by the difference between the present MCD and present OCD, i.e., the model bias. Therefore, the difference between these two runs indicates the effects of the climate-model bias on the present yield reproduction. The difference in the estimated future yields between Run-B and Run-D is caused by the difference between the future OCD and MCD, which is the same as the difference between the present MCD and OCD, as mentioned above. The difference in estimated yield between Run-B and Run-D indicates the effect of climate-model bias on future yield projections.

3.3. Results

3.3.1. Climate-model bias in the reproduced present climate

The result of Run-1 is compared with the present OCD to assess the accuracy of the RCM products. The differences in climate values over a 6-month period are shown in Figure 3.2 as the 2-year mean and area mean values of MCD - OCD. Area mean differences for all of Japan except for the southwestern islands are shown in Figure 3.3. The monthly mean temperature shows a cold bias of about 2 K in average. The monthly mean daily maximum temperature has a significant cold bias of about -5 to 0 K, which tends to be enhanced during summer. On the other hand, the monthly mean daily minimum temperature has a warm bias, prominent in September and October, of about 1 to 3 K. As a result, the diurnal range of the present MCD is smaller than that of the present OCD.

The monthly mean daily total solar radiation of the MCD agrees well with that of the OCD from May to July, although it is significantly smaller than that of the OCD from August to October. The monthly total precipitation also is in good agreement; however, the precipitation totals of the MCD are significantly underestimated in July, August, and September and overestimated in June and October.

Table 3.2 represents spatial correlation coefficients of five climate variables between the 2-year mean present MCD and OCD from May to October, the entire period of rice crop growth. The RCM shows high accuracy for the spatial distribution of temperature. The correlation coefficients are 0.369 - 0.669 for the monthly mean temperature, 0.252 - 0.378 for the monthly mean daily maximum temperature, and 0.401 - 0.620 for the monthly mean daily minimum temperature. The correlation coefficients of the maximum and minimum temperatures are quite poor in August.

The monthly mean daily maximum temperature has a warm bias in northern Japan and a -5 to 0 K cold bias in southwestern Japan in all months for which estimates were made. The cold bias in the daily maximum temperature is enhanced and extended in the area in summer. The

daily minimum temperature shows a higher accuracy in the spatial pattern than at the maximum temperature. The daily minimum temperature has a slightly warm bias in most of the Japanese mainland, although a slight cold bias appears in the central part in all months as well as in the Sea of Japan side from May to July. The warm bias of the daily minimum temperature is enhanced in September and October. As a result, the monthly mean temperature of the present MCD has a cold bias of 2 K, while the diurnal range of the MCD is smaller than that of the OCD.

The spatial correlation coefficients of the monthly mean daily total solar radiation are 0.211 - 0.451. The spatial pattern of the present MCD agrees fairly well with that of the OCD. However, daily total solar radiation of the present MCD tends to be overestimated in northern Japan, while it is underestimated in the southwestern part from August to October. The spatial correlation coefficients of the monthly total precipitation are quite poor, only 0.003 - 0.198. Although the spatial pattern of the present MCD agrees fairly well with the OCD in May and June, the spatial pattern of the present MCD disagrees with the observed data from July to October (The spatial correlation coefficients during 10 years can be seen in Appendix A).

3.3.2. Regional climate change in Japan

Figure 3.4 shows the 2-year mean regional projection of the different components obtained by Run-1 and Run-2. The monthly mean daily maximum and minimum temperatures increase by about 2 K until the 2070s. The monthly mean temperature increases more in October than in the other months. Total solar radiation slightly increases from June to October, while precipitation decreases from May to June but increases from July to October.

The spatial pattern of the differential components of the RCM is shown in Figure 3.4. The monthly mean daily maximum and minimum temperatures increase in all of Japan (Figures 3.4a and 3.4b). The temperature increases less in May and June than in the other months.

The monthly mean temperature increase of 0 to 2 K is associated with the same levels of increase in the minimum and maximum temperatures. The monthly mean daily total solar

radiation decreases in the northern islands and on the Pacific side of northern Japan during all months for which estimates were made (Figure 3.4c). It also decreases on the Sea of Japan side of the southwestern mainland in May and June.

Changes in monthly total precipitation depend on the area and the month. Precipitation slightly decreases in most of Japan from May to June, but it increases in southwestern Japan from September to October and from July to August, although the increments are quite small. Solar radiation slightly increases in August and October, while precipitation increases. The assumed reason is that the area of cloud cover shrinks while the frequency of heavy rainfall events increases due to the effects of global warming. By a numerical simulation using MRI-CGCM2, Yukimoto et al. (2001) suggested that heavy precipitation would increase due to global warming. Downscaling of the projection should take over the feature of MRI-CGCM2 (in addition, time series of projected regional climate change can be seen in Appendix B).

3.3.3. Effect of model bias on yield and impact of global warming

The results of Run-A and Run-C are validated by the actual yield record, "Crop Statistics," provided by Ministry of Agriculture, Forestry, and Fisheries of Japan. The estimated present yield agrees well with the record when it is estimated based on the present OCD (Figure 3.5c) but not on the present MCD. The estimated yield based on the MCD is significantly underestimated in southwestern Japan.

The projection of yield change is shown in Figure 3.6. The spatial distributions of yield change show a large difference between the two results obtained based on the OCD and MCD. The projected yield change based on the OCD shows a decrease in yield in most of southwestern Japan, but based on the MCD, it increases in all of Japan.

3.4. Discussion

To reproduce the present climate accurately using climate models is still challenging issue even in current days. The accuracy of climate models is not always high, and the reliability is sometimes insufficient. The accuracy of climate model products depends on climatic variables, area, seasons, and parameter setting in models. For example, Mearns et al. (2003) stated that the accuracy for extreme values, such as the maximum temperature in summer, is worse than that for the mean temperature in NCAR RegCM.

The model bias of the RCM products is summarized as follows. The daily minimum and maximum temperatures show a slight warm bias and a significant cold bias, respectively. The daily mean temperature indicates a cold bias of about 2 K as a result of a significant cold bias in the daily maximum temperature, as mentioned above. Thus, the diurnal range of temperature in MCDs is smaller than that in OCDs. The RCM gives a fair value for the area mean monthly total precipitation, while the accuracy of the spatial pattern depends on the season. Although the RCM tends to underestimate the monthly mean daily total solar radiation, it simulates the spatial pattern better than it simulates precipitation.

Climate-model bias, sometimes, seriously reduces the accuracy of the crop model. The cold bias in the daily maximum temperature causes the underestimation of yield damage due to heat stress. The warm bias in the daily minimum and mean temperatures leads to an underestimation of the yield damage by cold stress. The bias in the daily mean temperature reduces the accuracy of the flowering day period in the simulation. During the flowering period, crops are most sensitive to the heat, while cold stress is directly related to yield. Underestimating the daily total solar radiation leads to an underestimation of the total dry weight and yield at harvest time.

The spatial distribution of yield change until the 2070s shows a large difference between OCDs and MCDs. The projection based on MCDs indicates that the rice yield increases in most of Japan. On the other hand, the projection based on the OCDs shows that the yield decreases in most of southern Japan due to heat stress. The difference in the yield change is caused only by the climate-model bias since the crop-model runs assume the same condition except for the climate dataset. Appearance of the differences between the present and future climate data are common among MCDs and OCDs. The source of the difference derives only from the difference

in the baseline climate which exists between the present MCD and OCD.

The above-mentioned fact means that the projection of yield change is strongly affected by climate-model bias. Consequently, the careless use of climate-model products leads to capricious errors in impact projection due to non-linear effects of climate-model bias. Most of crop models use daily climate variables and their time-integrated value in each crop stage. Thus, climate-model bias sometimes expands its effects so much in crop models that the error in the estimated crop growth and yield becomes quite large.

Moreover, crop models respond non-linearly to changes in climate variables near the assumed thresholds. For example, the yield of a cultivar of rice is reported to decrease drastically due to heat stress when the daily mean temperature is above 26 ^{o}C (Kim et al., 1996). Rice yield also decreases when the daily mean temperature decreases below 20 ^{o}C during the microspore stage (Satake and Yoshida, 1978). Furthermore, water stress affects dominantly crop growth and yield in semi-arid and non-irrigated areas.

The accuracy of the spatial pattern in the estimated precipitation is often lower than that of temperature and solar radiation even though the monthly total or area mean precipitation agrees fairly well with the observation. Although changes in available water resources and the impact on crop production are of concern, the accuracy of the estimated precipitation by the model is often insufficient to input data to the crop models. The careless use of model-estimated precipitation reduces the reliability of impact projections. In order to maintain reliability, MCDs should be replaced by OCDs, which mitigate better the negative effects of climate-model bias for impact projection.

Generally, phenological parameters in the crop model have been adjusted to optimize the estimations of crop growth and yield formation. The phenological parameters include the development index and leaf area index as well as the threshold values mentioned above. The best-fit parameters are obtained from observational weather data and crop growth records in experimental fields, so the crop models can perform within the variation range of these weather data. On the other hand, it does not seem reasonable to fit phenological parameters to adjust to the relation between MCDs and the actual crop growth record in order to avoid a mismatch

between them because doing so may unacceptably modify the phenological meanings of the parameters because of climate-model bias. The present method allows the mismatch to be reduced without modifying the phenological parameters.

3.5. Summary

A simulated rice yield by the crop model agreed well with the actual yield record when OCDs were assumed for the input climate data. The accuracy of the estimated yield, however, was quite poor when it was simulated based on present MCDs. The latter significantly underestimated the yield and failed to reproduce the spatial distribution of the yield. These results indicate that climate-model bias sometimes seriously reduces the accuracy of the crop model simulations.

The estimated change in yield until the 2070s was estimated using present and future OCDs, and another estimation of the yield change was obtained using present and future MCDs. These two estimations differ considerably, although the components of climate change until the 2070s are common in OCDs and MCDs. The difference in the yield change is caused by the difference in the baseline climate, i.e., the present climate, in OCDs and MCDs, which means that the crop model responds non-linearly to changes in climate variables. The yield estimation tends to be quite sensitive when one climate variable is near the threshold value assumed in the model. The present method not only reduces the model bias induced by the climate models but also suppresses error enhancement by the non-linearity of the crop model. As a result, this method allows the reliability of the estimation of future yield to be maintained more easily.

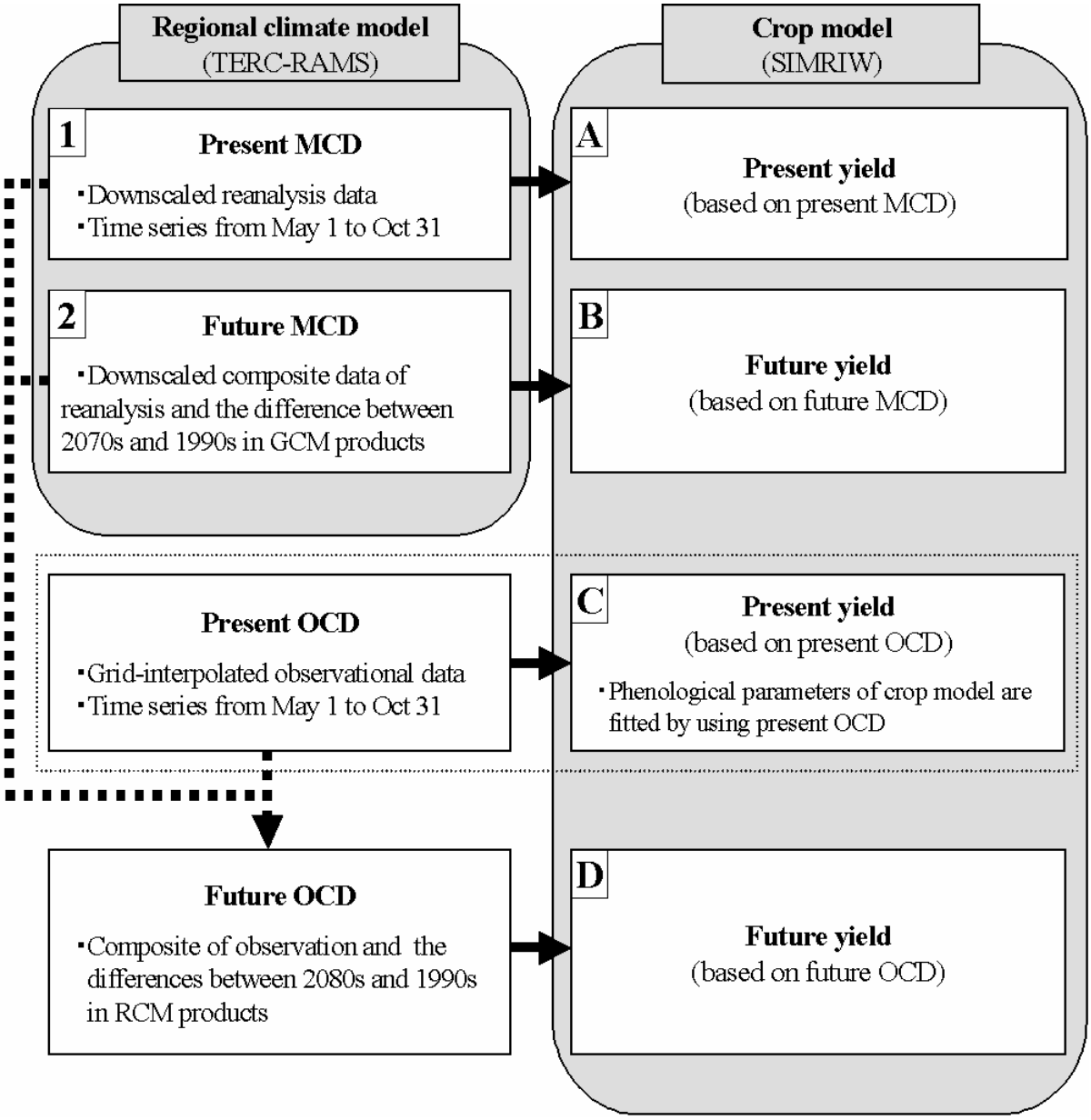

Figure 3.1: Relationship of two climate estimations by the RCM and four rice yield estimations by a crop model. OCD is the Observed Climate Dataset, while MCD is the Model output Climate Dataset (see Chapter 3.2.1). A solid arrow shows the climate data input to the crop model; a dotted arrow shows processing climate data for obtaining the future OCD.

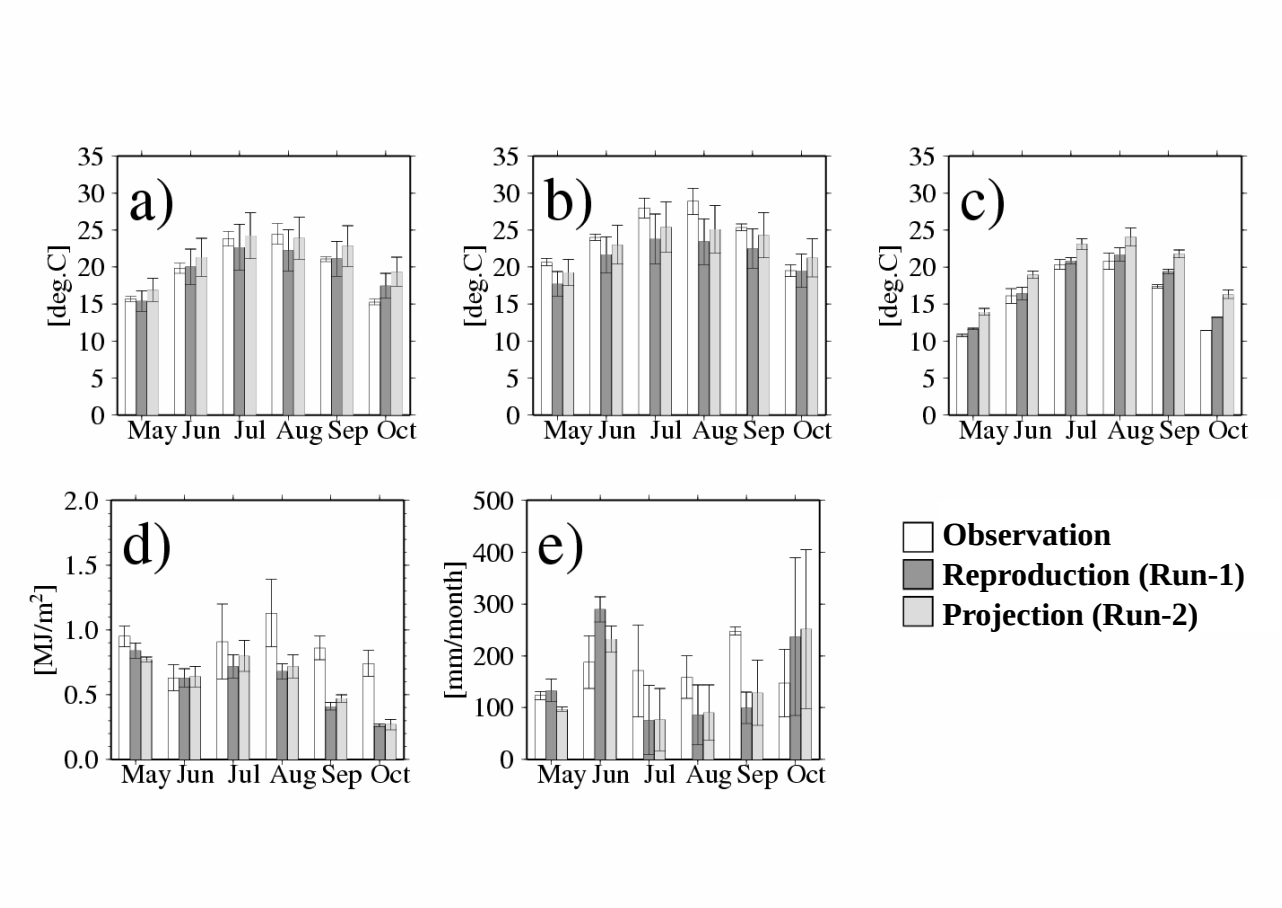

Figure 3.2: Two-year mean area means of five climate variables in observations, reproduction, and projection by the RCM. a) Monthly mean temperature. b) Monthly mean daily maximum temperature. c) Monthly mean daily minimum temperature. d) Monthly total precipitation. e) Monthly mean daily total solar radiation. The white bars correspond to the 2-year mean present OCD. The dark-gray bars and light-gray bars correspond to the reproduced present and future MCDs, respectively.

Climate-model bias

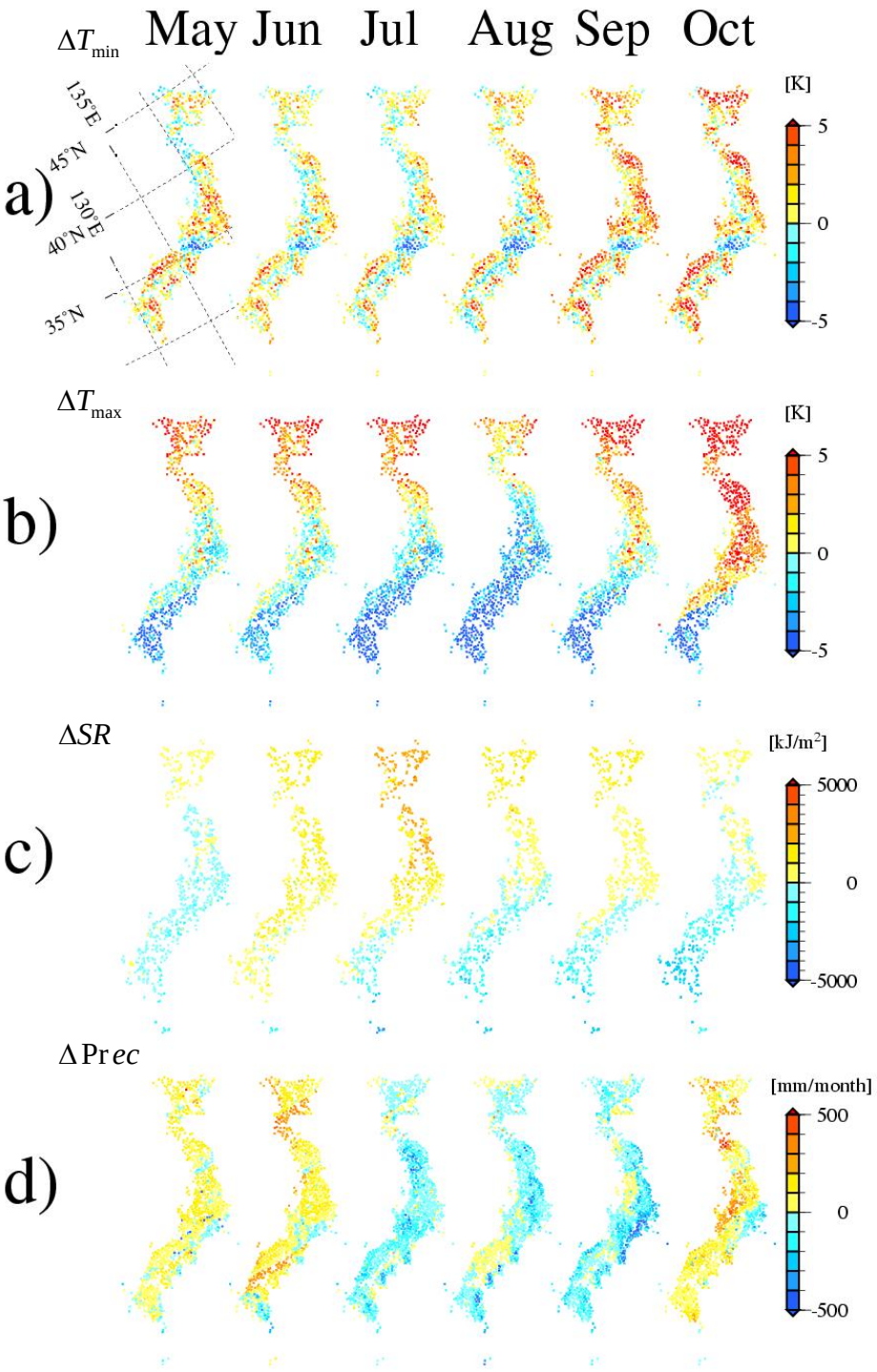

Figure 3.3: Differences in climate variables calculated by subtracting the present MCD from the present OCD. a) Monthly mean daily minimum temperature. b) Monthly mean daily maximum temperature. c) Monthly mean daily total solar radiation. d) Monthly total precipitation.

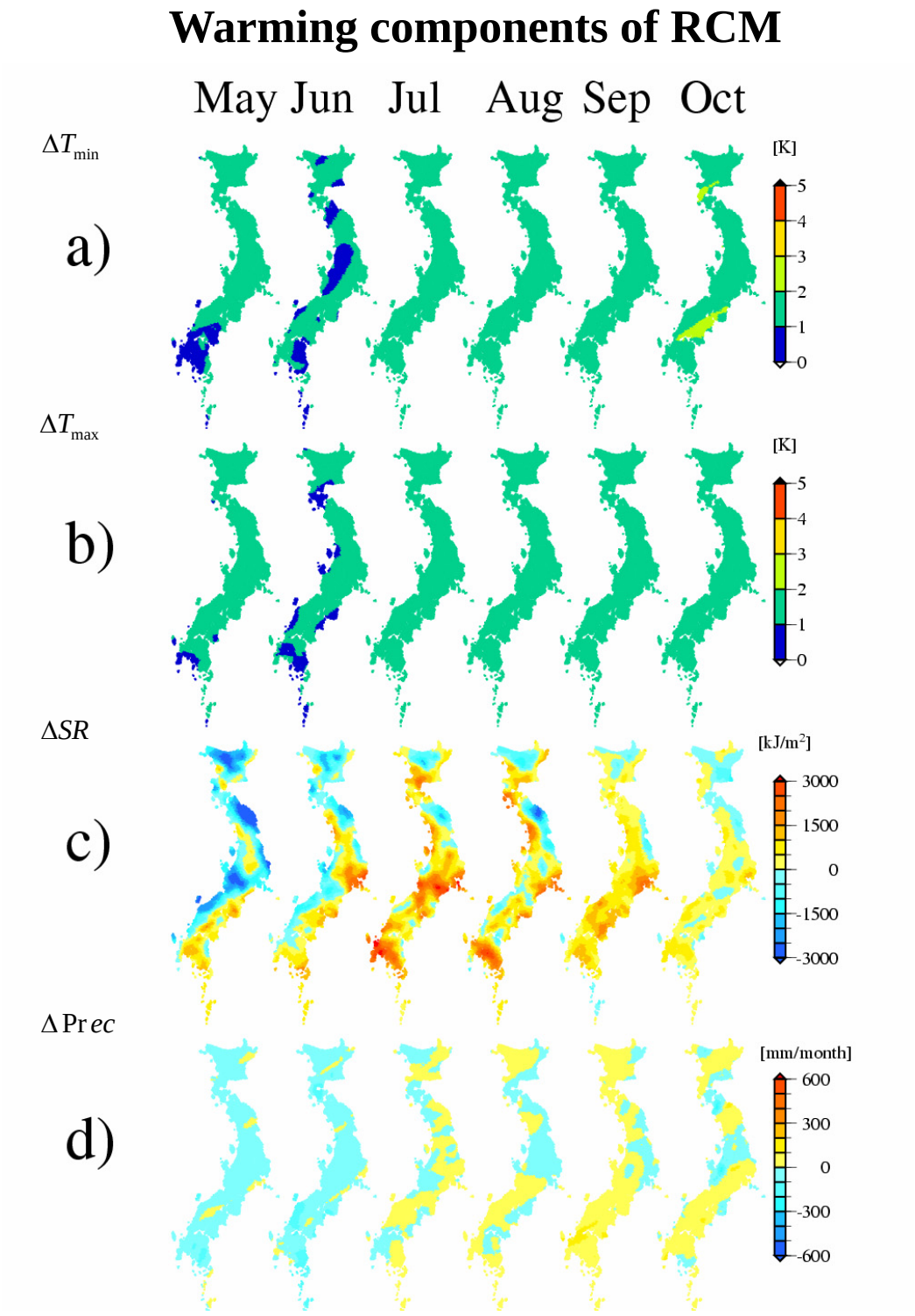

Figure 3.4: Changes in climate variables calculated by subtracting the present MCD from the future MCD. a) Monthly mean daily minimum temperature. b) Monthly mean daily maximum temperature. c) Monthly mean daily total solar radiation. d) Monthly total precipitation.

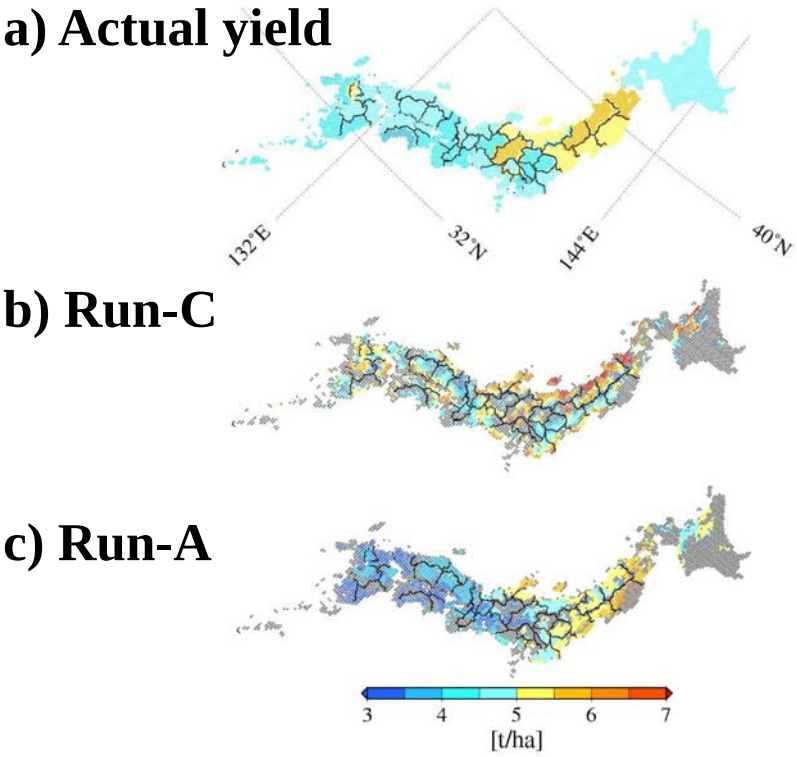

Figure 3.5: Comparison of two reproduced present yields versus the actual yield. Actual yield recorded in the crop statistics of each prefecture (top); estimated yield based on present OCD, which is the result of Run-C (middle); estimated yield based on present MCD, which is the result of Run-A (bottom). Gray area represents a non-paddy field. Solid line shows a prefectural border in Japan.

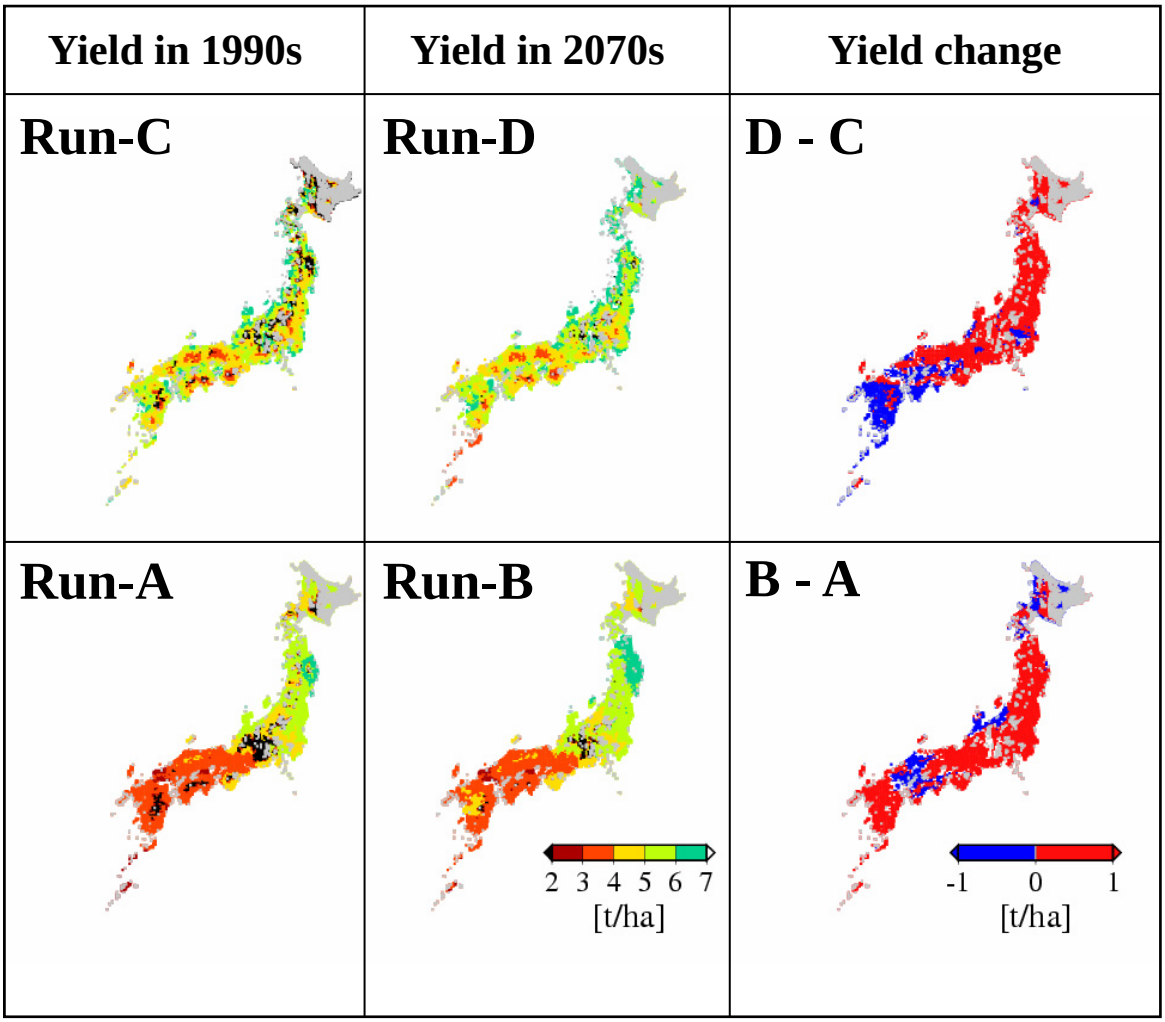

Figure 3.6: Simulated rice yield based on four climate data and their differences as yield changes due to global warming. Run-A, Run-B, Run-C, and Run-D correspond to the respective run names in Figure 1. The upper row shows the estimated present yields based on the present OCD (left), the future yield based on the future OCD (middle), and the projected yield change calculated from Run-C minus Run-D (right). The lower row shows the estimated present yields based on the present MCD (left), the future yield based on the future MCD (middle), and the projected yield change calculated from Run-B minus Run-A (right).

Table 3.1: Calculation conditions of the crop model

Breed type	1: Ishikari	4: Nipponbare
	2: Sasanishiki	5: Mizuho
	3: Koshihikari	
CO_2 concentration		330 ppm
Technical coefficient		1.00
Transplanting date		6 May - 10 Jul.
Initial development index		0.05 - 0.25
Initial leaf area index		0.01 - 0.1
Initial dry weight		10 - 20 g/m^2

Table 3.2: Spatial correlation coefficients of present OCD and present MCD

	Precipitation	Solar radiation	Mean temperature	Maximum temperature	Minimum temperature
May	0.152	0.233	0.547	0.351	0.596
Jun	0.198	0.451	0.511	0.330	0.620
Jul	0.047	0.234	0.446	0.378	0.426
Aug	0.003	0.211	0.369	0.252	0.401
Sep	0.062	0.292	0.669	0.373	0.511
Oct	0.052	0.248	0.632	0.361	0.406

4. Rice production in extreme weathers after global warming

4.1. Cool and hot summers

Antecedent impact projection studies only use the climatological mean condition in the future and present due to reliability limitations of GCMs. However, new dynamic downscaling methods are suggested to increase the reliability of GCM products, such as in Sato et al. (2006) and Misra and Kanamitsu (2004). They also use the GCM anomalies between the future and the present to reduce the GCM bias. Additionally, they estimate the regional-scale climate change by using a Regional Climate Model (RCM). In particular, the method suggested by Sato et al. (2006) allows us to estimate the regional-scale climate change in respective years. A new dynamic downscaling method has several limitations according to the use of climatological anomalies in the GCM and the capability of RCMs. For example, the method does not account for changes in inter-annual variability of future climates. Nevertheless, the method provides useful information for impact projection studies, such as changes in the spatial pattern of climate elements.

This chapter aims to show (1) the difference in the regional-scale climate change and (2) the influence on rice production between the cool summer year and the hot summer year after global warming.

4.2. Data and Methods

4.2.1 Use of climate data

We used the data of adjusted climate projection in current and pseudo years of 1993 and 1994, as the extreme years (relating to “adjusted climate projection”, see Chapter 2.2.2). The two years represent a typical cool summer year and a typical hot summer year in eastern Asia (Suh

and Lee, 2004) in the 1990s. Using the pseudo warming method, the synoptic condition of the simulated future year is very similar to that of the specific present year. Therefore, the simulated future year is called “pseudo-year”, and means a year after global warming that has very similar synoptic conditions to the present year.

4.2.2 Rice model simulations

The original version of SIMRIW was adapted. The rice model hindcasts the present yield when the model is based on a 330 ppm CO_2 concentration and observational climate datasets. The numerical experiment is named the “Yield-present-run”. The rice model projects the future yield when the model is based on a 550 ppm CO_2 concentration and the adjusted climate projection and this experiment is named the “Yield-warming-run”.

Despite its good capability, the SIMRIW has limited capability in climate acclimatization. The partial effect of climate acclimatization is included in the parameters regarding the phenology sub-model of the current model through the parameter optimization process. The current model implicitly considers the effect of climate acclimatization rather than explicitly. Thus, our simulation results have an uncertainty regarding the effect of climate acclimatization.

4.3. Results

4.3.1. Region-scale climate change over Japan as a result of global warming

Figure 4.1 shows the change in climate variables between the future and the present in the hot summer year, while Figure 4.2 shows the same changes but for the cool summer year. These changes are derived from the adjusted climate projection in Chapter 2.2.2. The following four changes in climate variables are shown as the warming components of the RCM: (a) the monthly mean daily minimum temperature ($\Delta T_{\min}$); (b) the monthly mean daily maximum temperature ($\Delta T_{\max}$); (c) the monthly mean daily total solar radiation (ΔSR); and, (d) the monthly total

precipitation ($\Delta Prec$).In the cool summer year after global warming (pseudo-year 1993), the monthly mean daily minimum temperature increases by 0.0 to 4.5 K throughout Japan from May to October. The increase is remarkable in northern Japan. The spatial patterns of the maximum temperature increase practically agree with those of the minimum temperature. And, the increase in the maximum temperature is smaller than that of the minimum temperature. The change in the monthly mean daily total solar radiation varies depending on month and area. Radiation decreases in northern Japan and increases in southwestern Japan from June to July. However, radiation increases in all of Japan in August and decreases in May. For September and October, the changes in radiation depend on area.

The change in monthly total precipitation also varies depending on the month and the area. Precipitation increases slightly in part of northern Japan in June and July. Precipitation tends to decrease in western Japan in September and October and increases in most of Japan in May. In the hot summer year after global warming (pseudo-year 1994), the monthly mean daily minimum temperature increases by 0.0 to 3.5 K throughout Japan in May. The minimum temperature increases 1.5 to 3.0 K from June to September, except for a greater increase in northern Japan. The minimum temperature increases by 2.0 to 4.0 K in October. The monthly mean daily maximum temperature shows the same spatial pattern as that of the minimum temperature. However, the increase in the maximum temperature is less than that of the minimum temperature from May through October. The monthly mean daily total solar radiation increases slightly in southwestern Japan and decreases in northern Japan from May to June. The radiation increases slightly over all of Japan from July to October, whereas the increase is less than 400 kJ/m^2. The change in monthly total precipitation varies depending on the month. Precipitation increases by 0 to 150 mm/month throughout most of Japan in May, July, August and October. Precipitation decreases slightly throughout Japan in June except for the area of facing Sea-of-Japan. Precipitation tends to decrease in northern Japan and increases in southwestern Japan in September.

The temperature increase in the hot summer year is slightly greater than that for the cool summer year. However, the increase in temperature in the cool summer year is greater that that

for the hot summer year in most target months in northern Japan. The minimum temperature increases are greater than the maximum temperature increases in both years. The changes in radiation are similar each year; i.e., radiation decreases in northern Japan from May to June but increases throughout Japan from July to October. Precipitation changes are different each year. Precipitation increases in southwestern Japan in May in the hot summer year and decreases in the cool summer year. Precipitation increases in most of Japan in May for both years. Precipitation changes show different spatial patterns from June to October. Precipitation tends to increase in southwestern Japan in the hot summer year, and decreases in this area in the cool summer year.

4.3.2. Global warming impact on rice growth and yield

Figure 4.3 shows the percentage of simulated change in yield formation elements, such as (a) the potential yield (PY); (b) the averaged daily maximum temperature during the flowering period ($\overline{T_{\max}}$); (c) the spikelet sterility (γ_c in the cool summer year and γ_h in the hot summer year); (d) the harvest index (h); and, (e) the total dry weight at maturity (W_t). These yield formation elements are shown for the two years, respectively.

In the cool summer year after global warming (pseudo-year 1993), the potential rice yield increases 5 to 50 percent throughout Japan as a result of global warming. However, the potential yield remains the same as that under the present climate condition in northern Japan. The area mean average daily maximum temperature during the flowering period increases by 1.82 K, caused by an increase in the maximum temperature shown in Figure 4.2. Spikelet sterility decreases by 50 percent in northern Japan and in the high altitude area of southwestern Japan as a result of a reduction in the damage from a cool summer. The change in the harvest index corresponds to the change in spikelet sterility. The harvest index increases in accordance with the decrease in spikelet sterility. The total dry weight of rice including roots increases throughout all of Japan.

In the hot summer year (pseudo-year 1994), the potential yield decreases by 5 to 20 percent in southwestern Japan. However, yield under the future climate condition continues to increase 5

to 50 percent in northern Japan, compared to the increase under the present climate condition. The area mean average daily maximum temperature during the flowering period increases by 2.89 K, as a result of the increase in the daily maximum temperature from July to August. Spikelet sterility increases by 40 percent throughout Japan except for northern Japan and in the high altitude area of southwestern Japan, as a result of heat stress. The harvest index decreases by 5 to 20 percent, caused by an increase in spikelet sterility and an increase in the average maximum temperature during the flowering period. However, the harvest index shows either an increase in the northern Japan. The total dry weight of rice including roots remains the same under the present climate condition in most of Japan. However, the total dry weight continues to increase in northern Japan.

Figures 4.4a and 4.4b show changes in total rice production in each agricultural area in the cool summer year and in the hot summer year. Figures 4.4c and 4.4d are the same as Figures 4.4a and 4.4b, but show mean rice yield. Total production is calculated assuming the same paddy acreage distribution as today. The land-use information is given by the DNLI.

In the cool summer year, the mean yield averaged over agricultural areas increases from 3.809 t/ha to 5.343 t/ha. The tendency for a yield increase is consistent across all areas, but the yield increase is significant in Hokkaido and Tohoku. Thus, the total production increases from 7.1×10^{6} t to 12.3×10^{6} t. On the other hand, in the hot summer year, the mean yield averaged over agricultural areas decreases from 4.990 t/ha in the present to 4.451 t/ha in a post-warming. Yield increases in Hokkaido, Tohoku, Kanto/Tozan, and Kyushu and decreases in Tokai, Kinki, Chugoku, and Shikoku. The yield in Kyushu, as well as the other areas in southwestern Japan (Figure 4.4), is affected by the increase in spikelet sterility caused by heat stress. However, the summation of a slight yield increase in the mountainous area is greater than the summation of the decrease in the lowland area. As the result of the change in yield, total production decreases from 11.9×10^{6} t in the present to 10.5×10^{6} t in a post-warming.

4.4. Discussion

The regional-scale climate change is projected by the dynamic downscaling method. This method allows us to obtain climate data under global warming conditions in respective years; i.e., the hot summer year and the cool summer year.

The projected regional-scale climate condition shows that the daily maximum and minimum temperatures increase by 0.0 to 4.5 K throughout Japan. In our simulations, the temperature increase in the hot summer year is slightly greater than the increase in the cool summer year. The cool summer year and the hot summer year changes to one with a moderate or slightly hot summer under present climate conditions and to one with an extremely hot summer under future climate conditions, respectively. Additionally, the climate change projection is also obtained for solar radiation and precipitation. The projected climate variables maintain their inter-variable relationships under physical laws within the limits of the climate model. Thus, our climate data progresses in the above point compared with the climate data obtained by variable-independent interpolation.

In the cool summer year, the monthly mean daily total solar radiation tends to increase slightly in most of Japan from July to August. These changes in climate conditions positively affect rice yield. The temperature increase obediently leads to an increase in the average maximum temperature during the flowering period. However, the daily maximum temperature increase remains moderate throughout Japan. Thus, the temperature increase causes a significant decrease in spikelet sterility in northern Japan, which has been suffering from damage caused by a cool summer in the present climate. Spikelet sterility decreases cause a direct increase in the harvest index. The total dry weight of rice including roots increases throughout Japan. As the result, the rice yield increases significantly in most of northern Japan as a result of a decrease in spikelet sterility. However, the yield increase is quite small in northern Tohoku and Hokkaido despite the decrease in spikelet sterility. In such areas, the damage due to a cool summer is found even in the year after global warming.

In the hot summer year after global warming, changes in climate conditions affect the rice yield both positively and negatively depending on the area. The average maximum temperature

increase obediently causes an increase in the maximum temperature during the flowering period. The daily maximum temperature increase causes a significant increase in spikelet sterility in central to southwestern Japan, as a result of heat stress. The increase in spikelet sterility causes a direct decrease in the harvest index. The total dry weight of rice including roots remains the same as under the present climate. As the result, the rice yield decreases in central to southwestern Japan because of the increase in spikelet sterility due to heat stress. However, the maximum temperature increase does not reach a critical level. The temperature increase and a slight solar radiation increase lead to a yield increase in northern Japan even in the hot summer year after global warming.

Damage from a cool summer is the most serious negative factor for rice production in northern Japan. The hazard is expected to lighten as a result of the temperature increase due to global warming. However, we notice the possibility of cool summer damage even after global warming by considering the inter-annual climate variability with paddy rice acclimatized to high temperatures. Additionally, the yield damage from heat stress is not found in southwestern Japan during the cool summer year after global warming. Yield damage by heat stress during the flowering period is expected to swell during the hot summer year after global warming. However, yield damage from heat stress is not found in northern Japan even in the hot summer year after global warming. These changes indicated that the hazard related to yield variability by climate condition shifts southward as a result of global warming.

4.5. Summary

This study updates the impact projection on rice production in Japan based on the dynamic downscaled MRI-CGCM2 products under the SRES-A2 scenario. The newly suggested dynamic downscaling method makes it possible to project the regional-scale climate change over Japan, and also allows us to extend the discussion to rice production hazards in the cool summer year and in the hot summer year after global warming.

The projected regional-scale climate changes are summarized as follows:

(1) The different changes in climate are found between the cool summer year and the hot summer year, although the boundary condition of the RCM in both years includes a common warming component of the GCM;

(2) In the cool summer year after global warming, the monthly mean daily maximum/minimum temperatures increase by 1.0 to 4.5 K throughout Japan. Additionally, the monthly mean daily total solar radiation slightly increases in the summertime over Japan, whereas radiation decreases in northern Japan in June and July;

(3) In the hot summer year after global warming, the monthly mean daily maximum/minimum temperatures increase by 0.0 to 4.0 K. The monthly mean daily total solar radiation shows an increase from July to October throughout Japan and a decrease in northern Japan from May to June.

The impact of region-scale climate changes on rice production is summarized as follows:

(4) The impact of global warming on rice production is different between the hot summer year and the cool summer year, and also varies by area.

(5) In the cool summer year after global warming, the temperature increase during the flowering period causes a spikelet sterility reduction derived from the damaged caused by a cool summer in northern Japan. Spikelet sterility reduction reflects the increase in the harvest index and leads to an increase in yield. The yield damage caused by heat stress is not found because the temperature increase remains at a moderate level in southwestern Japan;

(6) In the hot summer year after global warming, the temperature increase directly reflects the increase in the averaged daily maximum temperature over the flowering period. The temperature increase leads to a significant increase in spikelet sterility as well as a decrease in the harvest index. As the result, yield decreases in central and southwestern Japan while yield continues to increase in northern Japan;

(7) The hazard for yield variability by climate condition shifts southward as a result of global warming. The major hazard in the present climate, i.e. damage caused by a cool summer, is reduced in northern Japan. On the other hand, heat stress is enhanced, and becomes a new

serious hazard in central to southwestern Japan in the hot summer year.

Further study is required regarding estimating changes in frequency of the cool summer year and of the hot summer year after global warming based on GCM simulations. Another study is needed for impact projections based on the inter-annual variability of summer temperature simulated by the GCMs, as this study considers only the change in the mean climate and assumes that the inter-annual variability in the future climate is same as that in the present climate. Since our impact projection is based on one GCM, an ensemble of GCM products is required to improve the reliability of impact projection in future studies.

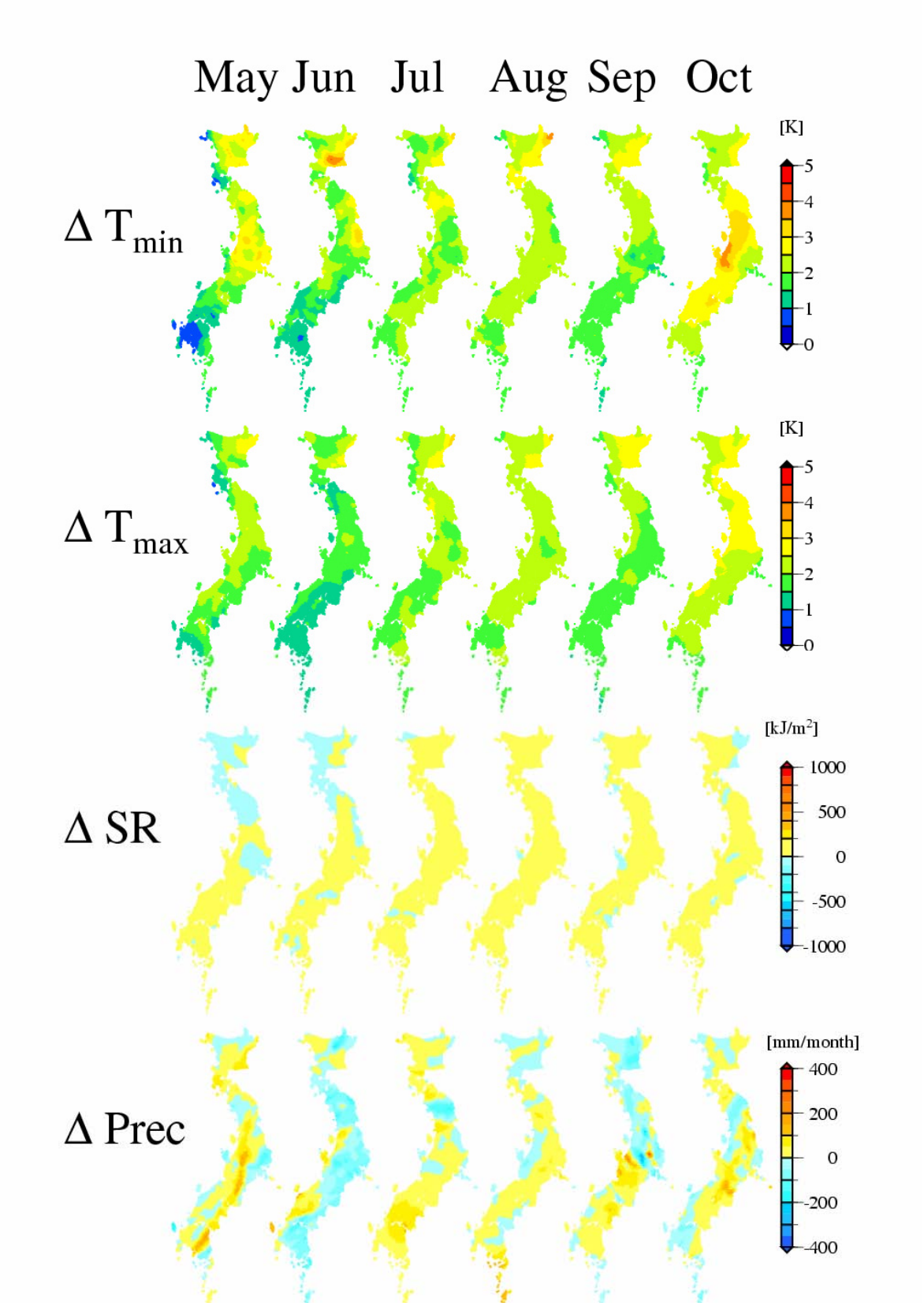

Figure 4.1: The warming components of the RCM (see in the Chapter 3.3.2) in the year with a hot summer.

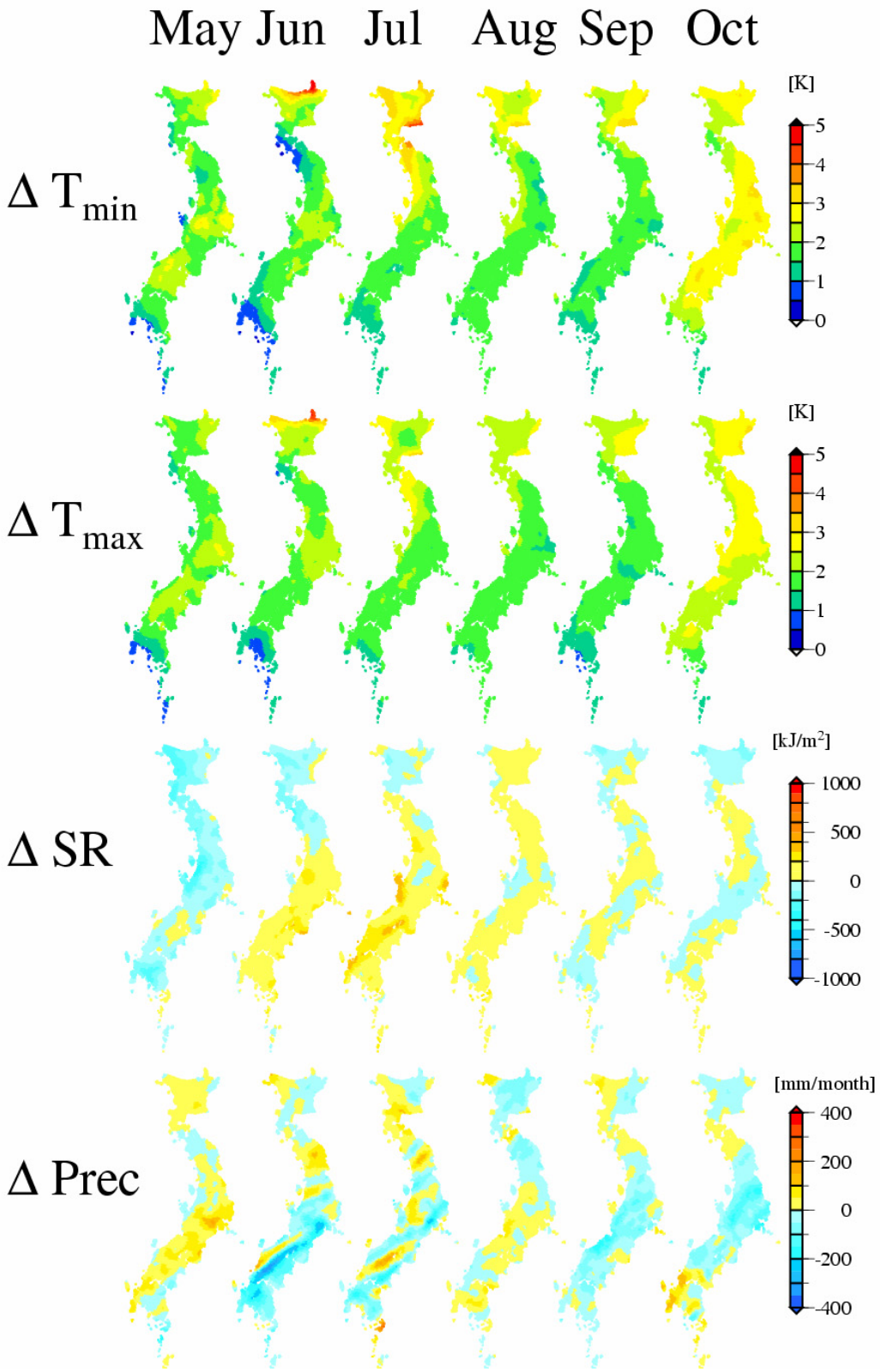

Figure 4.2: Same as Figure 4.1 but the year with a cool summer.

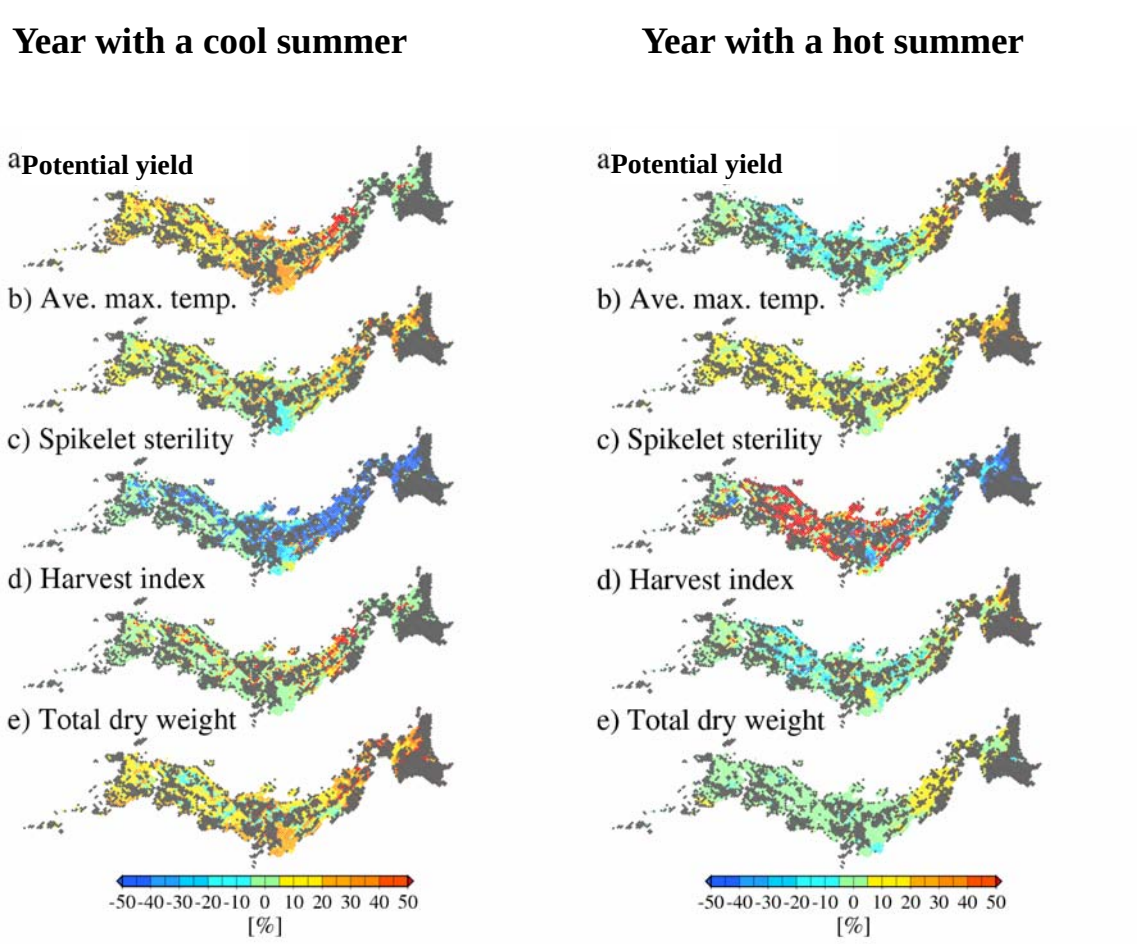

Figure 4.3: The percentage of change in the yield formation factors (see in the Chapter 2.3.1) in the year with a cool summer (left) and that with a hot summer (right).

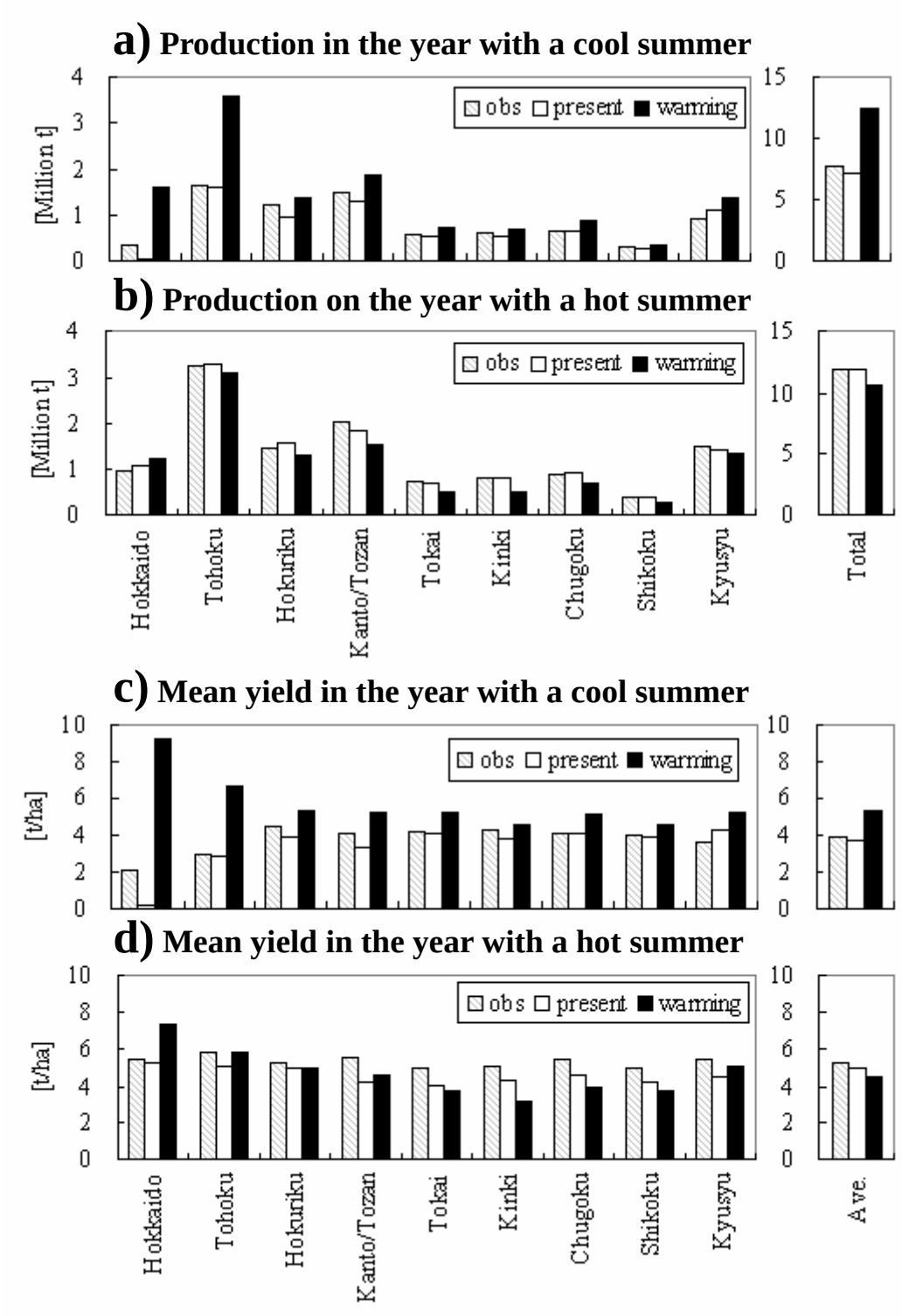

Figure 4.4: The simulated changes in the total rice production in the year with a cool summer (a) and that with a hot summer (b). Figure 4.4c and 4.4d are same with 4.4a and 4.4b but area mean of potential rice yield in agricultural area.

5. Economic assessment of global warming impact on rice production

5.1. Economic assessment

Rice production is frequently damaged by natural hazards, such as meteorological disasters, disease, and pests. Climate directly affects disease, pests, and other threats to rice production. Thus, climate is the most serious risk to agriculture. Crop insurance for rice, i.e. rice insurance, contributes to income stability in Japan and elsewhere (Ray, 1981; Hazell et al., 1986). Namely, rice insurance protects against climate risk even in the current climate. Farmers expect rice insurance to protect them even against global warming. However, global warming may influence rice insurance payouts through changes in production damage caused by natural hazards. Rice insurance payouts and premiums must be fairly balanced for robust management. Rice insurance is provided by the Japanese government, and, therefore, policymakers insist on having projections of potential payouts in the face of the threats from global warming. An objective of this study is to develop projections of the impacts of global warming on rice insurance payouts in Japan.

The crop model for rice used in this study has enough capability to assess the yield damage caused by cool summer and heat stress, which are the most serious threats in the current climate and after the global warming in Japan, respectively. However, although the rice insurance in Japan covers all damages caused by natural hazards, current crop models lack the capability to assess damage from disease, pests, and storms. Steady development is shown in the projection regarding disease and pests for rice that are caused by global warming (Yamamura et al., 2006); however, the accumulation is still insufficient for including such contributions to crop models as phenological parameterizations. Considering such limitations, a stochastic parameterization was developed as a yield damage assessment model. In spite of the limitation in our analysis framework relating to the lack of phenological parameterization in damage assessment, the

framework contributes to the presentation of a primary projection of global warming impact on the rice insurance payout.

5.2. Method

The analysis framework in this study was designed to project future rice insurance payouts after global warming in Japan (Figure 2.1). The framework was composed of the following four modules: (1) a climate-projection downscaling module that dynamically downscales global reanalysis datasets and GCM products to obtain regional high-resolution climate projections; (2) a yield estimation module that estimates the typical potential yield of paddy rice in a unit area by using daily weather datasets; (3) a yield damage-assessment module that estimates the yield damage caused by natural hazards; (4) a rice insurance payout projection module that simulates the insurance payout based on the estimated production and a long-term average production. The module details are described in Chapter 5.3.

5.3. Data and Models

5.3.1. Climate projection downscaling module

The adjusted climate projection was used for 10 years in 1990s and 2070s (from current and pseudo year 1991 to 2000). The detail can be seen in Chapter 2.2.

5.3.2. Rice yield estimation module

A modified version of SIMRIW was used as a Regional-scale Rice Model (RRM) and included into the analysis framework as the rice yield estimation module. The RRM simulates the rice yield in 10 years during 1990s and 2070s, respectively. The detail can be seen in Chapter 2.3.2.

5.3.3. Yield damage assessment module

Use of data regarding yield damage

The Regional Stochastic Damage Model (RSDM) was newly developed to supplement the RRM and included into the analysis framework as the yield damage assessment module. By coupling the RSDM with the RRM, it becomes possible to assess yield damages caused by not only cool summers and heat stress but also storms, disease, and pests.

The RSDM describes two kinds of relationships, one between weather conditions and yield damage caused by meteorological disasters, and the other between yield damage caused by meteorological disasters and that caused by disease and pests. The data regarding yield damage for the past 25 years, from 1979 to 2003, were obtained from the Crop Statistics. The governmental records include gross damaged acreage and gross damage due to 11 factors in each prefecture. The damage component includes four meteorological disasters, three diseases, three types of insects, and others, as shown in Table 5.1.

Both the net and gross yield damage is calculable from the record; however, there is a large disagreement between the net yield damage and the sum of the 11 types of gross damage. To correct the gross damage to the net one, the following process was conducted, in which the total yield damage in the *i* area and *j* year ($\Delta Y_{i,j}$) is defined by subtracting the 25-year mean yield ($\overline{Y_i}$) from the yield ($Y_{i,j}$) by

$$\Delta Y_{i,j} = Y_{i,j} - \overline{Y_i} . \qquad (5.3.3.1)$$

Since the $\Delta Y_{i,j}$ roughly corresponds to the net yield damage in the records, the relation $\Delta Y_{i,j} \cong a_i + b_i ND_{i,j}$ can be found, where a_i and $b_{,i}$ are the correction parameters in the *i* area; secondly, although the gross yield damage in the record tallies redundantly among damaging factors, the sum of the 11 types of yield damage should corresponds to the net yield damage after correction using the damaging factor weight (w_k). The w_k was estimated simply as the parameter of the multiple regression model given by

$$ND_{i,j} = w_0 + \sum_{k=1}^{n_3} w_k GD_{i,j,k} \quad (5.3.3.2),$$

where $ND_{i,j}$ and $GD_{i,j,k}$ are the net and gross yield damage of *i* area in *j* year caused by factor *k* and $n_3 = 11$. The estimated w_k is summarized in Table 5.1; then, the corrected yield damage for 25 years was obtained for each factor *k* in each prefecture.

Damage components regarding cool summer and heat stress

A cool summer is the most influential factor on rice yield, especially in northern Japan in the present climate, while heat stress is potentially the most influential factor in the central and southwestern areas after global warming. Even in current days, heat stress is observed in Chugoku, Shikoku, and Kyushu. Considering the importance and accumulation of studies relating to them, we adapted the phenological parameterization for cool summers and heat stress instead of the stochastic one. Details of the phenological parameterization can be found in Horie et al. (1995), Nakagawa et al. (2003), and Iizumi et al. (2007).

Damage component regarding storm

The corrected gross yield damage caused by storms ($GD_{i,j,1}$) is estimated by use of the multiple regression model given by Eq. 5.3.3.3.

$$GD_{i,j,1} = \beta_{0i} + \beta_{1i} PI_{i,j} + \beta_{2i} WI_{i,j}, \quad (5.3.3.3)$$

where β_{0i}, β_{1i}, and β_{2i} are the parameters in the *i* area. The model uses two climate indices, $PI_{i,j}$ and $WI_{i,j}$, defined by Eqs. 5.3.3.4 and 5.3.3.6, respectively.

$$PI_{i,j} = \sum_{m=DOI_b}^{DOI_h} P, \quad (5.3.3.4)$$

$$P = P\max_{i,j,m} - P_{0j} \quad , \quad (P\max_{i,j,m} > P_{0,i}),$$
$$P = 0 \quad , \quad (P\max_{i,j,m} \le P_{0,i}), \quad (5.3.3.5)$$

$$WI_{i,j} = \sum_{m=DOI_b}^{DOI_h} W, \quad (5.3.3.6)$$

$$\begin{cases} W = W\max_{i,j,m} - W_{0j} \quad , \quad (W\max_{i,j,m} > W_{0,i}), \\ W = 0 \qquad\qquad\qquad , \quad (W\max_{i,j,m} \le W_{0,i}). \end{cases} \tag{5.3.3.7}$$

These indices are given as follows: first, the values of daily maximum precipitation and wind speed ($P\max_{i,j}$ and $W\max_{i,j}$) above the thresholds ($P_{0,i}$ and $W_{0,i}$) are calculated at each calendar day; secondly, the values are accumulated throughout the influential period, yielding $PI_{i,j}$ and $WI_{i,j}$. The period of influence includes from the first day of the influence period (DOY_b) to harvest (DOY_h). The DOY_h is given by the phenological development sub-model in the RRM (Horie et al., 1995), whereas the DOY_b is fixed in each area. The DOY_b was optimized through the best-subset selection procedure on the basis of the corrected gross yield damage caused by storms and the observed climate dataset. The $P_{0,i}$ and $W_{0,i}$ were also optimized, as was the DOY_b.

The above parameters were estimated on the basis of the dataset in the odd years, and the estimated $GD_{i,j,1}$ was cross-validated with the corrected values in the even years. As a result of cross-validation, the mean value of the freedom-adjusted coefficient of determination (adj-R^2) among 46 prefectures was 0.527, with the RMSE of 0.143 t/ha.

Damage components regarding diseases and pests

Relating to disease and pests, yield damage is described by the linear regression model given by

$$GD_{i,j,k} = \alpha_{i,k} + \beta_{i,k} GD_{i,j,m}, \quad k = \{4,...,11\}, \quad m = \{1,2,3\}, \tag{5.3.3.8}$$

where $GD_{i,j,m}$ is the most influential meteorological damaging factor against gross yield damage caused by damaging factor *k* ($GD_{i,j,k}$). The suffix *m* in Eq. 5.3.3.8 is given as follows:

$$R_{k,m} = \max\left(R_{k,1}, R_{k,2}, R_{k,3}\right), \tag{5.3.3.9}$$

where $R_{k,m}$ is the adj.R^2 calculated by the gross yield damage of damaging factor k and that of meteorological disaster m. To fix the explanatory variable ($GD_{i,j,m}$) in the model, the matrix of adj.R^2 is prepared on the basis of the actual records of $GD_{i,j,k}$ and $GD_{i,j,m}$. One damaging factor is chosen among storms, heat stress, and cool summers as the most influential damaging factor m.

5.3.4. Rice insurance payout projection module

We adapted the concept of a simple insurance to project the rice insurance payout. The adapted model is frequently used and referred to in many studies, such as those by Ray (1967), Hazell et al. (1986), and Abbaspour (1994). The insurance payout in the *i* area in *j* year is given by two step procedure; firstly, the insurance-covered yield damage is given by Eq. 5.3.4.1, the modified Eq. 5.3.3.1,

$$\Delta Y_{i,j} = Y_{i,j} - \phi\overline{Y_i}\,, \tag{5.3.4.1}$$

where ϕ is the insurance coverage. The actual value of ϕ ranges from 0.7 to 1.0 in the rice insurance of Japan (Tsujii, 1986), while it takes unity in this study. Secondly, the insurance payout is given as follows,

$$L_{i,j} = A_{i,j} \times \mathrm{Pr}\,ice \times \Delta Y_{i,j}\,, \tag{5.3.4.2}$$

where $L_{i,j}$ is the rice insurance payout, $A_{i,j}$ is the planted acreage of paddy rice, and $\mathrm{Pr}\,ice$ is the mean price of rice in the 1990s. The value of $\mathrm{Pr}\,ice$ corresponds to 257,000 yen/t and was obtained by the actual crop insurance of Japan, which is called “mutual relief” (Tsujii, 1986; Iizumi, 2005).

Since the economic value of rice in a country varies depending on the changes in economic factors, i.e., demand, supply, exports, and imports, any future economic value of rice may be unequal to the present one. From such difficulty in future economic projection, simulated future insurance payouts are expressed by the economic value of rice in the 1990s.

5.4. Results

5.4.1. Changes in phenology and yield caused by global warming

Figure 5.1 shows the average of simulated rice phenological response to changes in regional climate over nine years. Figure 5.1a shows the Cooling Degree Days (CDD), i.e. an index of cooling stress, for the most sensitive period for the rice panicle to cool temperature (Horie et al., 1995), and the value decreases throughout Japan. On the other hand, Figure 5.1b shows the daily

maximum temperature averaged over the flowering period (Nakagawa et al., 2003), which also heavily affects the spikelet sterility in rice, and the value is shown to increase by 0.5 ^{o}C to 2.5 ^{o}C throughout Japan. Changes in both the CDD and the daily maximum temperature averaged over the flowering period are directly caused by the increase of temperature.

Figure 5.1c displays the dry weight, including roots at maturity, which can be used as the index of change in solar radiation during the growth period. The dry weight decreases in northern Japan, whereas it shows mixed responses depending on the area in the southwest. A different response in the dry weight between the north and southwest is derived from the change in the growth period and from that in solar radiation. The growth period, which is the time from planting to harvest, is shortened by more than 14 days in northern Japan and by 3 to 9 days in the southwest (Figure 5.1d and 5.1e), while the solar radiation increases in July to August in most of Japan (no figure). The shortening of the growth period is caused by the acceleration in the phenology development derived from the increase of the daily mean temperature.

Figure 5.2 shows the changes in yield damage caused by meteorological disasters, disease, and pests. The yield damage caused by storms, shown in Figure 5.2a, slightly increases in parts of Tohoku, Kanto, Kinki, Chugoku, and Kyushu. The yield damage caused by heat stress (Figure 5.2b) significantly increases in most areas, with some exceptions, such as the Pacific side of Tohoku and Hokuriku, while that caused by cool summers decreases remarkably in Hokkaido and Tohoku (Figure 5.2c). The yield damage caused by disease and pests (Figure 5.2d and 5.2e) changes mainly in parallel with the change in damage caused by storms and cool summers.

Figure 5.3 shows the 10-year-averaged changes in the mean yield and the Coefficient of Variance (CV) from the 1990s and 2070s, meanwhile the CV is defined by $CV = \sigma / \mu$ where σ is the standard deviation of yield during nine years and μ is the 10-year mean yield; these changes are summarized in Table 5.2 for each agricultural area. The mean yield shows mixed responses, and the yield increases in Hokkaido and Tokai. Furthermore, it shows a reduction in Tohoku, Hokuriku, and Kinki. The CV in yield decreases in Hokkaido, Tohoku, Hokuriku, Shikoku, and Kyushu but increases in Kanto, Tokai, and Kinki.

5.4.2. Projected change in rice insurance payout

The changes in the yield are recalculated as the insurance payouts (Table 5.3). In the estimation of insurance payouts, the distribution of paddy acreage in the 2070s was assumed to be same as that in the 1990s. The data regarding paddy acreage was given from the DNLI for each prefecture.

The mean insurance payout averaged over nine year decreases in most agricultural areas, with the exceptions of the increase observed in Kanto/Tozan and Kinki. However, the increase is considerably smaller than the decrease in the other areas. The increases in the mean insurance payout in Kanto/Tozan and Kinki are 474 and 30 million yen, respectively, while the decrease in the other areas ranges from 28 million yen in Tokai to 8,596 million yen in Hokkaido. The simulated total insurance payout decreases as a result of global warming from 3.18 billion yen in the 1990s to 2.24 billion yen in the 2070s.

The CV of the insurance payout for nine years increases in the four areas, i.e., Hokkaido, Hokuriku, Kinki, and Shikoku, while it decreases in five other areas. The increase in the CV ranges from 0.065 in Shikoku to 0.381 in Hokkaido, while the decrease ranges from 0.007 in Chugoku to 0.176 in Kyushu. The mean change in the CV averaged over all areas increases from 1.617 in the 1990s to 1.667 in the 2070s.

5.5. Discussion

5.5.1. Comparison with previous projections (mean yield)

Previous studies have simulated a significant increase in yield in Tohoku (Toritani et al., 1999; Nakagawa et al., 2003), whereas our results show a slight decrease. A significant increase is found in the simulated yield in years with cool summers, such as 1991 and 1993, in our simulation (Iizumi et al., 2007); however, the yield decreases in years without cool summers because of the shorter growth periods. Such differences between the previous projections and our

results are due to the assumption of adaptation and the climate data described in the next subsection.

Rice yields are sensitive to heat and cold during heading, which occurs from middle July to early August in Japan. Especially, rice yield drastically decreases when the panicle rice is exposed to the conditions of both high temperature and high CO_2 concentration (Kim et al., 1996; Nakagawa et al., 2003). Regarding such responses in rice, consistent results with previous projections were found in the decrease of yield damage caused by cool summers and the increase of damage due to heat stress.

Rice yields also decrease because of a reduction in the total biomass, and the response is evident in the model. A rapid development in rice is induced by an increase in the daily mean temperature, which results in a shorter growth period. The shorter growth period results in a reduction in the accumulation of solar radiation during the period, and such a response decreases the volume of the biomass. Although the change in solar radiation due to global warming is responsible for the biomass, the change in the growth period is more critical than that in solar radiation. Such rice responses can be found from the simulation results regarding the dry weight and maturity day.

Toritani et al. (1999) assumed an adaptation technique in which the planting day was moved ahead approximately two weeks from that currently applied. Our projection assumes no adaptations; thus, the shortened growth period causes the decrease of the yield in northern Japan. In addition, the difference in projection is due to the emission scenarios and GCMs. Nakagawa et al. (2003) shows four projections of mean yield change in the 2090s under IS92a scenario. Those projections use on the four GCM products i.e., CCSR/NIES (Emori et al., 1999), CGCM1 (Flato et al., 2000), CSIRO-Mk2 (Watterson et al., 1997), and ECHAM/OPY3 (Roeckner et al., 1992; Oberhuber et al., 1998). While three of the four projections in Nakagawa et al. (2003) show similar changes in yield as the projection of Toritani et al. (1999), the one of the four projections, ECHAM/OPY3, is relatively consistent with our simulation result.

5.5.2. Comparison with previous projections (interannual variability)

Nakagawa et al. (2003) present the CV of the yield in the 2090s in Japan based on the climate projection of the CCSR/NIES (Emori et al., 1999). There are considerable differences between the findings of Nakagawa et al. (2003) and our own. Especially, large differences were found in Tohoku, Hokuriku, Kinki, and Kyushu. Nakagawa et al. (2003) project a large increase of the CV in the above areas, while our result simulates a slight decrease.

The difference in the projected CV is mainly due to the climate data. The data used in the work of Nakagawa et al. (2003) is the composition of the sum of monthly mean anomalies and the climatological mean observed dataset, and the data assumes no change in the interannual variability in climate elements. In addition, these anomalies were obtained as a result of an interpolation technique (Yokozawa et al., 2003). On the other hand, the climate data in this study were obtained by the dynamic downscaling method. The results of dynamic downscaling show that the resultant increase of temperature in summer caused by global warming differs from year to year.

In our simulation, the interannual variability of the yield is smaller in northern Japan. Since the damage caused by cool summers seriously affects the yield in this area, the yield reduction under warming conditions is mitigated in comparisons with that in the present. The yields in the years without cool summers increase slightly as a result of increases in temperature and solar radiation or decrease slightly as a result of the shorter growth period. Such changes in the yield were found as a reduction in the interannual variability. On the other hand, in southwestern Japan, the interannual variability of the yield becomes smaller, as it does in northern Japan. Since there is no serious damage due to cool summers in the area, the yields in the years with cool summers or normal years decrease as a result of the shorter growth period, while the yields in the years with hot summers decrease as a result of heat stress. Both decreases in yield were found as a reduction in interannual variability. As a result of such yield responses to global warming, the interannual variability of the yield is reduced in six of the nine agricultural area in Japan, i.e., Hokkaido, Tohoku, Tokai, Chugoku, Shikoku, and Kyushu. In contrast, the interannual variability of the yield is enhanced in three of nine agricultural area, i.e., Hokuriku, Kanto/Tozan,

and Kinki.

5.5.3. Inconsistency of changes between yield and insurance payout

There is an inconsistency between the change in the yield and that in the insurance payout. The mean yield decreases in all areas except Hokkaido and Tokai, whereas the mean insurance payout increases only in Kanto/Tozan and Kinki. In addition, the CV of the yield increases in Hokuriku, Kanto/Tozan, and Kinki, whereas that of the insurance payout increases in Hokkaido and Shikoku as well as in Hokuriku and Kinki.

Such inconsistency is derived from the calculation method of rice insurance used to estimate the insurance payout. The insurance payout in this study is calculated by using ΔY, ϕ, and $\mathrm{Pr}ice$, and only ΔY varies throughout the years. Since $\overline{Y}$ changes according to the year-to-year changes in the yield, $\overline{Y}$ in the present is different from that in the warming condition. If Hokkaido is taken as an example, the decrease in yield caused by a cool summer is reduced by warming. However, the degree of the decrease from the $\overline{Y}$ in the warming condition is still large by the symmetric decrease of $\overline{Y}$. Since yield anomalies are small in a year without a cool summer, the CV of an insurance payout increases, whereas that of the yield decreases in Hokkaido.

On the other hand, a different response can be found in Shikoku. The mean and the CV of the yield both decrease in the area, while the mean insurance payout decreases, and the CV increases. The inconsistency is due to the relatively heavy decrease caused by heat stress from the $\overline{Y}$ in the warming condition. In other areas, the increase/decrease of the mean and the CV in yield are consistent with those in the insurance payout.

5.6. Summary

The analysis framework, namely, the combination of various models, is prepared to project the rice insurance payout in Japan caused by global warming under the SRES-A2 scenario. The

simulation results show slight decreases of the mean and interannual variability in yield in most areas of Japan under the no adaptation condition. On the other hand, the simulations show results according to which the projected insurance payout decreases in mean but increases in the interannual variability in most areas. Again, the insurance payout significantly decreases accompanying an increase in interannual variability, although the yield decreases in both mean and interannual variability. Their inconsistency is derived from the calculation method of rice insurance payout. The results suggest that the global warming impact in crop production is not necessarily parallel to that in the economic institution.

The simulation results also show that there is a difference in the change caused by global warming among areas even in a country. The result suggests that the change in the economic role of each agricultural area may emerge accompanying a shift of the main source area and a change in the stability of rice production after global warming. Agricultural production is also affected by such indirect impact of global warming as well as direct change in climatic resources.

To apply our analysis framework to other Asian countries, further improvements are required relating to the following issues: the inclusion of water resource models for application to non-irrigated areas and arid/semi-arid areas; and the inclusion of anthropologic effects in farm management into the yield damage assessment model, which is quite important, especially in developing countries.

Our results are based on only one climate scenario projected by the MRI-CGCM2 under the SRES-A2 scenario. Other SRES scenarios, such as A1b, possibly give another impact to the rice production and insurance payout in Japan. The projected change in climate strongly depends on GCMs as well as emission scenarios; thus, the adoption of other GCM products is expected to improve the reliability of our projection.

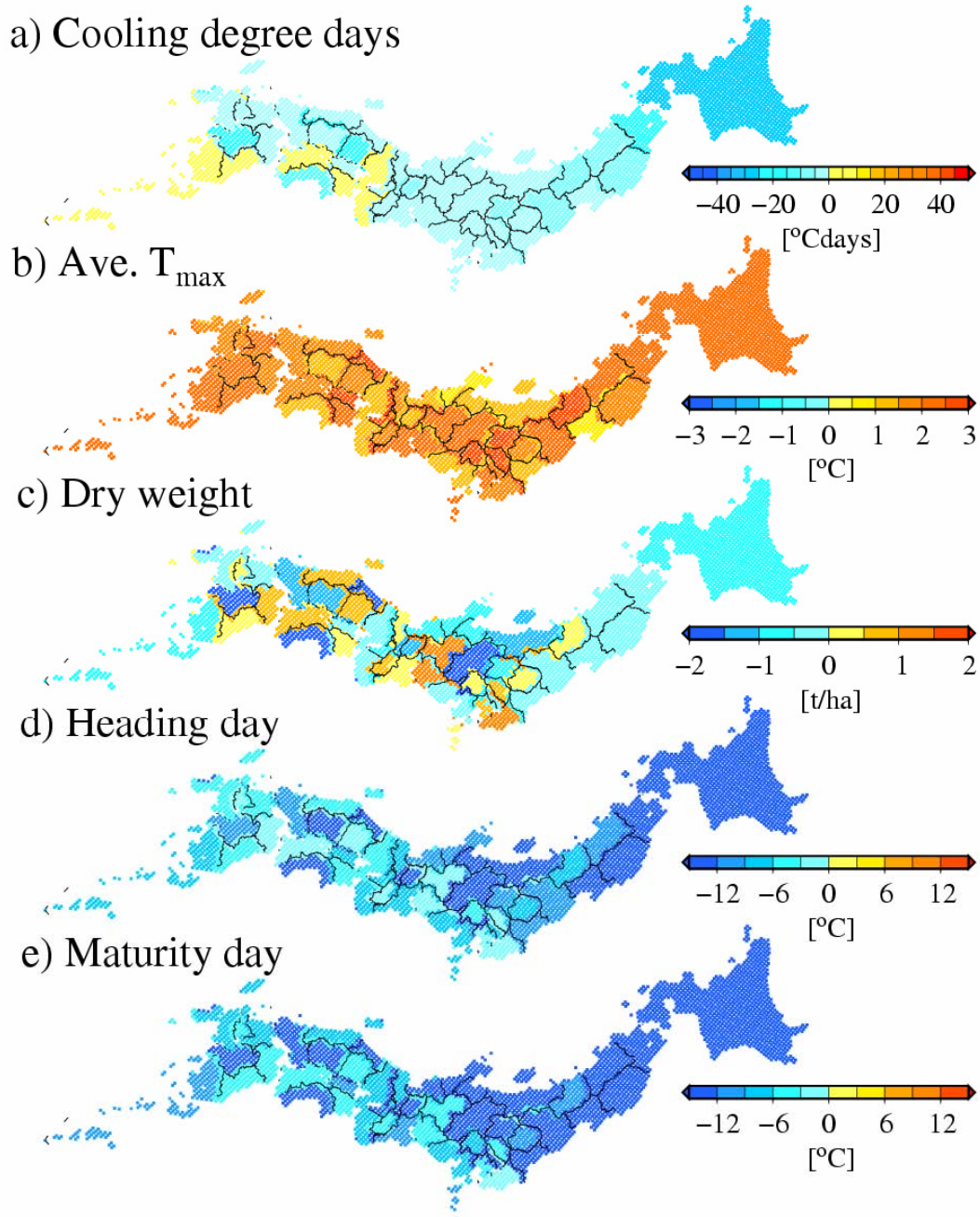

Figure 5.1: Spatial changes in regional climate found through the RRM and phenological responses i.e., (a) cooling degree days during the most sensitive period for the rice panicle, (b) daily maximum temperature averaged over the flowering period, (c) dry weight, including roots, at maturity day, (d) heading day, and (e) maturity day.

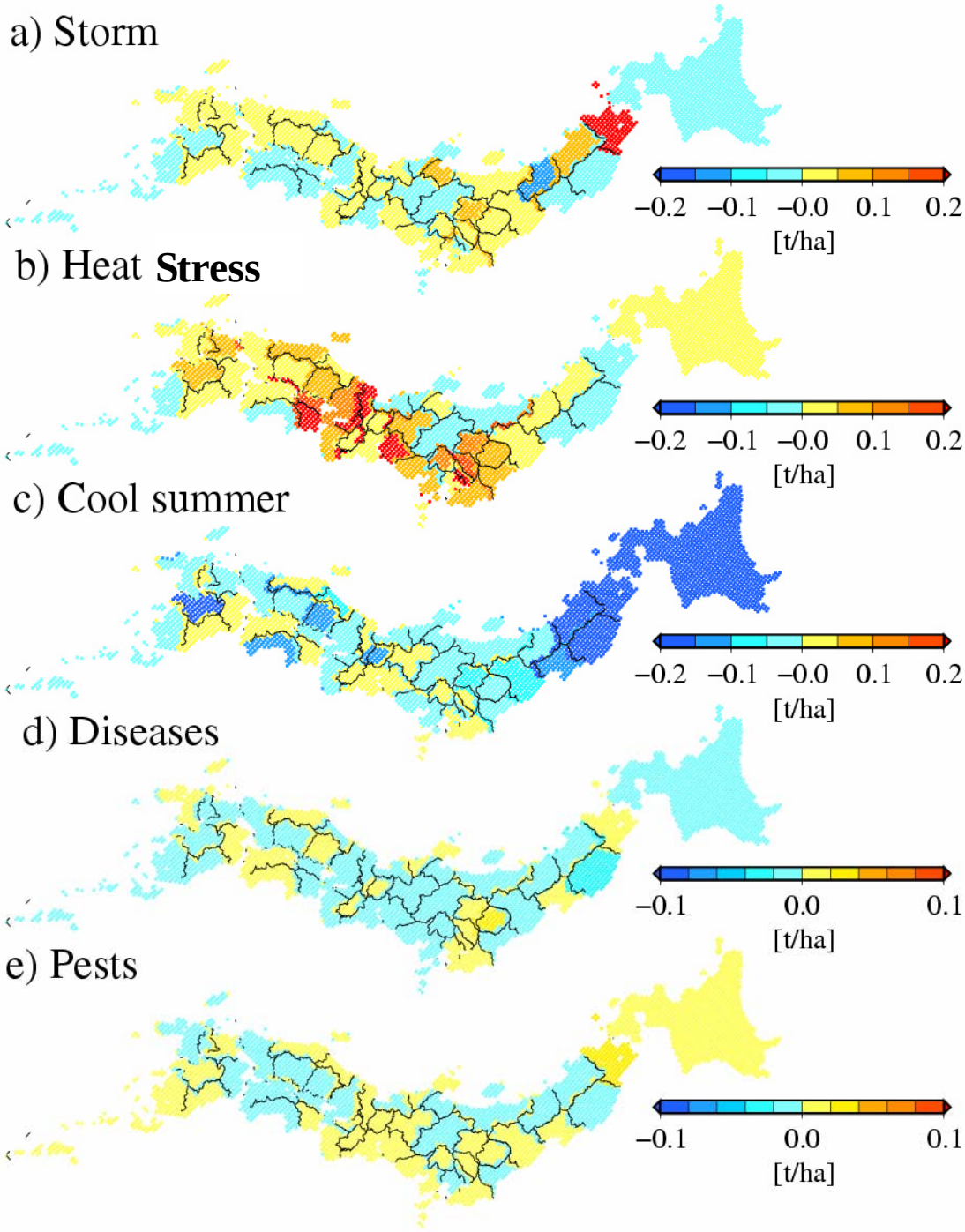

Figure 5.2: Spatial changes in yield damages caused by storms (a), heat stress (b), cool summers (c), disease (d), and pests (e).

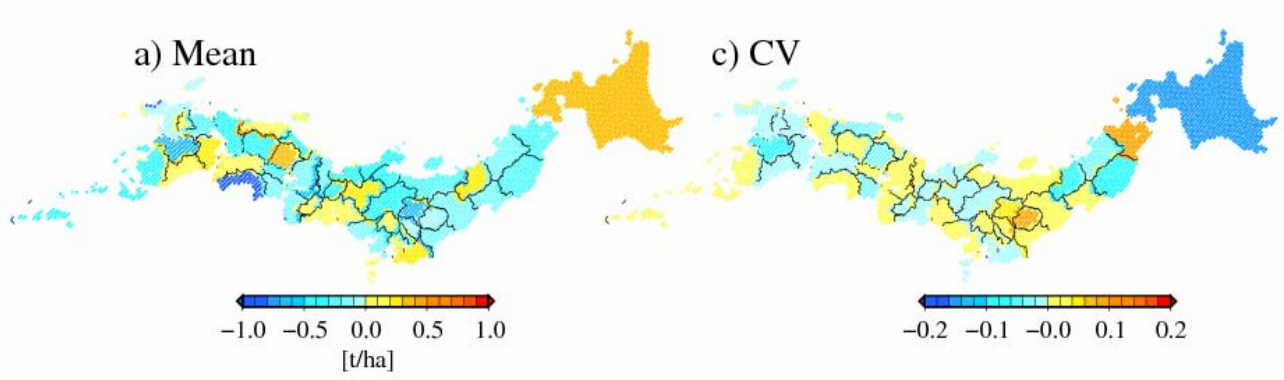

Figure 5.3: Spatial changes in the mean (a) and CV (b) of the yield.

Table 5.1: Estimated parameters in the multiple regression model given by Eq. 5.3.3.2. The two-tailed significance levels are denoted by asterisks, e.g., 0.1%, ***; 1%, **; and 5%, *.

Parameter	Damaging factor		Estimate	SE	P-value	
W_0	-	-	-0.023	0.010	0.022	*
W_1	Meteological	Storm	0.319	0.021	0.000	***
W_2	disasters	Heat stress	0.012	0.008	0.145	
W_3		Cool summer	0.318	0.010	0.000	***
W_4		Other meteorological disaster	0.010	0.009	0.282	
W_5	Diseases	Rice blast	0.264	0.025	0.000	***
W_6		Sheath blight	0.108	0.051	0.034	*
W_7		Other diseases	0.028	0.032	0.375	
W_8	Pests	Small brown planthopper	0.086	0.024	0.000	***
W_9		Rice stem border	0.071	0.051	0.165	
W_{10}		Other pests	0.258	0.058	0.000	***
W_{11}		Other	0.023	0.016	0.150	

Table 5.2: Changes in the mean and CV of the yield over nine years caused by global warming

	Yield			
	Mean [t/ha]		CV	
	Present	Warming	Present	Warming
Hokkaido	3.891	4.270	0.255	0.100
Tohoku	4.530	4.405	0.162	0.150
Hokuriku	4.675	4.312	0.105	0.110
Kanto/Tozan	4.470	4.330	0.094	0.112
Tokai	4.320	4.377	0.087	0.087
Kinki	4.171	3.966	0.080	0.093
Chugoku	4.623	4.497	0.106	0.098
Shikoku	4.176	3.907	0.119	0.116
Kyushu	4.366	4.243	0.145	0.131
Ave.	4.358	4.256	0.128	0.111

Table 5.3: Changes in the mean and CV of rice insurance payouts over 10 years caused by global warming

	Rice insurance payout			
	Mean [million yen]		CV	
	Present	Warming	Present	Warming
Hokkaido	13313	4717	2.005	2.386
Tohoku	6105	5614	1.900	1.836
Hokuriku	2282	2184	1.363	1.480
Kanto/Tozan	2254	2728	1.591	1.542
Tokai	1406	1378	1.666	1.628
Kinki	958	988	1.579	1.796
Chugoku	1862	1672	1.362	1.355
Shikoku	1056	964	1.426	1.491
Kyushu	2517	2202	1.666	1.490
Total	31755	22447	-	-
Ave.	3528	2494	1.617	1.667

6. Conclusions

In Chapter 3, a rice yield simulated by the crop model agrees well with the actual yield record when OCDs were assumed for the input climate data. The accuracy of the estimated yield, however, was quite poor when it was simulated based on present MCDs. The latter significantly underestimated the yield and failed to reproduce the spatial distribution of the yield. These results indicate that climate-model bias sometimes seriously reduces the accuracy of the crop model simulations.

The estimated change in yield until the 2070s was estimated using present and future OCDs, and another estimation of the yield change was obtained using present and future MCDs. These two estimations differ considerably, although the components of climate change until the 2070s are common in OCDs and MCDs. The difference in the yield change is caused by the difference in the baseline climate, i.e., the present climate, in OCDs and MCDs, which means that the crop model responds non-linearly to changes in climate variables. The yield estimation tends to be quite sensitive when one climate variable is near the threshold value assumed in the model. The present method not only reduces the model bias induced by the climate models but also suppresses error enhancement by the non-linearity of the crop model. As a result, this method allows the reliability of the estimation of future yield to be maintained more easily.

In Chapter 4, this study updates the impact projection on rice production in Japan based on the dynamic downscaled MRI-CGCM2 products under the SRES-A2 scenario. The newly suggested dynamic downscaling method makes it possible to project the regional-scale climate change over Japan, and also allows us to extend the discussion to rice production hazards in the cool summer year and in the hot summer year after global warming.

The projected regional-scale climate changes are summarized as follows:

(1) The different changes in climate are found between the cool summer year and the hot summer year, although the boundary condition of the RCM in both years includes a common warming component of the GCM;

(2) In the cool summer year after global warming, the monthly mean daily maximum/minimum

temperatures increase by 1.0 to 4.5 K throughout Japan. Additionally, the monthly mean daily total solar radiation slightly increases in the summertime over Japan, whereas radiation decreases in northern Japan in June and July;

(3) In the hot summer year after global warming, the monthly mean daily maximum/minimum temperatures increase by 0.0 to 4.0 K. The monthly mean daily total solar radiation shows an increase from July to October throughout Japan and a decrease in northern Japan from May to June.

The impact of region-scale climate changes on rice production is summarized as follows:

(4) The impact of global warming on rice production is different between the hot summer year and the cool summer year, and also varies by area.

(5) In the cool summer year after global warming, the temperature increase during the flowering period causes a spikelet sterility reduction derived from the damaged caused by a cool summer in northern Japan. Spikelet sterility reduction reflects the increase in the harvest index and leads to an increase in yield. The yield damage caused by heat stress is not found because the temperature increase remains at a moderate level in southwestern Japan;

(6) In the hot summer year after global warming, the temperature increase directly reflects the increase in the averaged daily maximum temperature over the flowering period. The temperature increase leads to a significant increase in spikelet sterility as well as a decrease in the harvest index. As the result, yield decreases in central and southwestern Japan while yield continues to increase in northern Japan;

(7) The hazard for yield variability by climate condition shifts southward as a result of global warming. The major hazard in the present climate, i.e. damage caused by a cool summer, is reduced in northern Japan. On the other hand, heat stress is enhanced, and becomes a new serious hazard in central to southwestern Japan in the hot summer year.

In Chapter 5, the analysis framework, namely, the combination of various model, is prepared to project the rice insurance payout in Japan caused by global warming under the SRES-A2 scenario. The simulation results show slight decreases of the mean and interannual variability in yield in most areas of Japan under the no adaptation condition. On the other hand,

the simulations show results according to which the projected insurance payout decreases in mean but increases in the interannual variability in most areas. Again, the insurance payout significantly decreases accompanying an increase in interannual variability, although the yield decreases in both mean and interannual variability. Their inconsistency is derived from the calculation method of rice insurance payout. The results suggest that the global warming impact in crop production is not always proportion to that in the economic institution.

The simulation results also show some differences in the change by global warming among areas even in a country. The result suggests that the change in the economic role of each agricultural area may emerge accompanying a shift of the main source area and a change in the stability of rice production after global warming. Agricultural production is also affected by such indirect impact of global warming as well as direct change in climatic resources.

From the multidisciplinary standpoints, this study concludes that (1) assessment of global warming impact requires the reduction of climate-model bias to achieve reliable projection for policymakers; (2) disturbance of climate-model bias on impact assessment indicates that no meaningful projections can result from the simple coupling of response models with climate models; (3) the global warming causes the change in the rice insurance payout as well as the rice production. However change in the insurance payment is caused not only by production change due to climate change but also institutional design itself. Thus, simple parameterization relating to economic damage and climate change has no meaning. Increase of temperature causes increase of economic loss in some area. However it also causes decrease of economic loss in another area; (4) change in crop productivity and production stability results from global warming in Japan. It suggests a shift of main agricultural source area due to the economic factors as well as climatic resources.

Further study is required regarding estimating the change in frequency in the cool summer year and in the hot summer year after global warming based on GCM simulations. Another study is needed for impact projections based on the inter-annual variability simulated by the GCMs, as this study considers only the change in the mean climate and assumes that the inter-annual variability in the future climate is same as that in the present climate. Since our impact projection

is based on one GCM, an ensemble of GCM products is required to improve the reliability of impact projection in future studies. To apply our analysis framework to other Asian countries, further improvements are required relating to the following issues; the inclusion of water resource models for what the application to non-irrigated area and arid/semi-arid areas; the inclusion of anthropologic effects in farm management into the yield damage assessment model, which is quite important especially in developing countries.

Our results base on the only one climate scenario projected by the MRI-CGCM under SRES-A2 scenario. Other SRES scenario, such as A1b, possibly gives more moderate impact to the rice production and insurance payment in Japan. And the projected change in climate strongly depends on GCMs as well as emission scenarios, thus the adoption of other GCM products is expected to improve the reliability of our projection.

Acknowledgements

I would like to show my appreciation to all members who have helped the progress of this study. Without the supports from multidiscipline members, the interdisciplinary study could have been deadlocked. Especially, I acknowledge Dr. Akio Kitoh in the Meteorological Research Institute of Japan Meteorological Agency for provision of climate projection by MRI-CGCM2 (Yukimoto et al., 2001). This study bases on the projection.

Firstly, I would like to show my sincerest appreciation to two advising professors, Prof. Yousay Hayashi and Prof. Fujio Kimura who have supported over research activities in the Graduate School of Life and Environmental Sciences, University of Tsukuba. Especially, I have been so grateful to Prof. Fujio Kimura for acceptance into his laboratory in spite of drastic change in my major at the transfer admission. My appreciation is extended to his encouragements and supports during my student time. Many parts of climate model setup in this study were owed to his supports. I also express my appreciation to Prof. Kimura for his introduction me to Prof. Yousay Hayashi. The supports and advices given by Prof. Yousay Hayashi improved many parts of this study relating to rice model setup and assessment of global warming impact. Many ideas on analysis in this study were raised at brainstorming with him both in personal and at seminars. I have been so grateful to Prof. Yousay Hayashi for his encouragement and accommodation regarding resources in the National Institute for Agro-Environmental Sciences. Countless comments and suggestions from the viewpoints of meteorology and climatology to this impact assessment study are given from Prof. Hiroshi L. Tanaka, Prof. Hiroaki Ueda, Prof. Kenichi Ueno, and Prof. Hiroyuki Kusaka in the University of Tsukuba, which aid in proceeding development of this study. Additionally, I would like to show my special thanks to Dr. Tomonori Sato, research fellow of the Japan Science and Technology Agency (JST), Ms. Tomoe Kurokawa in the Terrestrial Environmental Research Center, University of Tsukuba, Mr. Hiroaki Kawase, Ms. Sachiho Adachi in the Graduate School of Life and Environmental Sciences, University of Tsukuba for their kind supports and comments relating to use of climate model. Appreciation is extended to my colleagues Dr. Masatake E. Hori

in the Nagoya University, Mr. Tadao Inoue, Mr. Tomotsugu Inoue, Mr. Mio Matsueda, Ms. Noriko Ishizaki, and Mr. Masamichi Oba of the University of Tsukuba.

Secondly, I would like to show my great appreciation to Dr. Masayuki Yokozawa, Mr. Toshihiro Sakamoto and Dr. Akihiko Kotera in the National Institute for Agro-Environmental Sciences, and Hiroshi Nakagawa in the Ishikawa Prefectural University for their fruitful comments, suggestions and accommodation regarding use of newly developed rice model. The development of regional-scale rice modeling and yield damage assessment model in this study owes to their suggestions and cooperation.

Thirdly, I also acknowledge Prof. Masakazu Nagaki, Dr. Ruriko Nouguchi, and Dr. Yusuke Fukuda in the University of Tsukuba. Their open minded discussions help to build the economic part of analysis framework in this study. Especially, I would like to express my appreciation to Prof. Masakazu Nagaki for his support during my student time in the undergraduate school and master's program of the University of Tsukuba. My appreciation extends to Dr. Kenji Ishida in the National institute for Rural Engineering and Shintaro Hirako in the National Agricultural Research Center for their close supports and suggestions from the viewpoints of agricultural economics and farm management.

Fourthly, I acknowledge the members of ICCAP (Impact of Climate Changes on Agricultural Production system in arid areas) project, especially the project leader Prof. Tsugihiro Watanabe, in the Research Institute for Humanity and Nature for inspiring projection framework. The part of this study is supported by the Global Environmental Research Fund (S4) by the Ministry of the Environment of Japan and partially supported by the Ministry of Education, Science, Sports and Culture, Grant-in-Aid for Scientific research Category B, 1731000.

Finally, I would like to show special thanks to my parents, grandparents, uncles, and aunts. They have kept supporting me mentally and financially. Deepest and particular appreciation should be brought to Ms. Eri Kumagawa. The achievement of this study is essentially due to her mental supports and encouragements.

References

Abbaspour, C. K., 1994: Bayesian risk methodology for crop insurance decisions, *Agric. and Forest Meteorol.*, **71**, 297-314.

Arakawa, A., and W. H. Schubert, 1974: Interaction of a cumulus cloud ensemble with the large-scale environment. Part I, *J. Atmos. Sci.*, **31**, 674-701.

Doherty, R. M., L. O. Mearns, K. R. Reddy, M. W. Downton, and L. McDaniel, 2003: Spatial scale effects of climate scenarios on simulated cotton production in the southeastern U.S.A., *Climatic Change*, **69**, 99-129.

Flato, G. M., G. J. Boer, W. G. Lee, and N. A. McFarlane, 2000: The Canadian center for climate modeling and analysis global coupled model and its climate, *Clim. Dyn.*, **16**, 451-467.

Emori, S., T. Nozawa, A. Abe-Ouchi, A. Numaguchi, M. Kimoto, and T. Nakajima, 1999: Coupled ocean-atmosphere model experiments of future climate change with an explicit representation of sulfate aerosol scattering, *J. Meteorol. Soc. Jpn.*, **77**, 1299-1307.

Hazell, P., C. Pomareda, A. Valdes, and J. S. Hazell, 1986: Crop insurance for agricultural development: issues and experience, Johns Hopkins University Press.

Horie, T., and H. Nakagawa, 1990: Modeling and prediction of the development process in rice, *Jpn. Crop. Sci.*, **59**, 687-695.

Horie, T., H. Nakagawa, M. Ohashi, and J. Jakano, 1995a: Rice production in Japan under current and future climates, In: R.B. Matthews et al. (ed.), Modeling the Impact of Climate Change on Rice production in Asia, IRRI and CAB International, Wallingford, 143-164.

Horie, T., H. Nakagawa, H. G. S. Centeno, and M. J. Kropff, 1995b: The rice crop simulation model SIMRIW and its testing. In: R.B. Matthews et al. (ed.), Modeling the Impact of Climate Change on Rice production in Asia, IRRI and CAB International, Wallingford, 51-66.

Iizumi, T., 2005: Evaluation of the preference for tentative revenue insurance on rice farmers by Conjoint analysis, *Jpn. J. Farm Manage.*, **43**, 69-72. (in Japanese)

Iizumi, T., M. E. Hori, M. Yokozawa, H. Nakagawa, Y. Hayashi, and F. Kimura, 2006: Impact of

global warming on rice production in Japan based on five coupled Atmosphere-Ocean GCMs, *SOLA*, **2**, 156-159.

Iizumi, T., Y. Hayashi, and F. Kimura, 2007: Influence on Rice Production in Japan from Cool and Hot Summers after Global Warming, *J. Agric. Meteorol.*, **63**. (in press)

IPCC, 1996: Climate Change 1995 – Impacts, adaptations, and mitigation of climate change: Scientific-technical analysis, Cambridge University Press, New York.

IPCC, 2000: Special Report on Emissions Scenarios, Cambridge University Press, U.K.

IPCC, 2001: Climate Change 2001: The Scientific Basis, Cambridge University Press, U.K.

Kim, H. Y., T. Horie, and K. Wada, 1996: Effects of elevated CO_2 concentration and high temperature on growth and yield of rice. II. The effect on yield and its component of Akihikari rice, *Jpn. J. Crop Sci.*, **65**, 644-651.

Kimura, F., 2005: Trend in precipitation during the next 80 years in Turkey estimated by pseudo warming experiment. In: Research Team for the ICCAP Project (ed.), The Progress Report of ICCAP, Research Institute for Humanity and Nature, Kyoto, Japan, 11-12.

Louis, J. F., 1979: A parametric model of vertical eddy fluxes in the atmosphere, *Bound.-Layer Meteor.*, **17**, 187-202.

Mearns, L. O., F. Giorgi, L. McDaniel, and C. Shields, 2003: Climate scenarios for the southeastern U.S. based on GCM and regional model simulations, *Climatic Change*, **60**, 7-35.

Misra, V. and M. Kanamitsu, 2004: Anomaly nesting: A methodology to downscale seasonal climate simulations from AGCMs, *J. Clim.*, **17**, 3249-3262.

Nakagawa, H., T. Horie, and T. Matsui, 2003: Effects of climate change on rice production and adaptive technologies. In: T. W. Mew, D. S. Brar, S. Peng, D. Dawe, and B. Hardy (ed.), Rice Science: Innovations and impact for livelihood. Proc. Int. Rice Res. Conf., Sept. 2002, Beijing, China. IRRI, Chinese Academy of Engineering and Chinese Academy of Agricultural Sciences, 635-658.

Nakajima, T., M. Tsukamoto, Y. Tsushima, A. Numaguti, and T. Kimura, 2000: Modeling of the radiative process in an atmospheric general circulation model, *Appl. Opt.*, **39**, 4869-4878.

Oberhuber, J. M., E. Rockner, M. Christoph, M. Esch, and M. Latif, 1998: Predicting the ’97 El Nino event with a global climate model, *Gyophys. Res. Lett.*, **25**, 2273-2276.

Pielke, R. A., W. R. Grasso, M. E. Nicholls, M. D. Moran, D. A. Wesley, T. J. Lee, and J. H. Copeland, 1992: A comprehensive meteorological modeling system-RAMS, *Meteor. Atmos. Phys.*, **49**, 69-91.

Ray, P. K., 1967: Agricultural insurance, principles, and organization and application to developing countries, Pergamon Press, London.

Reynolds, R. W., N. A. Rayner, T. M. Smith, D. C. Stokes and W. Wang, 2002: An improved in situ and satellite SST analysis for climate, *J. Climate*, **15**, 1609-1625.

Roeckner, E., K. Arpe, L. Bengtsson, S. Brinkop, L. Dumenil, M. Esch, E. Kirk, F. Lunkeit, M. Ponater, B. Rockel, M. Suasen, U. Schlese, S. Schubert, and M. Windelband, 1992: Simulation of the present-day climate with the ECHAM4 model: Impact of model physics and resolution, Max Planck Institute for Meteorology, Report No. 93, Hamburg, 171.

Satake, T., and S. Yoshida, 1978: High-temperature-induced sterility in Indica rice at flowering, *Jpn. J. Crop Sci.*, **47**, 6-17.

Sato, T., and F. Kimura, 2005: Diurnal cycle of convective instability around the central mountains in Japan during the warm season, *J. Atmos. Sci.*, **62**, 1626-1636.

Sato, T., F. Kimura, and A. Kitoh, 2006: Projection of global warming onto regional precipitation over Mongolia using a regional climate model, *J. Hydro.* (in press).

Seino, H., 1993: An estimation of distribution of meteorological elements using GIS and AMeDAS data, *J. Agric. Meteorol*, **48**, 379-383.

Suh, M.-S., and D.-K. Lee, 2004, Impacts of land use/cover changes on surface climate over east Asia for extreme climate cases using RegCM2, *J. Geophys. Res.*, ***109***, D02108, doi:10.1029/2003JD003681.

Tanaka, K., Y. Fujihara, T. Watanabe, T. Kojiri, and S. Ikebuchi, 2006: Projection of the impact of climate change on the surface energy and water balance in the Seyhan River Basin Turkey, *Annual Journal of Hydraulic Engineering*, **50**, 31-36.

Tao, F., M. Yokozawa, Y. Hayashi, and E. Lin, 2003: Future climate change, the agricultural water cycle, and agricultural production in China, *Ecosystem and Environment.*, **95**, 203-215.

Thomson, A. M., N. J. Rosenberg, R. C. Izaurralde, and R. A. Brown, 2005: Climate change impacts for the conterminous USA: An integrated assessment, Part 5. Irrigated Agriculture and National Grain Crop Production, *Climatic Change*, **69**, 89-105.

Tokioka, T., A. Noda, A. Kitoh, Y. Nikaidou, S. Nakagawa, S. Motoi, S. Yukimoto and K. Takata, 1995: A transient CO2 experiment with the MRI-CGCM, *J. Meteor. Soc. Japan*, **73**, 817-826.

Toritani, H., S. Yonemura, and M. Yokozawa, 1999: Potential rice yield in the 21st Century in Japan under the climate change scenario based on MRI-CGCM, *J. JASS*, **15**, 8-16.

Tremback, C. J., and R. Kessler, 1985: A surface temperature and moisture parameterization for use in mesoscale numerical models. Preprints, Seventh Conf. on Numerical Weather Prediction, Montreal, QC, Canada. *Amer. Meteor. Soc.*, 355-358.

Tsujii, H., 1986: An economic analysis of rice insurance in Japan. In: P. B. R. Hazell, C. Pomareda, and A. Valdes (ed.), Crop Insurance for Agricultural Development: Issues and Experience, Johns Hopkins University Press, Baltimore, 143-155.

Tsvetsinskaya, E. A., L. O. Mearns, T. Mavromatis, W. Gao, L. McDaniel, and M. W. Downton, 2003: The effect of spatial scale of climatic change scenarios on simulated maize, winter wheat, and rice production in the southeastern United States, *Climatic Change*, **60**, 37-72.

Ueda, T., H. Nakagawa, K. Okada, and T. Horie, 2000: Varietical differences in yield and spikelet fertility of rice in response to elevated CO2 concentration and high temperature, *Jpn. J. Crop Sci.*, **69**, 112-113.

Walko, R. L., W. R. Cotton, M. P. Meyers, and J. Y. Harrington, 1995: New RAMS cloud microphysics parameterization. Part 1: The single-moment scheme, *Atmos. Res.*, **38**, 29-62.

Watterson, I. G., S. P. O'Farrell, and M. R. Dix, 1997: Energy and water transport in climates simulated by a general circulation model that includes dynamic sea ice, *J. Gyophy. Res.*, **102**, 11027-11037.

Yamamura, K., M. Yokozawa, M. Nishimori, Y. Ueda, and T. Yokosuka, 2006, How to analyze long-term insect population dynamics under climate change: 50-year data of three insect pests in paddy fields, *Popul. Ecol.*, **48**, 31-48.

Yokozawa, M., S. Goto, Y. Hayashi and H. Seino 2003: Mesh Climate Change Data for Evaluating Climate Change Impacts in Japan under Gradually Increasing Atmospheric CO_2 Concentration, *J. Agric. Meteorol.*, **59**, 117-130.

Yonemura, S., M. Yajima, H. Sakai, and M. Morokuma, 1998: Estimation of rice yield of Japan under the conditions with elevated CO_2 and increased temperature by using third mesh climate data, **54**, 235-245.

Yoshikane, T., and F. Kimura, 2003: Formation mechanism of the simulated SPCZ and Baiu front using a regional climate model, *J. Atmos. Sci.*, **60**, 2612-2632.

Yukimoto, S., A. Noda, A. Kitoh, M. Sugi, Y. Kitamura, M. Hosaka, K. Shibata, S. Maeda, and T. Uchiyama, 2001: A new meteorological research institute coupled GCM (MRI-CGCM2) – its climate and variability – *Pap. Met. Geophys.*, **51**, 47-88.

Appendices

Appendix A: Accuracy of the climate model

To diagnose the reproductive capability of the RCM (see in Chapter 2.2), the Spatial Correlation Coefficients (SCCs) between observations and dynamically downscaled products were calculated for monthly value during May to October in 1990s. The Standard Errors (SEs) between them are also calculated as well as the SCCs. The nearest grid values to observation points were searched and adapted as the datasets to calculate above statistics.

Relating to the monthly mean temperature, the SCCs show relatively high values from 0.490 to 0.915 (Figure A1a), and they mostly concentrate the range from approximately 0.7 to 0.9 (mean=0.799, max=0.273, and min=-3.518). However, the SCCs in August are consistently low for the target period. On the other hand, those in May and June show an opposite tendency and are consistently high for the period. The cold bias significantly appears in the monthly mean temperatures in the downscaled products through the period, and the bias averaged over all period is -1.48 K (max=0.27 and min=-3.52).

Relating to the monthly mean daily total solar radiation, the SCCs vary depending on years and months. If we take years 1994 and 1999 as the examples, the SCCs relatively concentrate in the range of 0.4 to 0.8 in 1994, while they distribute in the range of 0.1 to 0.8 in 1997 (Figure A2). The SCCs of October tend to show relatively high value; on the other hand, those of June are low (mean=3.30, max=0.83, and min=-0.32). The SEs show significant underestimations through the all period. The SEs show tendencies that the downscaled products in October have serious underestimations, whereas those in summer season i.e., June, July, and August, have slight underestimations (mean=-139.9, max=-58.0, and min=-239.3).

In the monthly total precipitation, the SCCs remarkably vary depending on years and months as well as those of solar radiation. For examples, the SCCs in 1991 concentrate in the range of 0.3 to 0.7, while those in 1996 also concentrate in the range of 0.1 to 0.3. On the other

hand, the SCCs in 1993, 1997, and so on, vary depending on months in the range of 0.0 to 0.8 (mean=0.305, max=0.745, and min=-0.247). The SEs tend to vary depending on months, and those in July and August show significant underestimation, while those in October show overestimates through the period (mean=-27.2, max=78.0, and min=-151.0).

From the viewpoint of spatial pattern in the climate elements, the reproductive capabilities of the RCM are comparatively high in temperature, and those in solar radiation and precipitation significantly vary depending on years and months. In addition, there are estimation errors i.e., climate-model bias, such as cold bias in the temperature, underestimation in solar radiation, and underestimation/overestimation in precipitation. Such climate-model biases derive from the spatial resolution, physical parameterizations, approximation in the dynamic process, and so on.

Above mentioned climate-model bias in spatial patterns could cause non-realistic spatial changes in impact projection regarding crop productions. In addition, the cold bias in temperature affects estimations of crop phenology development and causes underestimations of damage due to heat stress. Such underestimations are a serious problem for policymakers, researchers, and farmers. Especially in Japan, temperature works as a limiting factor of cultivation, and it also work a main factor of yield variability in northern area. The underestimations in solar radiation cause reductions of estimated biomass, and finally lead estimations of decrease in yield. Especially, the underestimations/overestimations in precipitation are quite serious problem when the elements are used as an input data to crop models. Since soil moisture is a strongly related with precipitation, and soil moisture is the essential factor to crop yield in arid and semi-arid areas. Thus, reliable projection of precipitation is a essential to assess a change in cultivable area and yield variability,

Climate models are the only tool to project climate changes as a result of global warming. Simulated changes in climate certainly cause changes in crop phenology responses. However, climate-model bias also causes changes in crop phenology responses. The distinction between simulated climate change and climate model bias is essential to conduct a reliable impact assessment of global warming. However, climate-model bias is inconsistent regarding models, objective climatic variables, and simulated seasons. Thus, the methods should be examined to

cancel the climate-model bias from climate model products. This study suggests a simple method i.e., the use of differential components in climate model products between future and current, namely the “adjusted climate projection”. The Model Output Statistics (MOS) has been contributing to reduce climate-model bias in the scene of weather forecasts. The MOS can be possible to be replaced above method. Development of the MOS for climate change scenario is an area where should be address in future studies to secure reliable impact projection of global warming.

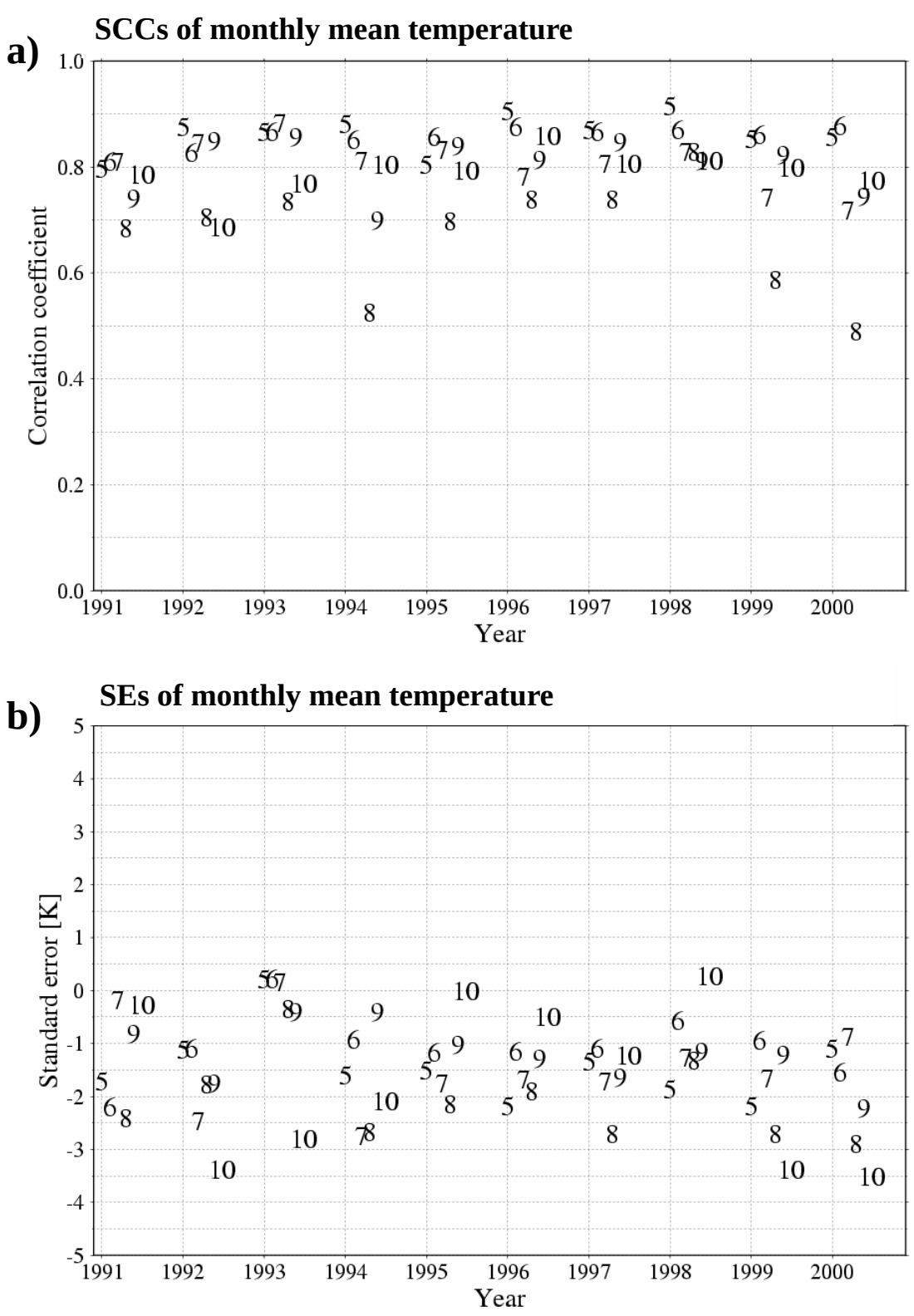

Figure A1: Spatial Correlation Coefficients (SCC; a) and Standard Errors (SE; b) between observations and dynamically downscaled products in monthly mean temperature for the 1990s.

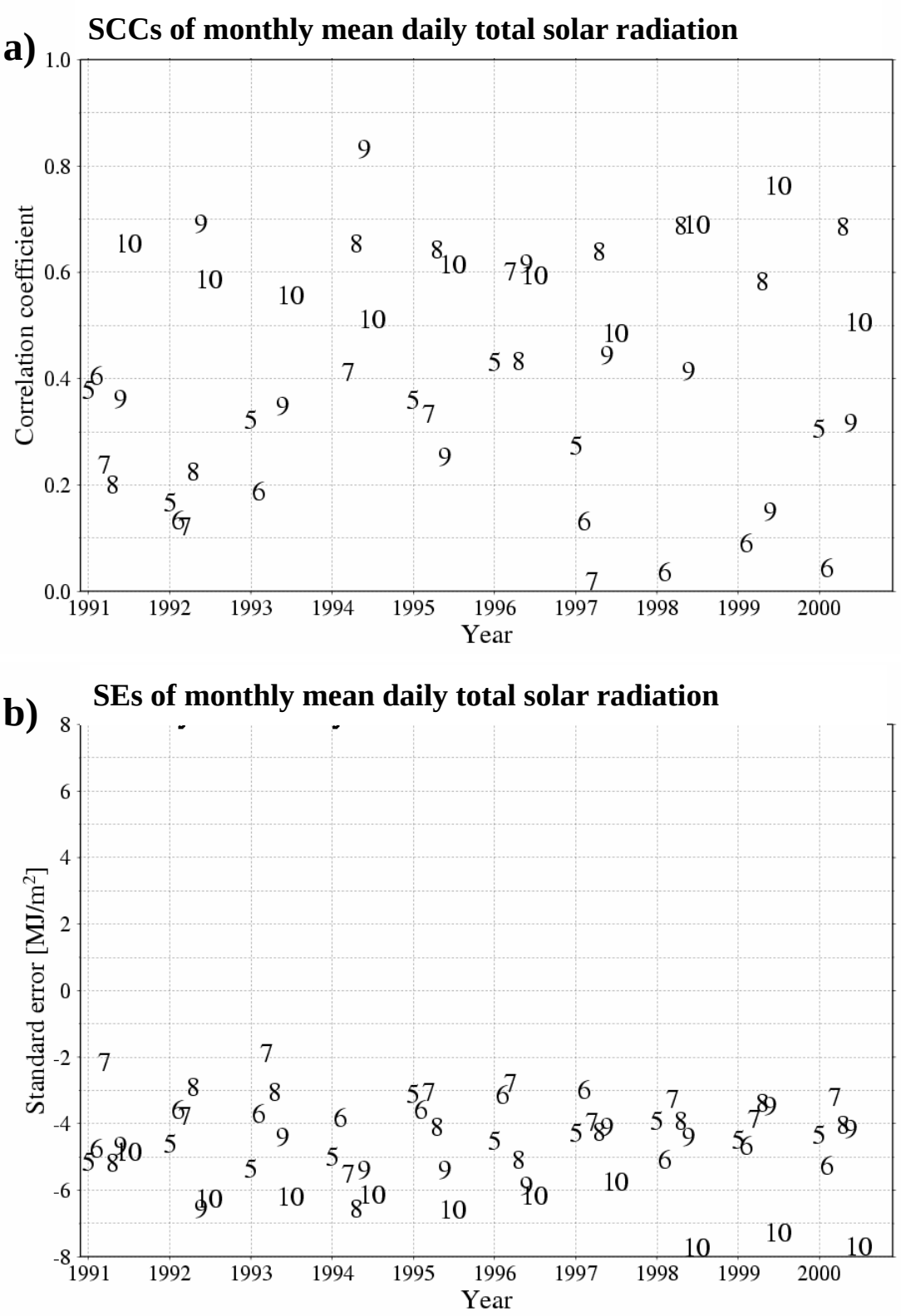

Figure A2: Same with Figure A1 but monthly mean daily total solar radiation for the 1990s.

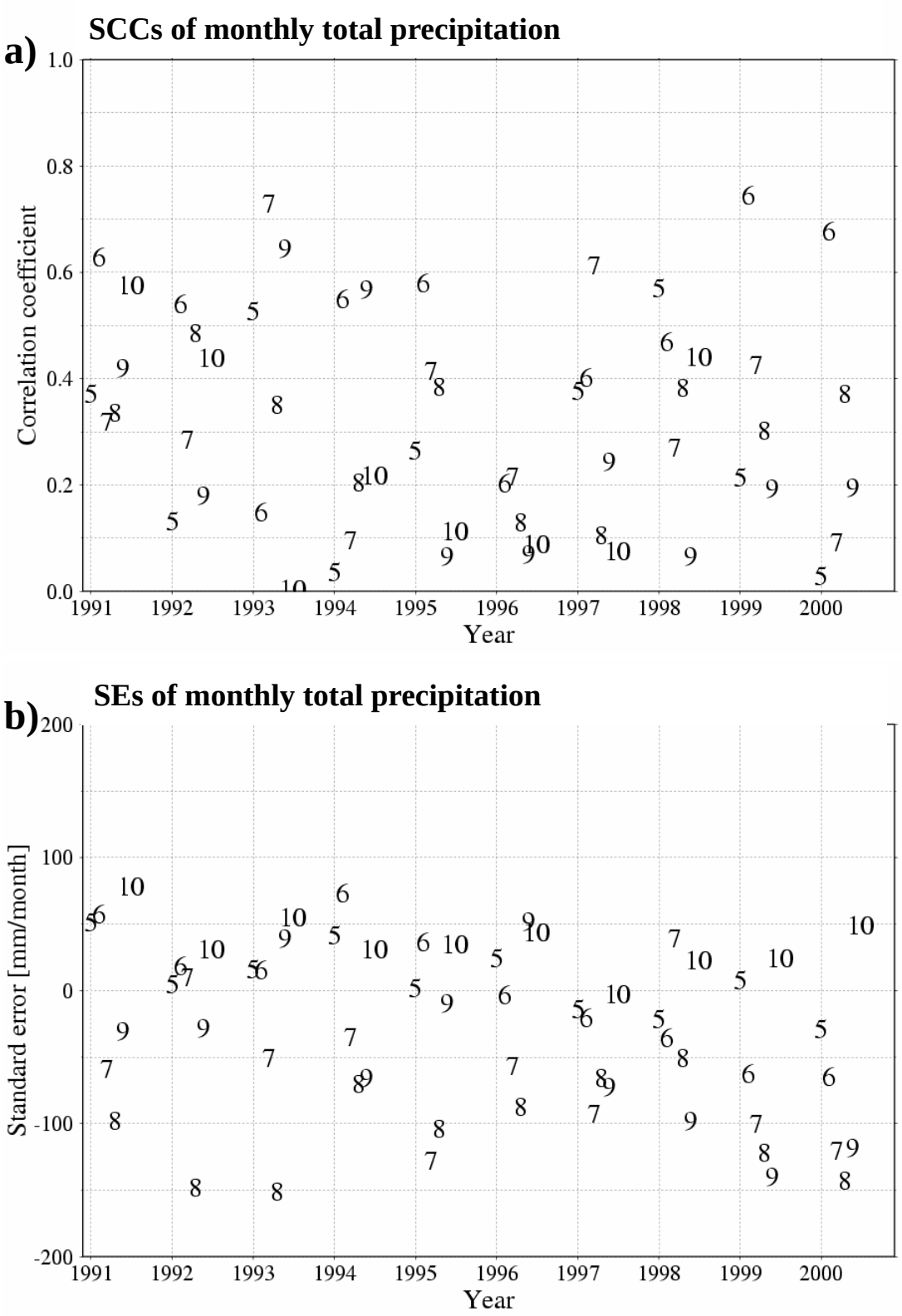

Figure A3: Same with Figure A1 but monthly total precipitation for the 1990s.

Appendix B: Projected regional climate change in 2070s under SRES-A2 scenario

Regional climate changes are projected by using a combination of the GCM products and the RCM, and summarized in Chapter 3.3.2. However, presented climate changes are only the 2-year mean climate change, thus the 10-year mean climate changes are newly shown here for every prefectures in Japan with the exception Okinawa, the southwestern islands. The climate changes data were used as the input data for the RRM and the DSRM, and the detail of data processes are described in Chapter 2.2.2, 2.3.2, and 5.3.3.

Hokkaido area

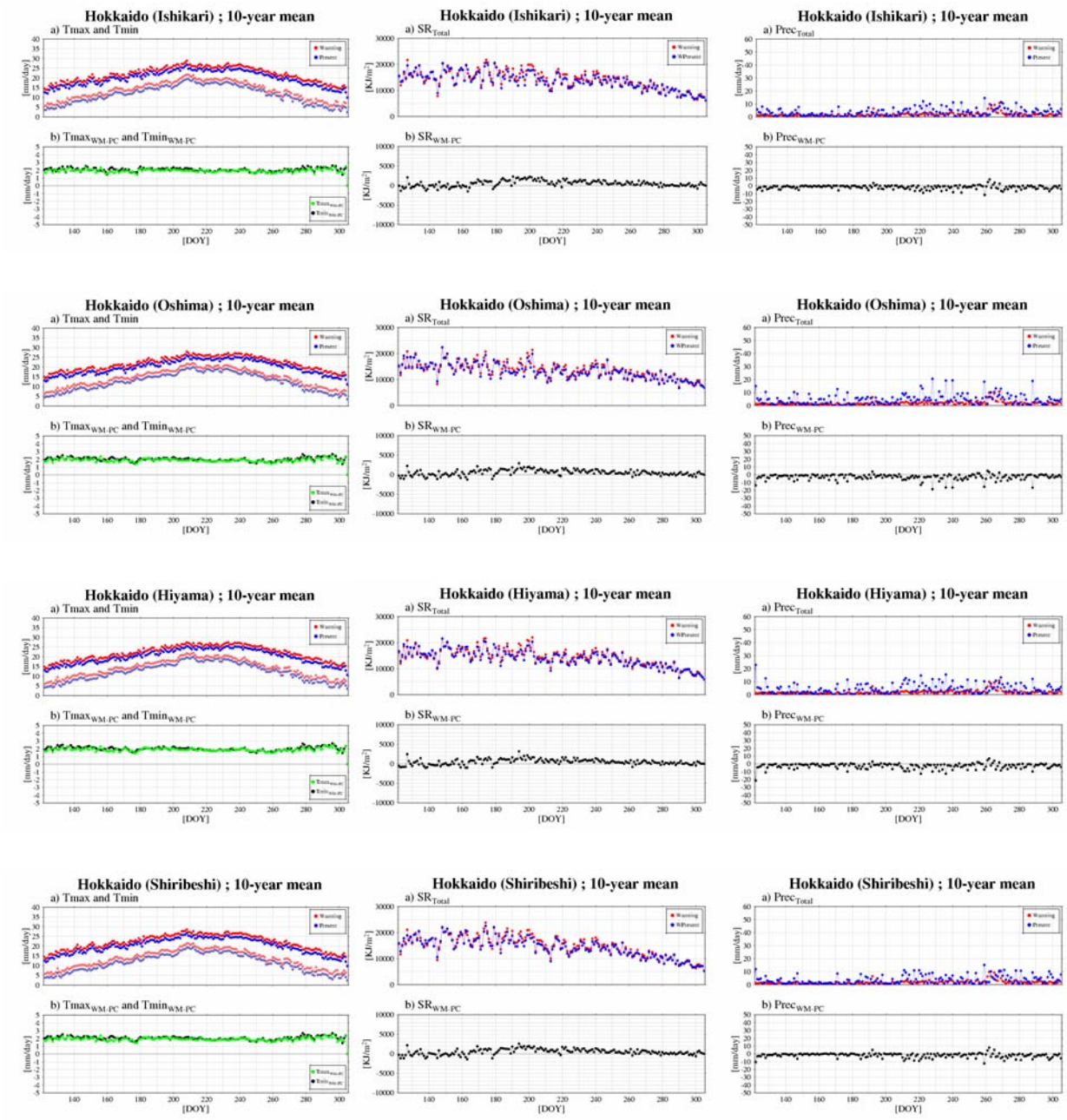

Figure B1: Time series of observational climate in 1990s and projected climate in 2070s regarding daily maximum/minimum temperatures (left), daily total solar radiation (middle), and daily total precipitation (right) in Hokkaido area. The bottom figures show each anomalies caused by global warming.

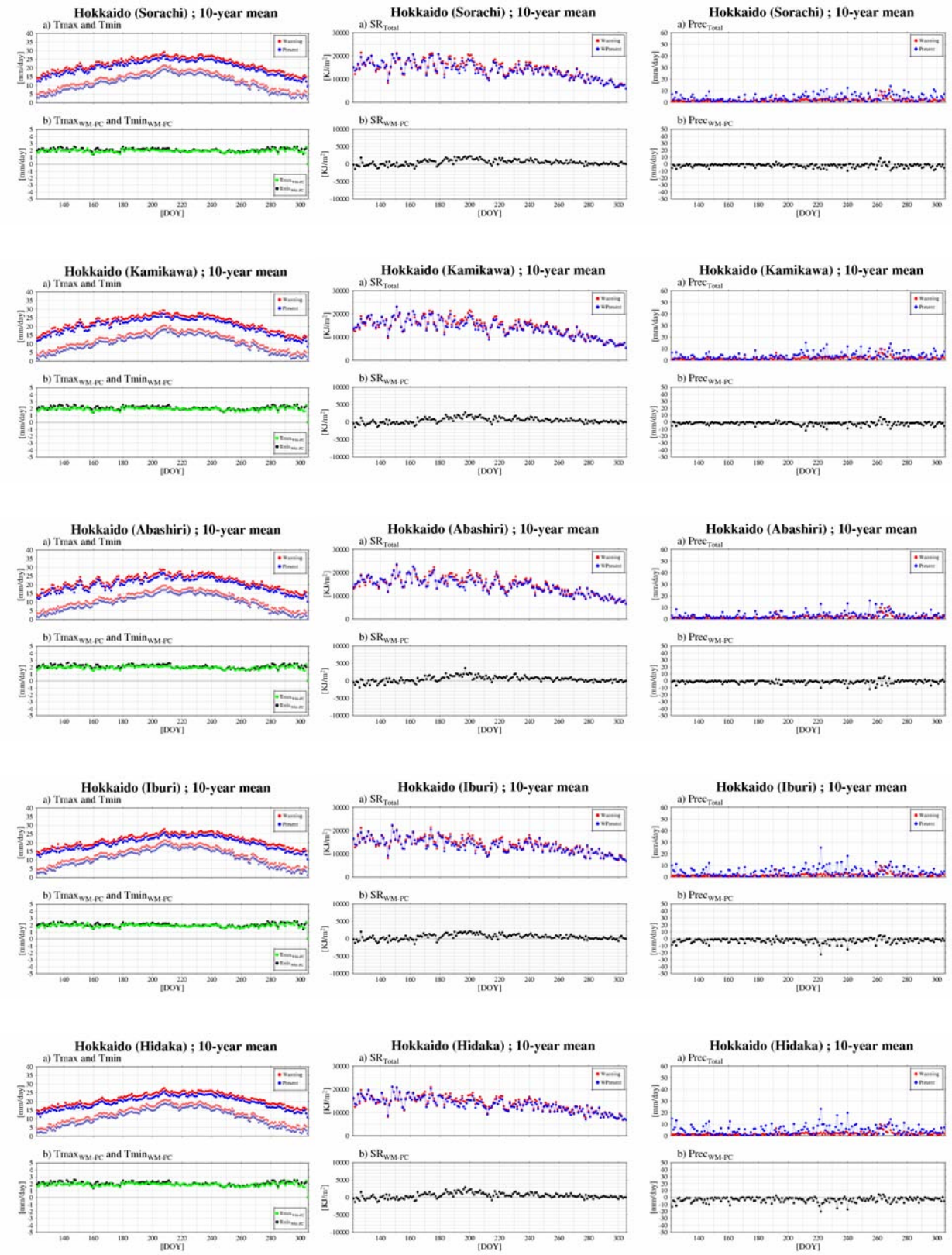

Figure B1: (continued)

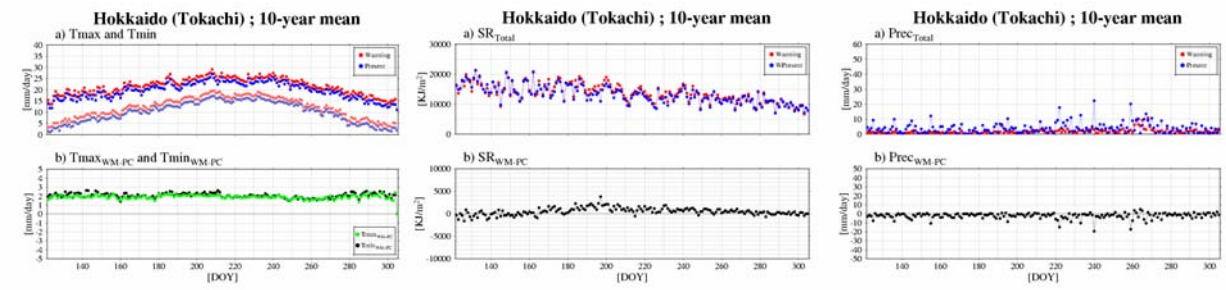

Figure B1: (continued)

Tohoku area

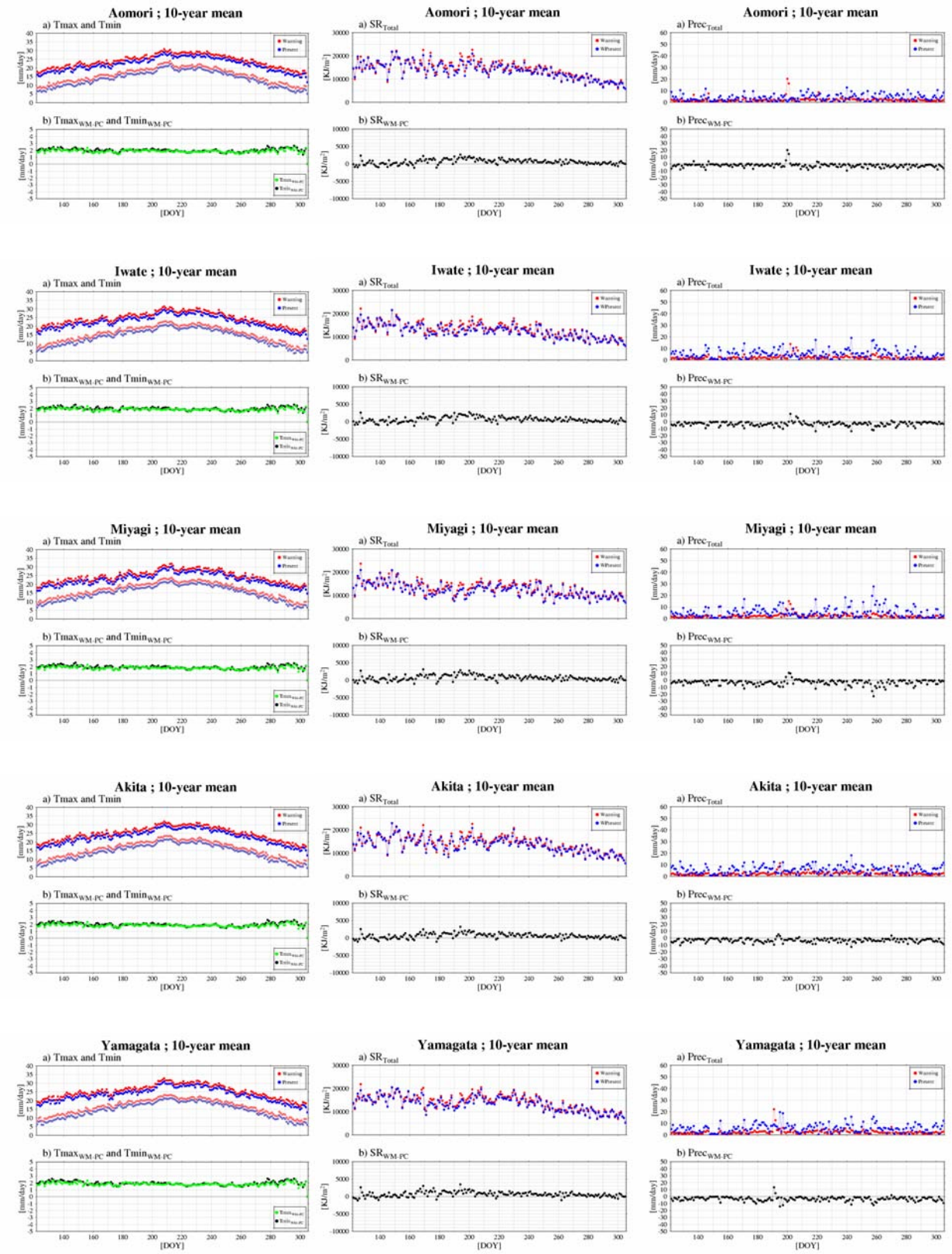

Figure B2: Same with Figure B1 but in Tohoku area.

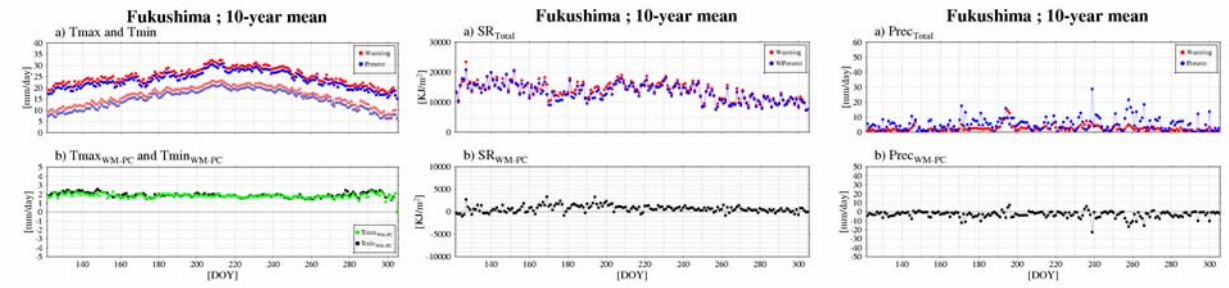

Figure B2: (continued)

Kanto/Tozan area

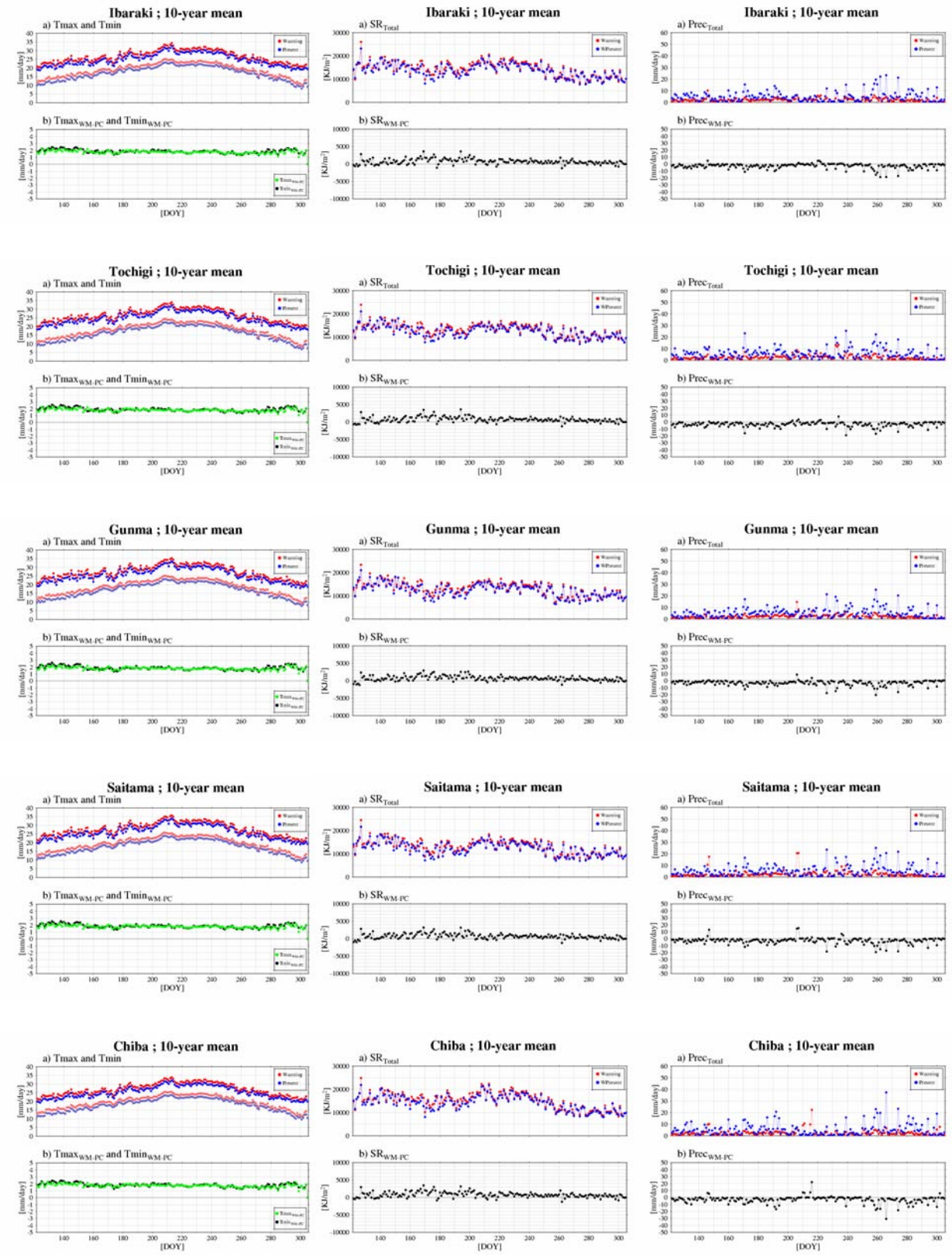

Figure B3: Same with Figure B1 but in Kanto/Tozan area.

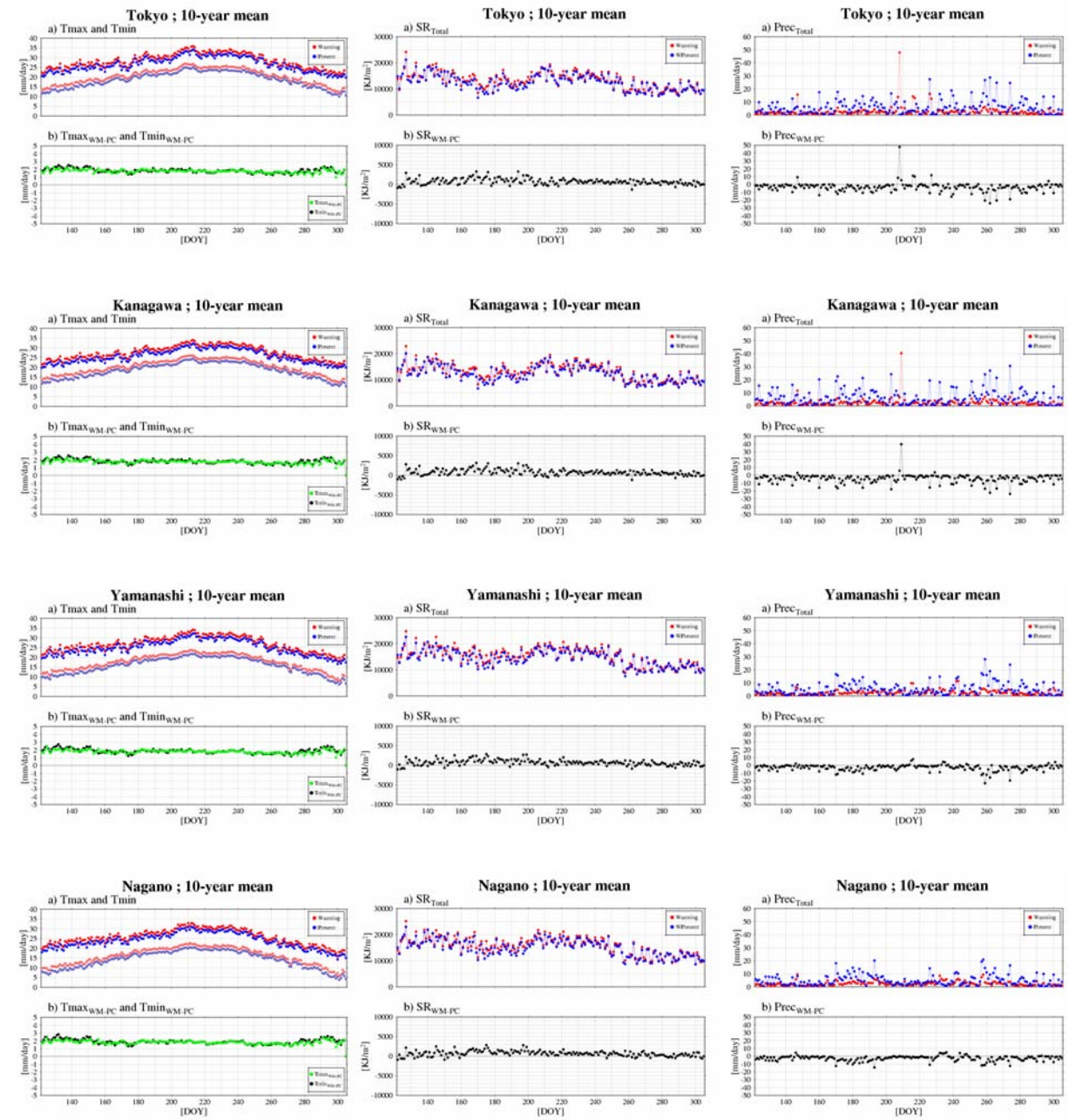

Figure B3: (continued)

Hokuriku area

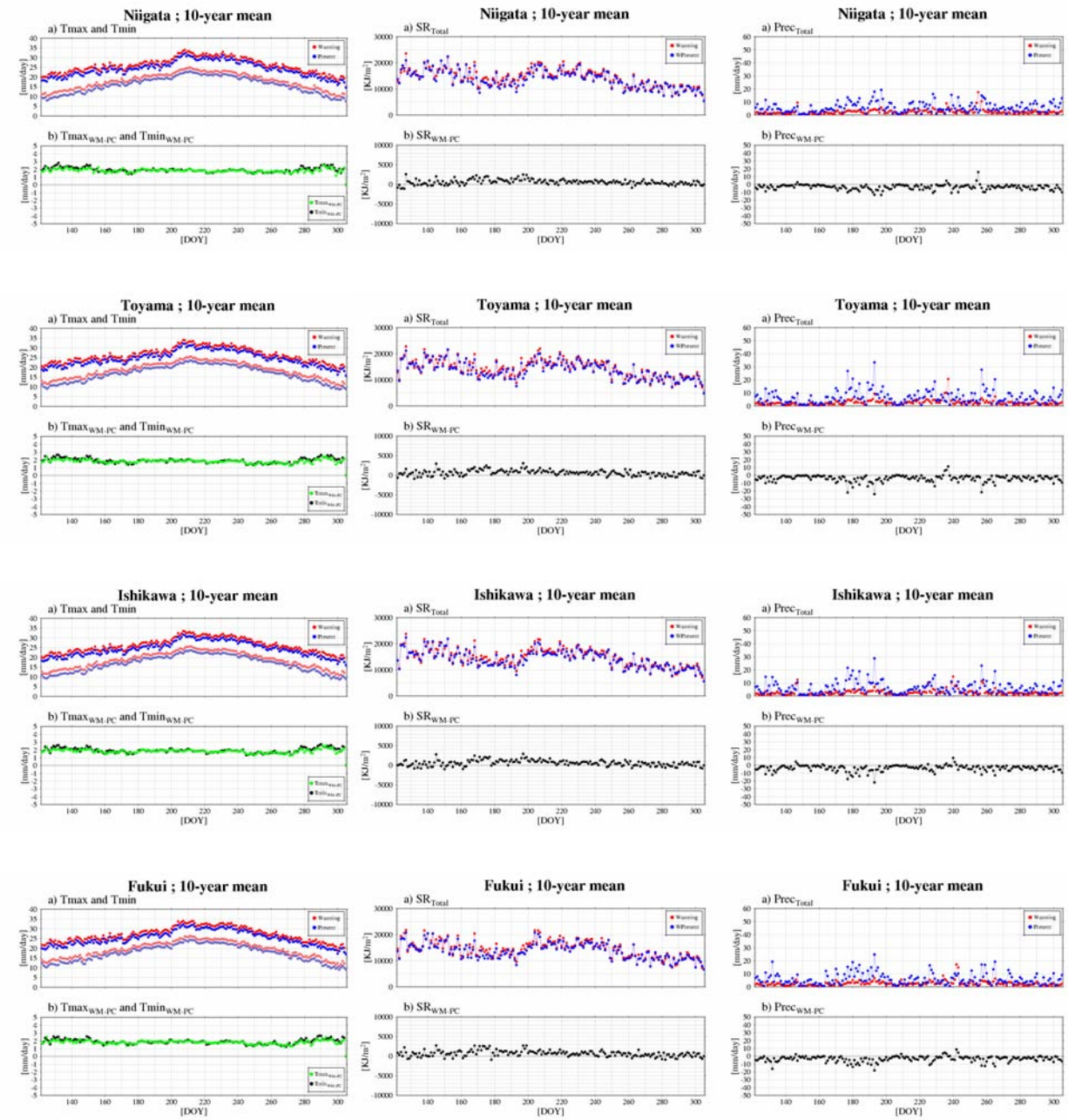

Figure B4: Same with Figure B1 but in Hokuriku area.

Tokai area

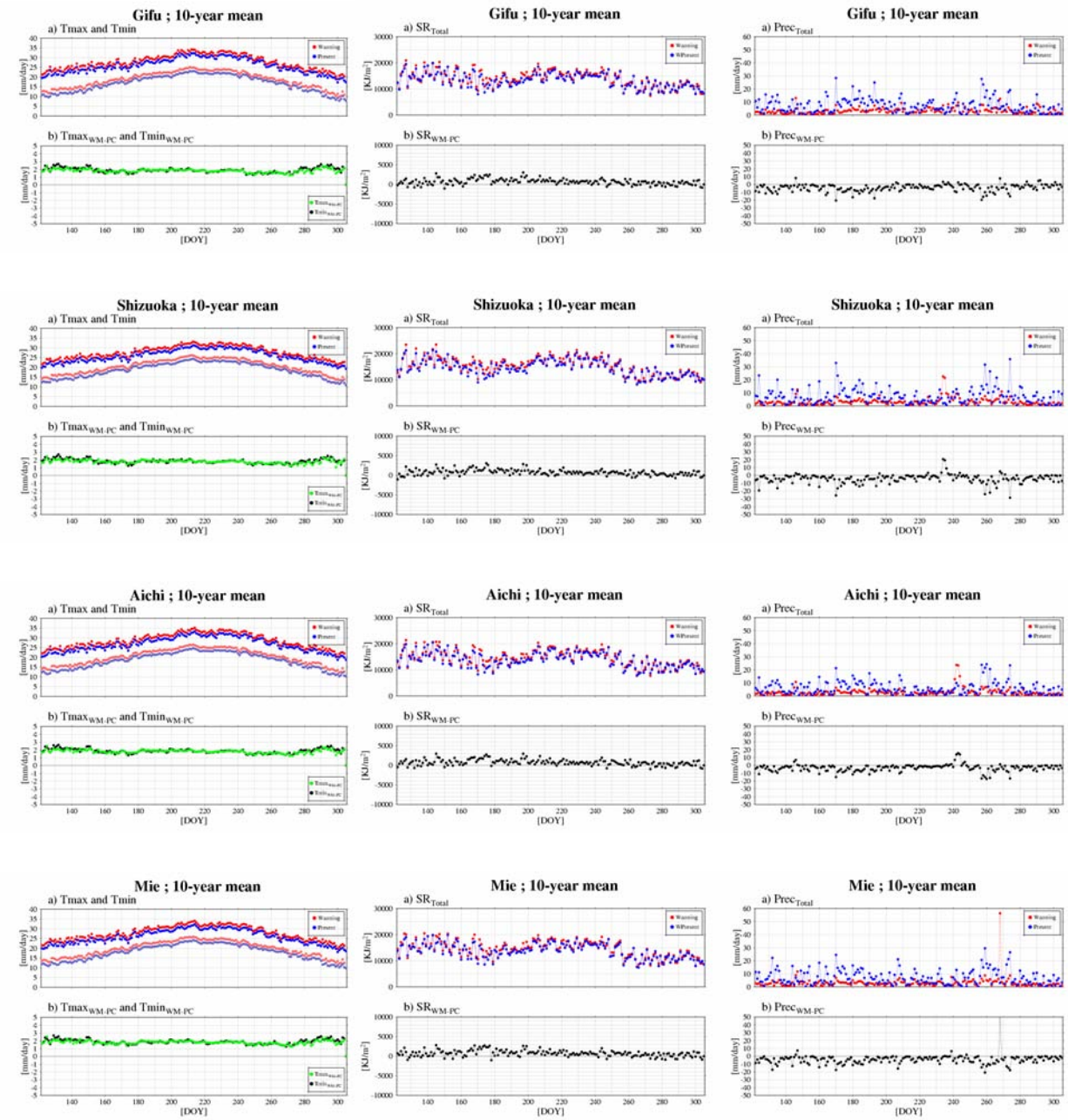

Figure B5: Same with Figure B1 but in Tokai area.

Kinki area

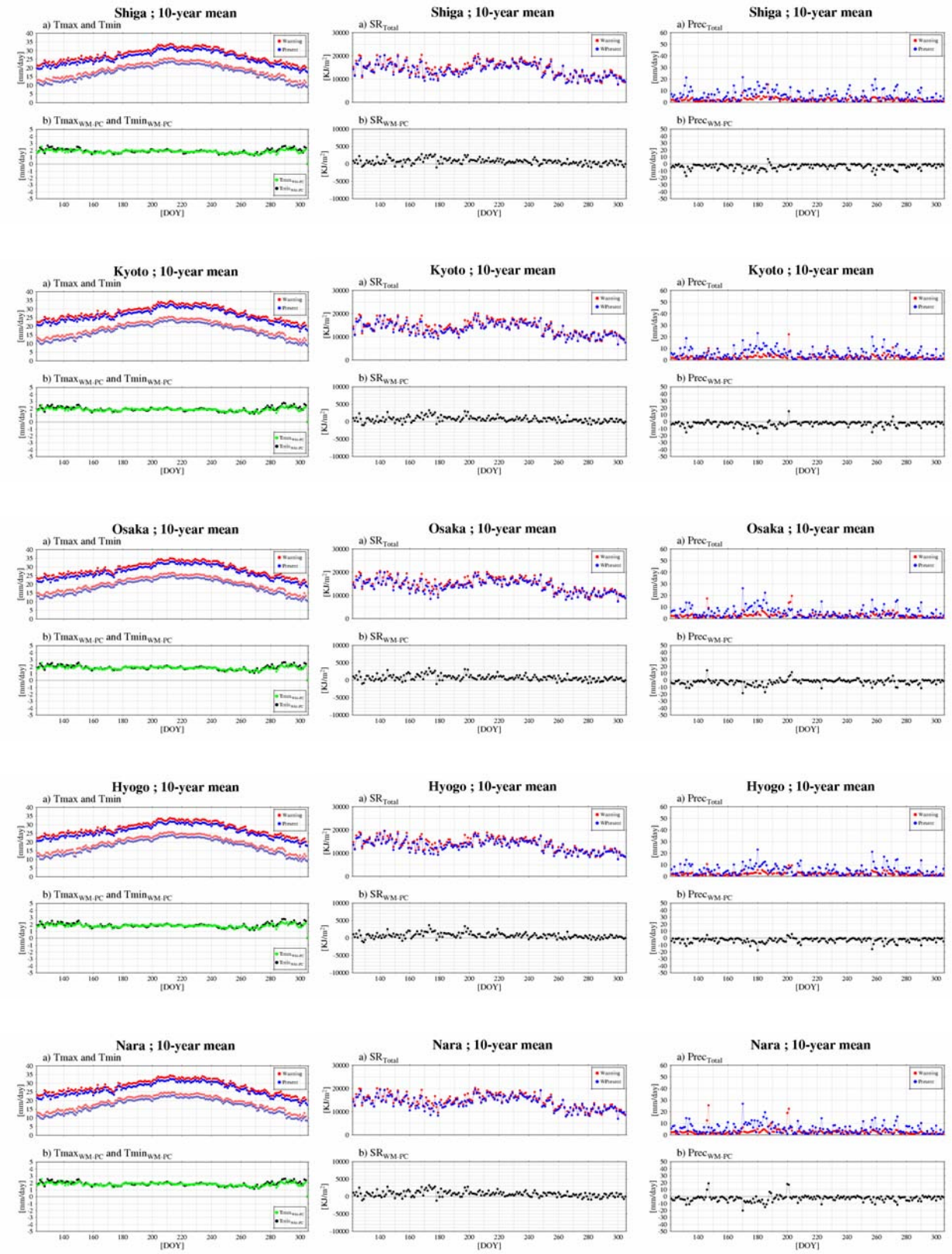

Figure B6: Same with Figure B1 but in Kinki area.

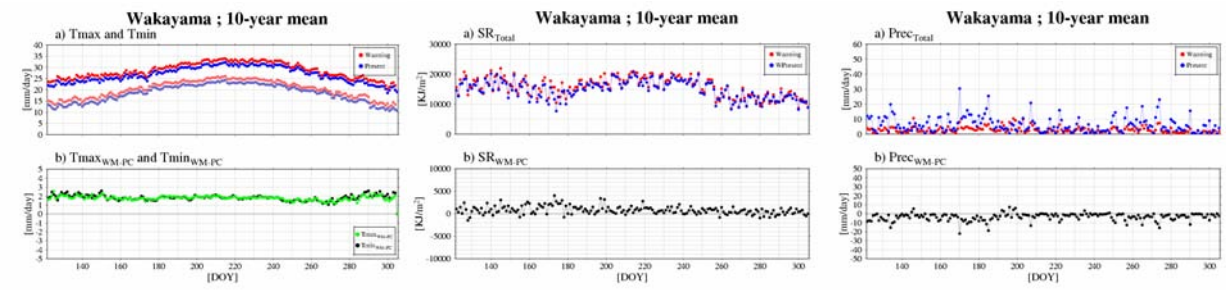

Figure B6: (continued)

Chugoku area

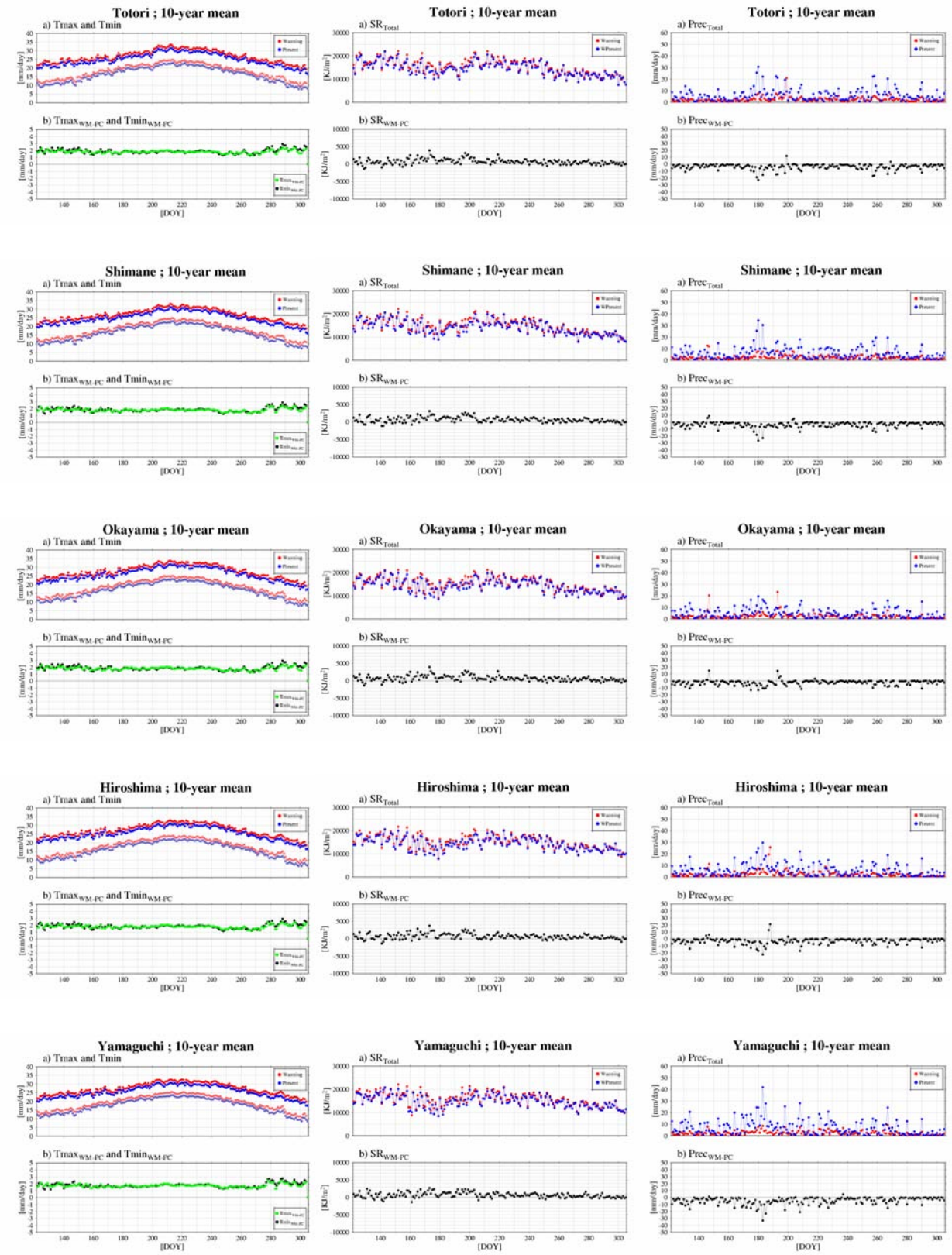

Figure B7: Same with Figure B1 but in Chugoku area.

Shikoku area

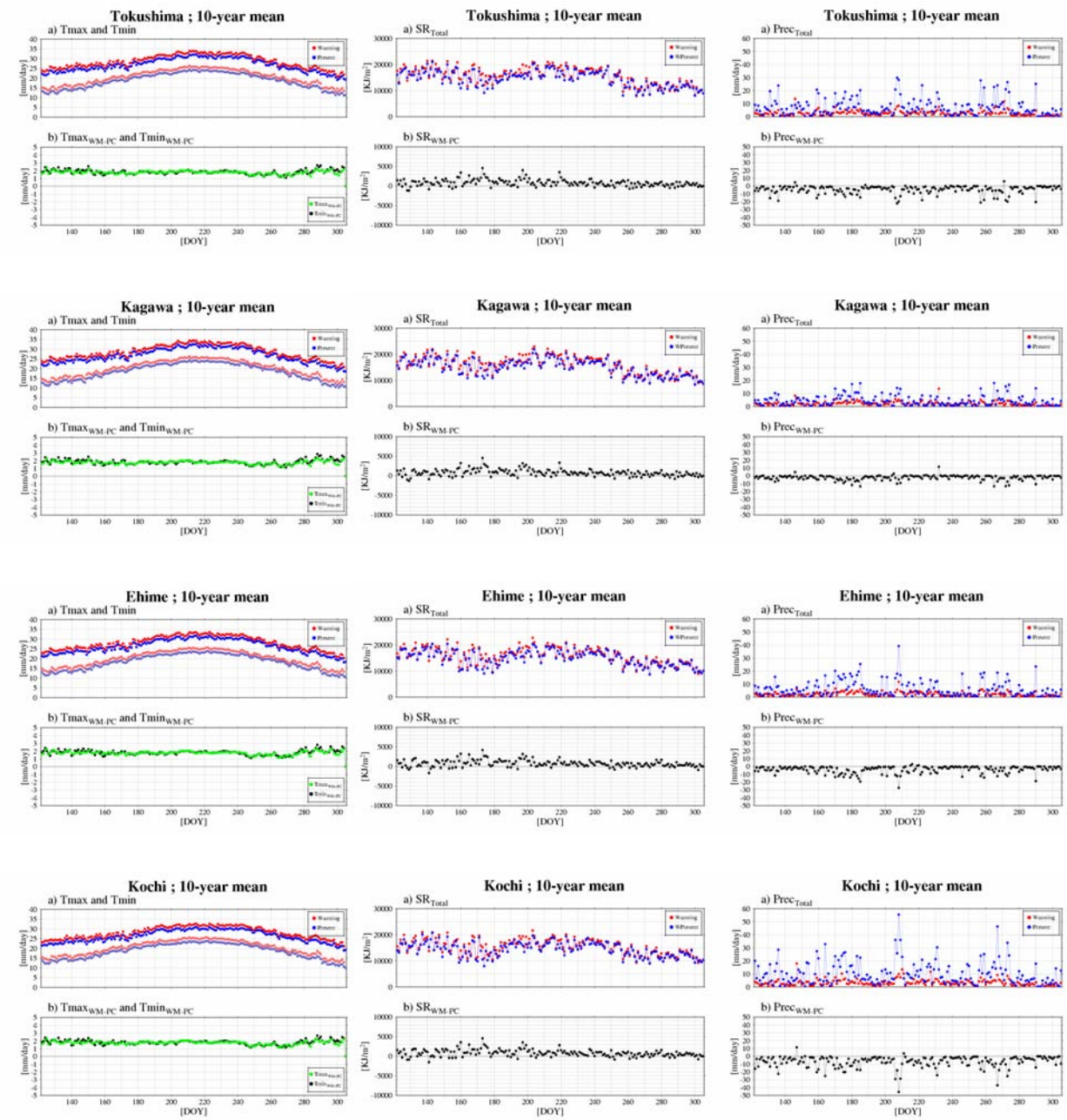

Figure B8: Same with Figure B1 but in Shikoku area.

Kyushu area

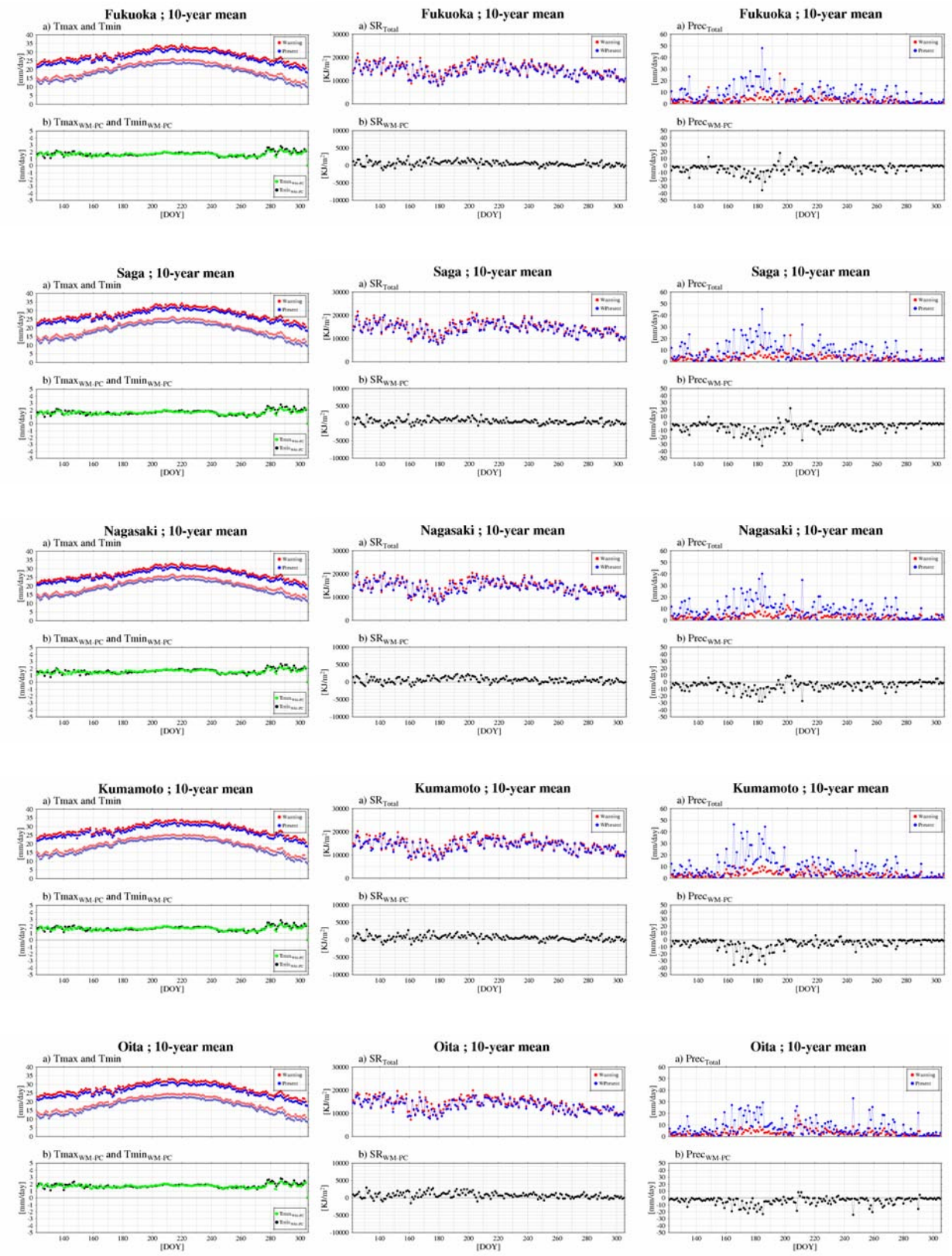

Figure B9: Same with Figure B1 but in Kyushu area.

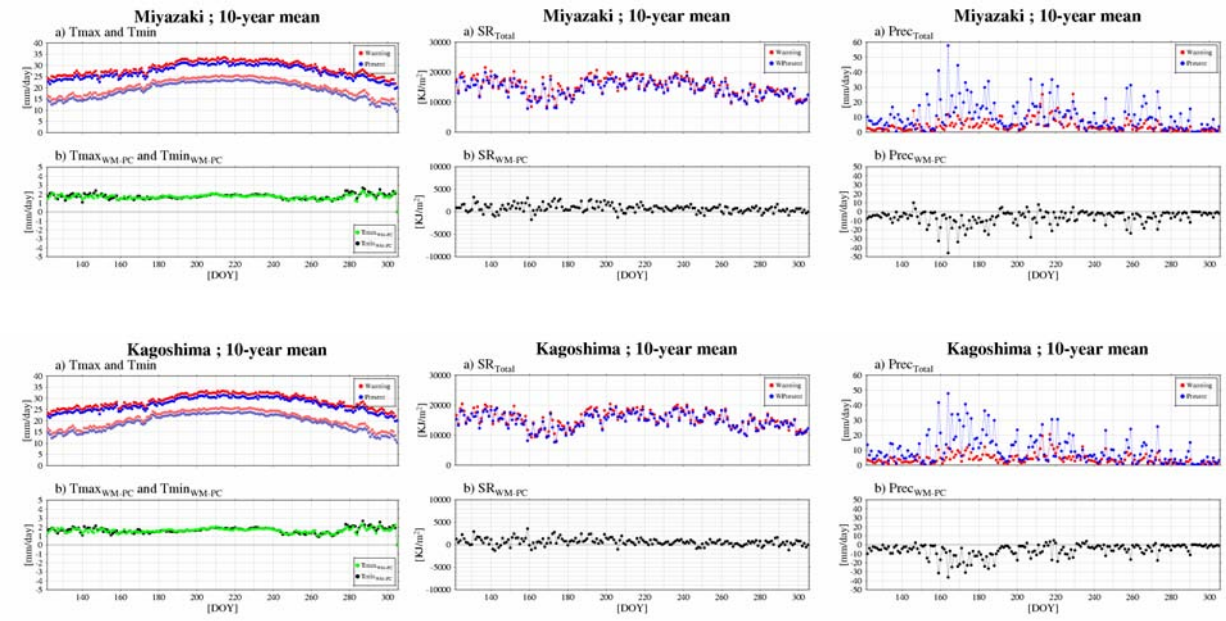

Figure B9: (continued)

Appendix C: List of abbreviation

AMeDAS: Automated Meteorological Data Acquisition System

AR: Assessment Report

CCSR/NIES: Center for Climate System Research, the University of Tokyo / National Institute for Environmental Studies

CDD: Cooling Degree Days

CGCM1: Canadian Global Coupled Model ver.1

CSIRO-Mk2: Australia's Commonwealth Scientific and Industrial Research Organization global coupled ocean-atmosphere-sea-ice model Mark 2

CV: Coefficient of Variance

DNLI: Digital Numerical Land Information

DVI: DVelopment Index

ECHAM/OPY3: ECMWF model and a comprehensive parametrisation package developed at HAMburg / Ocean and isoPYCnal coordinates ver.3

GCM: General Circulation Model

IPCC: Intergovernmental Panel on Climate Change

LAI: Leaf Area Index

MAFF: Ministry of Agriculture, Forestry and Fisheries of Japan

MCD: Model-output Climate Dataset

MOS: Model Output Statistics

MRI-CGCM2: Meteorological Research Institute - Coupled GCM ver.2

NCEP/NCAR: National Center for Environmental Prediction / National Center for Atmospheric Research

NIAES: National Institute for Agro-Environmental Sciences

OCD: Observed Climate Dataset

RCM: Regional Climate Model

RMSE: Root Mean Square Error

RRM: Regional-scale Rice Model

SCC: Spatial Correlation Coefficient

SE: Standard Error

SIMRIW: SImulation Model for RIce and Weather-relationship

SRES: Special Report on Emission Scenario

SST: Sea Surface Temperature

TERC-RAMS: Regional Atmospheric Modeling System modified by the Terrestrial Environmental Research Center, University of Tsukuba